Qaleh Kurd Cave (Qazvin, Iran): Oldest Evidence of Middle Pleistocene Hominin Occupations and a Human Deciduous Tooth in the Iranian Central Plateau

Hamed Vahdati Nasab, Gilles Berillon, Seyyed Milad Hashemi, Jean-Jacques Bahain, Noémie Sévêque, Mozhgan Jayez, Stéphanie Bonilauri, Guillaume Jamet, Mohammad Akhavan Kharazian, Asghar Nateghi, et al.

QALEH KURD CAVE (QAZVIN, IRAN): OLDEST EVIDENCE OF MIDDLE PLEISTOCENE HOMININ OCCUPATIONS AND A HUMAN DECIDUOUS TOOTH IN THE IRANIAN CENTRAL PLATEAU

Hamed Vahdati Nasab [1,2-*], Gilles Berillon [2-*], Seyyed Milad Hashemi [1,2], Jean-Jacques Bahain [2], Noémie Sévêque [3], Mozhgan Jayez [4], Stéphanie Bonilauri [2], Guillaume Jamet [5-6], Mohammad Akhavan Kharazian [2-6-12-13], Asghar Nateghi [7], Alieh Abdollahi [7], Pierre Antoine [6], Iraj Beheshti [8], Nicolas Boulbes [2], Cécile Chapon-Sao [2], Xavier Gallet [2], Christophe Falguères [2], Lisa Garbé [2], Mandan Kazzazi [9], Ahmad Zavar Mousavi [10], Sareh Nematollahinia [1], Jonathan Özçelebi [2], Emmanuelle Stoetzel [2], Olivier Tombret [2], Valéry Zeitoun [11]

1. Department of Archaeology, Tarbiat Modares University, Tehran, Iran, *corresponding author, vahdati@modares.ac.ir
2. UMR7194 CNRS-MNHN-UPVD / Département Homme et Environnement, Musée de l'Homme - Palais de Chaillot, Paris, France, *corresponding author, gilles.berillon@mnhn.fr
3. UMR7044 ArcHiMèdE, Strasbourg, France
4. Department of Archaeology, University of Tehran, Tehran, Iran
5. INRAP, Department Grand Ouest, Paris, France
6. UM8591 CNRS/Université Paris 1/UPEC, Laboratoire de Géographie Physique, Environnements Quaternaires et Actuels, Thiais, France
7. Department of Archaeology, Islamic Azad University, Tehran, Iran
8. Center for Conservation and Restoration Research, Research Institute of Cultural Heritage and Tourism (RICHT), Tehran, Iran
9. Sustainable Computing Lab, Vienna University of Economy and Business (Wirtschaftsuniversität Wien, WU), Wien, Austria
10. Department of Archaeology, Marlik Institute for Higher Education, Nowshahr, IRAN
11. Centre de recherche en paléontologie-Paris CR2P, UMR7207 MNHN-SU-CNRS, Paris, France
12. School of Geography, Earth and Atmospheric Sciences, University of Melbourne, Victoria, Australia
13. Department of Geography, School of Environment, Education and Development, University of Manchester, Manchester, United Kingdom

* Hamed Vahdati Nasab and Gilles Berillon are both first co-authors, equally contributing to the research design and the preparation of the manuscript.

Abstract

The Iranian Central Plateau (ICP) with the Alborz and the Zagros Mountains is located at the crossroads between the Levant and the Caucasus to the west, and Central Asia and East Asia to the east. These two regions yielded key paleoanthropological and archaeological sites from the Middle Pleistocene period. These discoveries highlight a large human biological and cultural diversity in this area during the Middle Pleistocene, and raise questions about the interactions these humans had. Yet, despite decades of field research, no Middle Pleistocene assemblage in a clear chronological and stratigraphic context was known in the ICP, the Zagros and the Alborz Mountains that could contribute to this debate; so far, the earliest of the area is dated of 80ka. The Joint Iranian and French Paleoanthropological Project reinvestigated the cave of Qaleh Kurd (Qazvin). The Qaleh Kurd cave is located at 2137m asl at the very western limit of the ICP, at its boundary with the Zagros Mountains. Here we report on the discovery of *in situ* middle Pleistocene archaeological assemblages, including a human deciduous first upper molar associated with a rich lithic and faunal material, and a first description of the chrono-stratigraphic framework of the deposits. The excavation, the archaeological and geoarchaeological analyses show that humans occupied the site during the Middle Pleistocene, during a period ranging from ca 452 ± 32 and 165 ± 11 ka . This chronology pushes back the earliest dated evidence of human settlement in the ICP by more than 300ka. The human deciduous first upper molar comes from the upper part of the middle Pleistocene sequence. The crown of the tooth is widely impacted by wearing and carries that limit taxonomic inferences. The study of the three upper archaeological assemblages shows that the cave was recurrently occupied by humans of early Middle Paleolithic cultures. These assemblages recall by some traits sub-contemporary assemblages known in the Caucasus and the Levant but also the later Middle Paleolithic of the Zagros. The faunal assemblage is mainly composed with horse's remains. The remains are very fragmented and show numerous anthropogenic stigmata that indicate important butchery activities on site. From a large regional and chronological perspective, these findings make Qaleh Kurd Cave a key site for the knowledge of early human settlements and dispersals between the Levant and Asia.

Keywords: Iranian Central Plateau, Hominin, Middle Pleistocene, Paleolithic, Qaleh Kurd Cave, Qazvin

Introduction

The Iranian Central Plateau (ICP1) with the Alborz and the Zagros Mountains is located at the crossroads of two vast regions: the Levant and the Caucasus to the west, and Central Asia and East Asia to the east. These two regions have yielded numerous archaeological assemblages in chrono-stratigraphic contexts. These assemblages are essential for investigating hominin biological and cultural diversity and dispersal during the Early and Middle Pleistocene between the Levant (e.g., Bar-Yosef, 1994; Bar-Yosef and Belfer-Cohen, 2001; Bar-Yosef and Meignen, 2001), Europe (e.g., Mihailović et al., 2022) and Asia (e.g., Dennell, 2008; Narasimhan et al., 2019; Finestone et al., 2022) (Fig. 1). These researches demonstrate that several hominin species have settled this large area during the Middle Pleistocene, some of which may have interacted: late *Homo erectus*, Denisovans, Neanderthals and *Homo sapiens* in the east (e.g., Chen et al., 2019; Jacobs et al., 2019; Pan et al., 2020; Finestone et al., 2022; Han et al., 2022) and in the west, Neanderthals, *Homo sapiens* and possibly other species (e.g., Mercier and Valladas, 2003; Hershkovitz et al., 2021). However, despite decades of field research in the ICP and its immediate surrounding areas (the Zagros and the Alborz), no archaeological assemblage related to the Early and Middle Pleistocene in a clear chronological and stratigraphic context has been reported in this vast region so far. The earliest assemblage in a clear stratigraphic and chronological context is dated of 80ka (Gareh Boof, Heydari et al., 2021). However, surface finds (such as Dehtal in the Southeast Zagros Mountains, Ganj Par in the Alborz Mountains and Kaftar Kouh of Ferdous in the Khorasan) as well as test excavations (such as Darband Cave in the Alborz Mountains) may advocate an early settlement of the region (e.g., Biglari and Shidrang, 2006; Biglari and Jahani, 2011; Sadraei et al., 2019, 2023; Biglari et al., 2014, 2023).

1 - The ICP is the large area surrounded by the Zagros Mountains to the west, the Alborz Mountains in the north, the Kopet Dagh Mountains in the east, and the central Iranian block (mainly the Lut Desert) in the south.

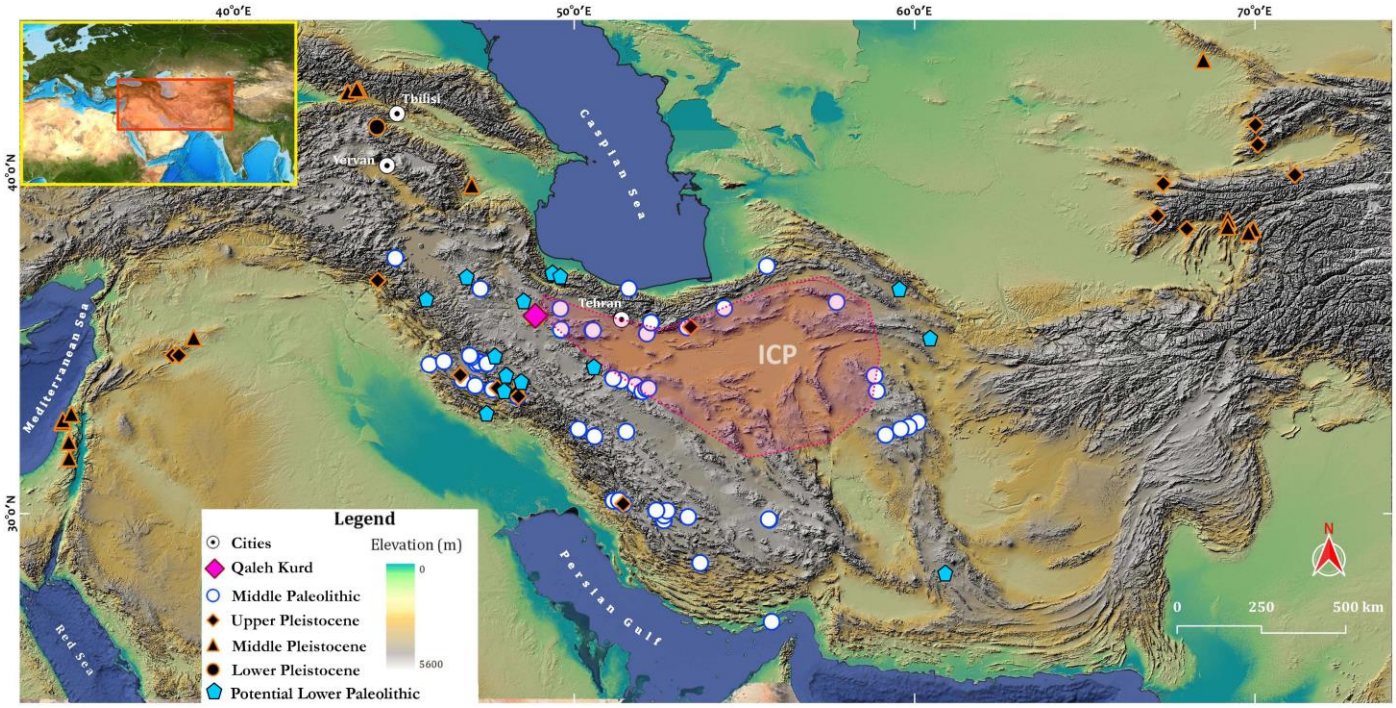

Figure 1. Location of the cave of Qaleh Kurd and the main Pleistocene archaeological sites of the Iranian Central Plateau (ICP) and surrounding areas, from the Levant to Central Asia (© M. Alirezazadeh, QGIS). ICP: the large area surrounded by the Zagros Mountains to the west, the Alborz Mountains in the north, the Kopet Dagh Mountains in the east, and the central Iranian block in the south.

In contrast, the Upper Pleistocene from the Zagros Mountains to the northern part of the ICP and the Alborz Mountains is relatively well documented by decades of excavations and discoveries. In the Zagros chain, they allow addressing the existence of local facies of Middle and Upper Paleolithic, and how the Upper Paleolithic originated (e.g., for early field works: Coon, 1951; Solecki, 1963; Braidwood et al., 1961; Hole and Flannery, 1967; McBurney, 1964; see Vahdati Nasab, 2010 for a synthesis; e.g., for more recent works: Otte et al., 2009, 2011, 2012; Jaubert et al., 2009; Tsanova, 2013; Shidrang et al., 2016; Bazgir et al., 2017; Becerra-Valdivia et al., 2017; Ghasidian et al., 2017, 2019; Heydari et al., 2021; Heydari-Guran et al., 2021). In the Northern part of the ICP and the Alborz chain, discoveries address the diversity of Middle and Upper Paleolithic cultures and their relationships to those of the Zagros (e.g., Chevrier et al., 2006; Berillon et al., 2016; Bonilauri et al., 2019; Vahdati Nasab et al., 2019). These debates are also supported by numerous surface finds, from the Zagros Mountains (e.g., Roustaei et al., 2004), the Alborz chain (e.g., Biglari and Jahani, 2011), the northern ICP (e.g.,

Vahdati Nasab and Clark, 2014; Vahdati Nasab and Hashemi, 2016; Hariryan et al., 2021) to the eastern ICP (e.g., Nikzad et al., 2015). Finally, in a broader context, including the Caucasus and Central Asia, these decades of discoveries demonstrate the significance of the ICP and surrounding areas as a dispersal corridor for hominin populations during the Upper Pleistocene (e.g., Vahdati Nasab et al., 2013; Shoaee et al., 2021; Ghasidian et al., 2023).

From the paleoanthropological point of view, human remains are scarce in the ICP, the Zagros Mountains and the Alborz Mountains, and they are all related to the Upper Pleistocene so far. The Neanderthals at Shanidar cave represent a large palaeoanthropological assemblage in a Middle Paleolithic archaeological context (Solecki, 1959; Trinkaus, 1983). The other human fossils consist in isolated bones and teeth: the right radius proximal diaphysis at Bisitun rock shelter (Trinkaus and Biglari, 2006), a deciduous canine at Bawa Yawan (Heydari-Guran et al., 2021), an isolated unerupted P3 at Wezmeh 1 (Trinkaus et al., 2008; Zanolli et al., 2019). Finally, one possibly Upper Paleolithic modern human lower molar was reported at Eshkaft-e Gavi (Scott and Marean, 2009) as well as nine specimens from the Epipaleolithic sequence. Such scarcity in Upper Pleistocene human remains in this wide area, contrasts with the paleoanthropological corpus in the Levant (e.g., Tobias, 1966; Vandermeersch, 1981; Hershkovitz et al., 2021), the Caucasus (e.g., Vekua et al., 2002; Ferring et al., 2011; Vasilyev and Amirkhanov, 2018), Central and East Asia (e.g., Glantz et al., 2008; Glantz, 2010; e.g., Reich et al., 2010; Chen et al., 2019). This corpus represents several human species dated from the Lower Pleistocene to the Upper Pleistocene.

In this context, the Joint Iranian and French Paleoanthropological Project reinvestigated the cave of Qaleh Kurd (Qazvin). Located at the western edge of the ICP and its boundary with the Zagros (Fig. 1), its potential prehistoric significance was recently demonstrated (Soleymani and Alibaigi, 2018). Here we report on the discovery of *in situ* Middle Pleistocene archaeological assemblages, including a human deciduous tooth associated with a rich lithic and faunal material, and the first description of the chrono-stratigraphic framework of the deposits.

The Qaleh Kurd Cave and excavation methodology

Qaleh Kurd cave (35°47'50"N 48°51'26"E) is located near the village of Qaleh Kurd (Avaj district) at the northwestern limit of the ICP, in the southwestern boundaries of Qazvin province. The cave belongs to a wide karstic network that developed in the Oligo-Miocene Qom Formation (Fig. 2) (Mehterian et al., 2017). The entrance of the cave opens at 2137m. It faces toward the southwest, and is located 140m above a seasonal creek that follows the valley. The archeological deposits are preserved in two chambers (Fig. 2): the main chamber of the cave that is 8m wide, 6m high, and 20m long (maximum dimensions) and oriented south-east-northwest, and at the back, a narrow corridor of 12m length and 1.5m high on average that deviates toward the west.

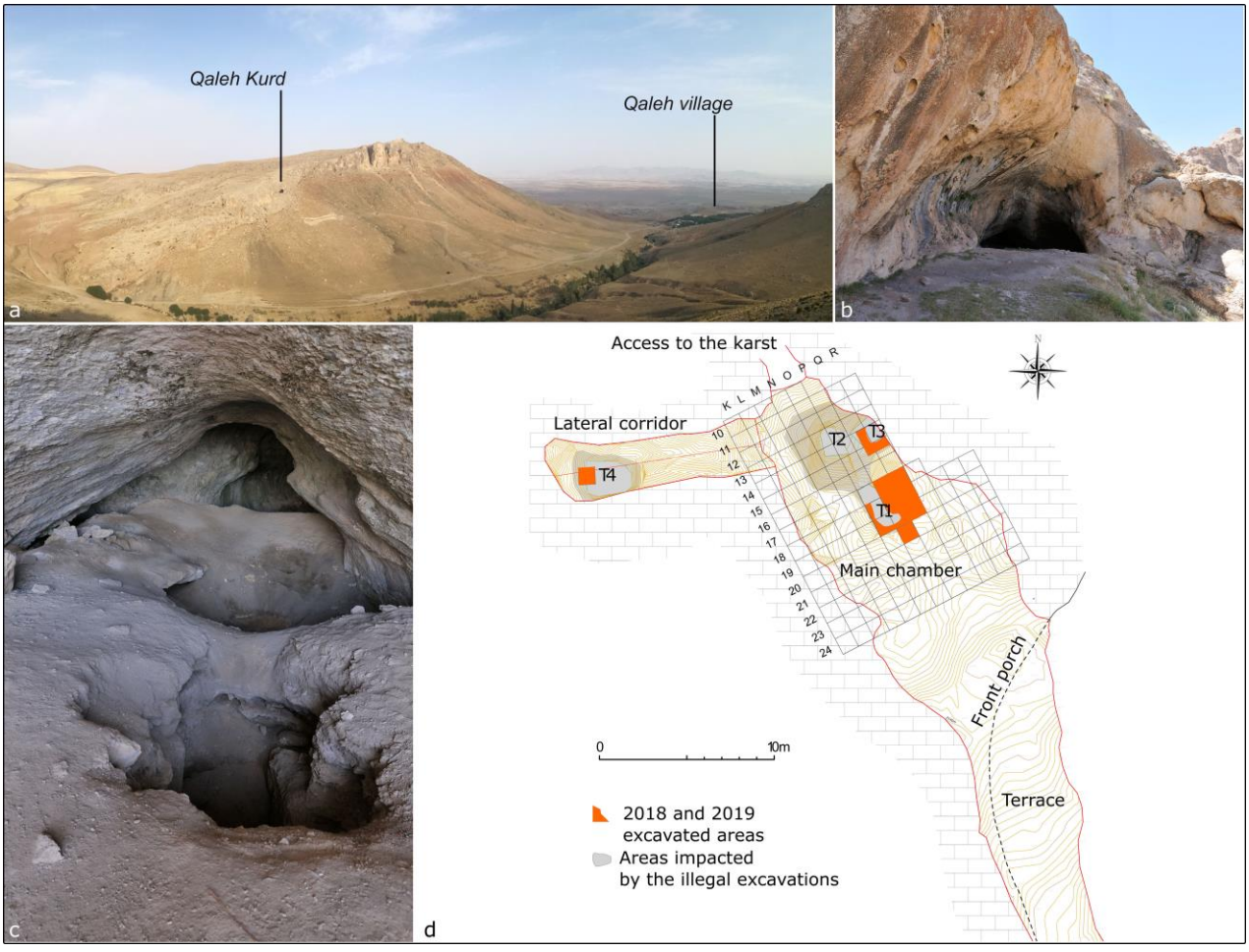

Figure 2. The Qaleh Kurd cave: Context, mapping and excavated areas. The Qaleh Kurd Valley (a); the entrance (b) and the damages visible in the main chamber (c) at the time of first visit by the joint Iranian and French team; mapping of the cave and the excavated areas (d) (© FIPP 2019).

The Qaleh Kurd cave is originally known among the cavers for its active karstic network and calcareous concretions. S. Alibaigi noticed its archaeological potential in 2011. Surface lithic artefacts were then collected and analyzed by Soleymani and Alibaigi (2018). Based on Middle Paleolithic diagnostics (e.g., the presence of Mousterian and Levalloisian artifacts), they proposed similarities with the surface Middle Paleolithic assemblage of Mirak known in the northern ICP (Vahdati Nasab et al., 2013). Qaleh Kurd cave has also been investigated for oxygen isotopes based palaeoclimatic reconstruction of the last Interglacial and early glacial periods (73–127ka) and early Holocene (6500–7500 BP) (Mehterian et al. 2017). At the time we reinvestigated Qaleh Kurd, the deposits had been extensively damaged by recent illegal human activities. Four large clandestine pits revealed a stratigraphy of at least 2.5m depth, including Paleolithic archaeological deposits with well-preserved faunal remains and lithic artifacts.

The excavations allowed to investigate the nature of archaeological deposits and their chrono-stratigraphic context. For some preservation and safety reasons, the excavation strategy was adapted to the presence of the clandestine pits. Indeed, they largely affected the deposit of the main chamber on a surface of 25m² and 2.5m in depth. We first dry-sieved the whole reworked sediment next to the pits; several thousand objects were collected in this reworked sediment. We then initiated the excavation by enlarging two pits located in the main chambers (labelled Trench 1 T1 and Trench 3 T3, see Fig.2). The excavation was then conducted by m² following the stratigraphic main units and 3D referencing the archaeological finds. A total area of 11m² and an average depth of 130cm were excavated in T1 and 250cm in T3; trench 4 (T4) was additionally prepared for ongoing geological investigation. The whole excavated sediments underwent dry and wet sieving using 1mm mesh sizes in order to collect microfauna, small chips, and debris.

Depositional setting and chrono-stratigraphic framework of Qaleh Kurd

The Qaleh Kurd stratigraphic sequence

The excavations enabled us to observe the stratigraphy of the deposits in three trenches. Concerning T4, deposits at the bottom take the form of broad, wedge-shaped sheets characteristic of secondary deposits. Some of these

sheets have also been extensively reworked in a second step by recent human activities. Concerning T1 and T3, Figure 3 and Table 1 provide a synthesis of the results of the fieldwork analysis of the deposits, auger drilling, and laboratory analyses (including grains size analysis, micromorphology; see SI1). These analyses reveal a sedimentary succession represented by a 6 m-thick karstic and clastic record made up of two sequences: Sequence I and Sequence II, separated by a discontinuity (an incision surface and limestone blocks). The deposits are in the form of centimetric to decimetric-thick sheets. These sheets correspond to laterally non-continuous units (unit numbers are proper to each section). Descriptions of the units are given in SI2 for T3 (where the excavation reaches is maximum depth and the sequence is observed continuously). Correlations have been made secondarily based on field and sedimentological data (see Table 1).

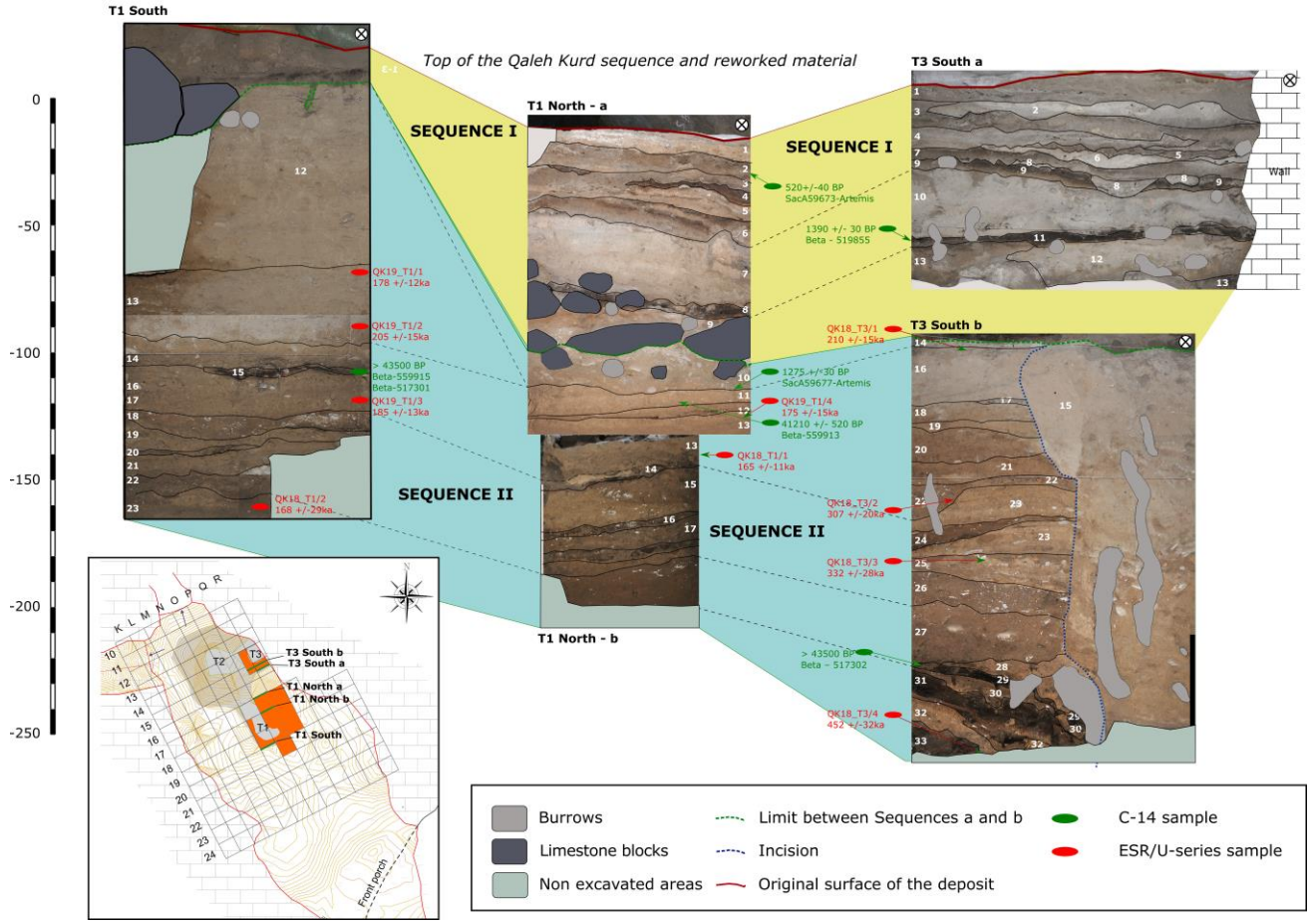

Figure 3. Synthetic stratigraphy of the Qaleh Kurd sequence and chronological data. (Full page, landscape) (© G. Berillon, J.-J. Bahain, M. Akhavan Kharazian and G. Jamet).

Table 1 – Simplified stratigraphic succession of the Qaleh Kurd deposits (See SI2 for the description of the units).

QALEH KURD SEQUENCE	T1 southern section	T1 northern section	T3 southern section	Proposed age
SEQUENCE I	T1S U1-3	T1N U1-6	T 3 U 1-9	Holocene
		T1N U 7-8	T3 U 10-13	
		T1N U 9		
SEQUENCE II	T1S U12-13	T1N U10	T3 U14-15	Late Pleistocene??
	T1S U14-16	T1N U11-13	T3 U16-21	MIS 7-6
	T1S U17-21	T1N U14- 17	T3 U22-26	MIS 9
	T1S U22-23		T3 U27	??
			T3 U28-33	MIS12-11

Sequence I consists of 8 units (1–8) in T1 (Northern Section, where it is best preserved) and 13 units (1–13) in T3. Its thickness varies laterally; from high in T3 and the northern T1 section (80cm on average) it thins towards the entrance of the cave on the southern T1 section (10cm). Sequence I exhibits a granular to massive structure. It contains predominantly whitish-grey ashy silt-sized sediments with episodical occurrence of cobbly to gravelly erosional surfaces and local calcareous flat stones, with inclusions of dark humic lenses. Anthropogenic components are frequent, such as shepherd deposits (charcoals, spherulites, animal dung, ashy remains, and occasionally pot fragments). The boundary with sequence II corresponds to a roof- and/or wall-collapse deposit (Units 9 and 10 in T1 northern section, unit 13 in T3) that is characterized by angular to subangular calcareous clasts of varying sizes, from gravel to large blocks.

Sequence II consists of a ca. 170 cm-thick deposit in both trenches; its basis has not been reached yet. It was subdivided into 12 units (12–23) in T1 (Southern Section, where it is best preserved) and 20 units (14–33) in T3. It is composed mainly of silt-sized material and displays a generally slightly granular to massive structure. Micromorphological traits, such as strongly degraded calcic clasts reduced to very coarse sand (as observed in Unit 15), are indicative of post-depositional alterations of the units linked to fluctuating seasonal temperature and water levels in the karst. This sequence has also recorded several cryoclastic episodes (e.g., Unit 15 in the Northern T1 section, within Units 13, 26 and 27 in T3) and display lenticular humic silty layers (e.g., Unit 17, 20, 22, 24 in Upper Sequence II of T3). Humic lenses are also numerous in the lowest units of T3 as well (Units 29, 31, 33) where they superimposed with lenticular gravelly silt layers. These humic lenses contain abundant

charcoal, heated bones and vegetal remains. They could represent paleosoils and may be in relation with anthropic activities. These traits are indicative of a long time-range deposition.

Generally speaking, sequence II delivered numerous archaeological levels and remains, including the human deciduous tooth recovered in the upper part of Unit 13, close to the T1 Northern section. The upper units of sequence II appear truncated from the entrance to the back of the chamber. Together with the roof-collapse episode with large blocks (units 9 and 10 of the T1 northern section), this indicates a major sedimentary hiatus between sequences I and II.

Chronology of the Sequences based on AMS and ESR/U-series dating

Numerous samples were collected for chronological analysis. The obtained ages, when applicable, are provided in Figure 3. Concerning Sequence I, two radiocarbon dates were obtained on organic sediments and micro-charcoals from the lower and upper units, which provided ages of 1390 +/- 30 BP (Beta-519855) and 520 +/-40 BP (SacA59673). Such recent dates are in agreement with the general composition of the collected archaeological assemblages and sediments, indicating the recent nature of the sequence.

Concerning Sequence II, five samples of organic sediments from the upper to the lower units were analysed by radiocarbon and provided an age above the limit of the AMS method (> 43500 BP). In parallel, 10 equid teeth were also sampled for C14 analysis, but the low collagen content made it impossible to attempt any radiocarbon dating. They were then used for analysis by the ESR/U-series dating method using the analytical protocol described by Bahain et al. (2021) and detailed in SI3. The obtained results are displayed in Table 2 and Figure 4. They range from 205 ± 15 ka to 165 ± 11 ka in T1, and from 452 ± 32 to 210 ± 15 ka in T3. These results allow assigning the whole sequence II to the Middle Pleistocene and a period that spans at least 300 ka.

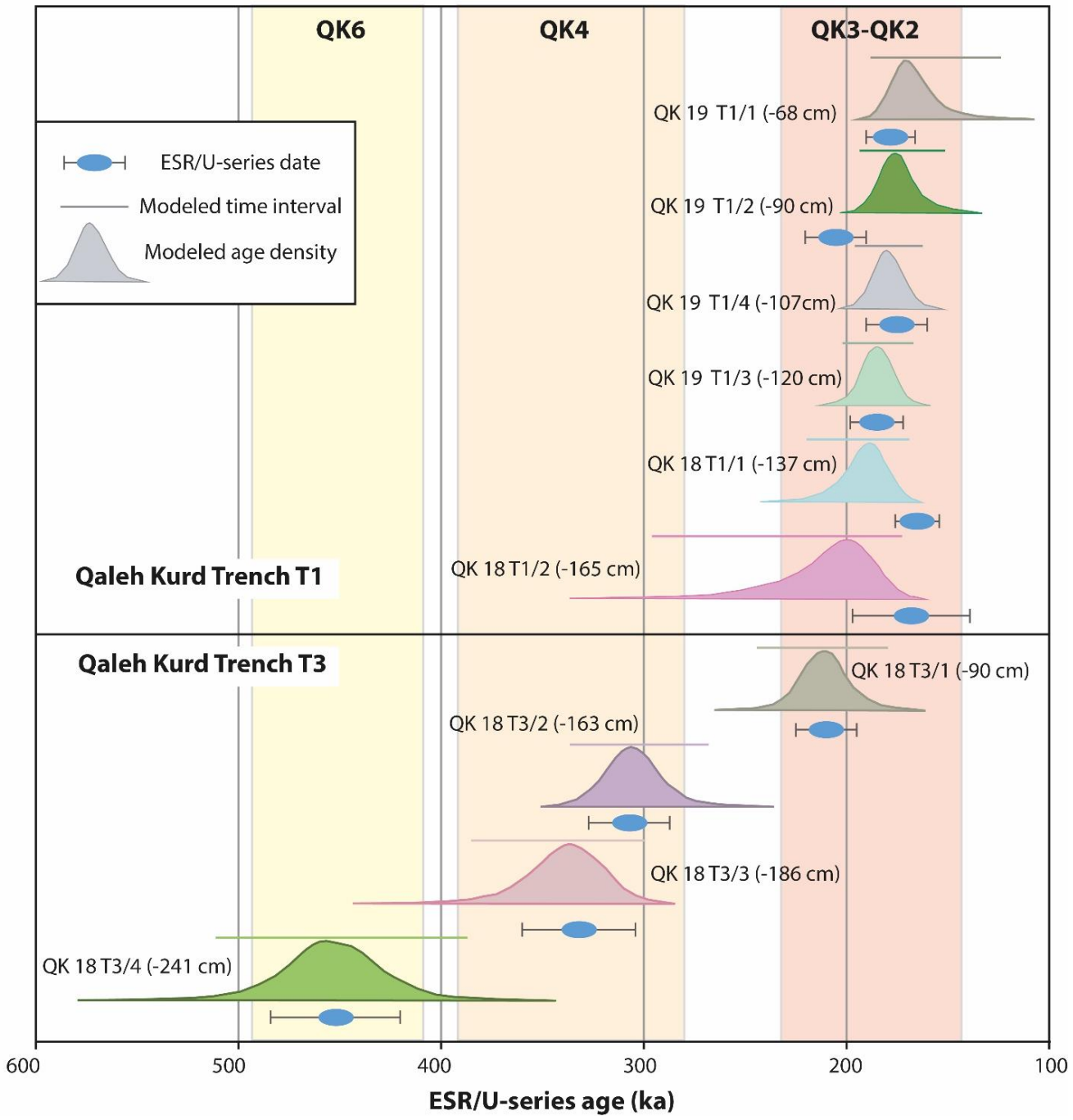

220

221 Figure 4. Bayesian model (Chnonomodel, 95% of confidence) of the ESR/U-series ages obtained on analyzed

222 Qaleh Kurd teeth. (© J.-J. Bahain).

Table 2 – ESR/U-series ages of the analyzed Qaleh Kurd teeth. Uncertainties are given at 2 σ (95% of confidence).

Samples (laboratory number)	Samples (Excavation number)	Trench	Unit	Depth	ESR/U-series ages (ka)
QK19 T1/1	Tooth n°5118	T1	12	-68cm	178 ± 12
QK19 T1/2	Tooth n°5353	T1	15	-90cm	205 ± 15
QK19 T1/4	Tooth n°4895	T1	13	-107cm	175 ± 15
QK19 T1/3	Tooth n°6158	T1	23	-120cm	185 ± 13
QK18 T1/1	Tooth n°2381	T1	C3	-137cm	165 ± 11
QK18 T1/2	Tooth n°2500	T1	C4	-165cm	168 ± 29
QK18 T3/1	Tooth n°495	T3	C1	-90cm	210 ± 15
QK18 T3/2	Tooth n°3148	T3	C1	-163cm	307 ± 20
QK18 T3/3	Tooth n°3310	T3	C1	-186cm	332 ± 28
QK18 T3/4	Tooth n°1721	T3	C1	-241cm	452 ± 32

Context and history of the deposits

The stratigraphic and sedimentary characteristics of Sequence II support the idea of low-energy sheet deposits in which seasonal temperature variations as well as human activities played an important role. Some features indicate contrasted climatic conditions along the sequence with colder periods marked by cryoclastic deposits and more temperate ones, marked by humic deposits. These humic deposits may represent palaeosoils and may be in relation with anthropic activities (see above). According with the ESR/U-series chronology, these climatic changes can correspond to the local record of the late Middle Pleistocene climatic cyclicity. This first phase of sedimentation started prior 450ka and lasted at least 300 ka. It seems to have ended during the late Middle Pleistocene. No further deposits were recorded until the late Holocene (around 1.5 ka).

This long sedimentary gap between Sequence II and Sequence I could be linked to the closure of the cave leading a decrease in sedimentation or karstic processes within the cave, as well as the end of anthropic activities. The top part of the Pleistocene sequence (T1 South) in the central current main chamber has been eroded. No data is available so far to date this event precisely and to address its possible natural causes, yet recent human activities cannot be excluded. The cave opened up during the last two millennia. A level of

gelifracts and large blocks that presumably collapsed from the ceiling, covers the eroded Pleistocene sequence in this area; it seems to signify the restart of sedimentation. The cave has since been used by humans.

The archaeological assemblages

The archaeological levels

Excavations at T1 and T3 yielded more than 5800 *in situ* finds, within which around 2/3 are large mammals' bones and teeth, 1/3 are lithic artifacts, and one is a human tooth. Figure 5 represents the vertical distribution of the finds in both trenches across the whole sequence. Sequence I delivered isolated remains, mainly pottery fragments and remains of wild and domesticated animals. Isolated artifacts of Paleolithic affinities were also collected in reworked contexts, such as animal burrows or the units 8–10 of T1 at the contact of the collapsed rocks.

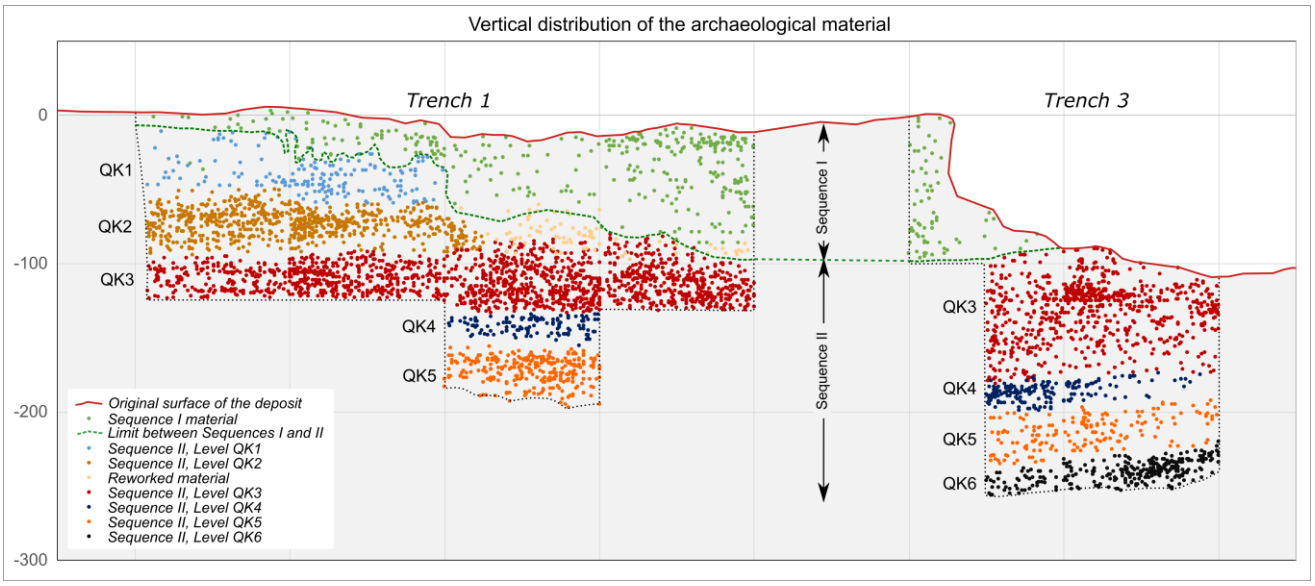

Figure 5. Vertical distribution from South to North of the *in situ* collected archaeological material in Trench 1 and Trench 3 of Qaleh Kurd (© G. Berillon, M. Hashemi and H. Vahdati Nasab). Full page, landscape.

In sequence II, finds are distributed in at least six archaeological levels, named QK1 to QK6, from the top of the sequence in T1 (around 10cm in depth) at the entrance of the cave until the deepest excavated area in T3 (around 250 cm in depth). Archaeological levels extend sub-horizontally, with a depth of several decimeters. Both lithics

and faunal materials show fresh ridges and are very well preserved. The fauna is locally covered with carbonated encrustation. The upper part of sequence II (until 90cm depth) is preserved in the southern half of T1 only where the deposits have not been incised (see above). QK1 appears largely impacted by animals' burrows and as a consequence, appears fragmented with a low average density of objects. QK2 could be observed in the southern part of T1 only as well, while QK3 was preserved in all excavated areas of T1. The lower material has been allocated to at least 3 levels, QK4 to QK6. These lower deposits could be observed on a very limited surface; these allocations thus need to be improved based on new excavations. The bottom of the sequence has not been reached by the excavations. Auger drillings down to the depths of 6m in both T1 and T3 indicates that older archaeological layers are preserved in the non-excavated part of the sequence (at least 3m depth).

The deciduous human tooth

A human deciduous left first upper molar (n°QK19-6169) was discovered in Trench 1, square R17, at a depth of 105cm. This tooth was deposited in unit 13 (Section T1 North). It belongs to the upper half of the QK3 level that spreads from unit 13 to unit 16 of the stratigraphy (Section T1 North). The current chronological framework places thus this human tooth between 205 ± 15 ka and 165 ± 11 ka. Here we present the preliminary results of the analysis of this tooth.

The morphology of the tooth is widely impacted by wearing, root resorption and carries (Fig. 6). In occlusal view, the outline of the crown is trapezoidal and asymmetrical. The occlusal surface of the crown shows extensive wear (stage 5) (Molnar, 1971); only a small chip of enamel is preserved and no cuspid can be identified. At the mesial and distal levels, the crown is affected by two large millimetric lacunae, from the enamel to the dentine; the largest (mesial) communicates with the pulp cavity. Both lacunae appear to be caries: the edges and inner surfaces are smooth, and neither enamel nor dentine show any signs of abrasion or breakage. The resorption of the root appears almost achieved with some remaining flaps at the vestibular and linguo-distal borders. The state of resorption of the root suggests that this tooth was close to be shed if not shed naturally during the child's life; by way of comparison, in modern humans, this upper first molar (if not been shed) would came from a child around the age of 11 (AlQahtani et al., 2014). However, the life history evolution may be

dissociated with the timing of tooth eruption within hominins; if the tooth represents for example a Neanderthal or an archaic *Homo sapiens* then the individual was probably younger (e.g., Smith et al., 2007). Such degrees of crown wear and root resorption suggest that the tooth may have been functional for a long period of time.

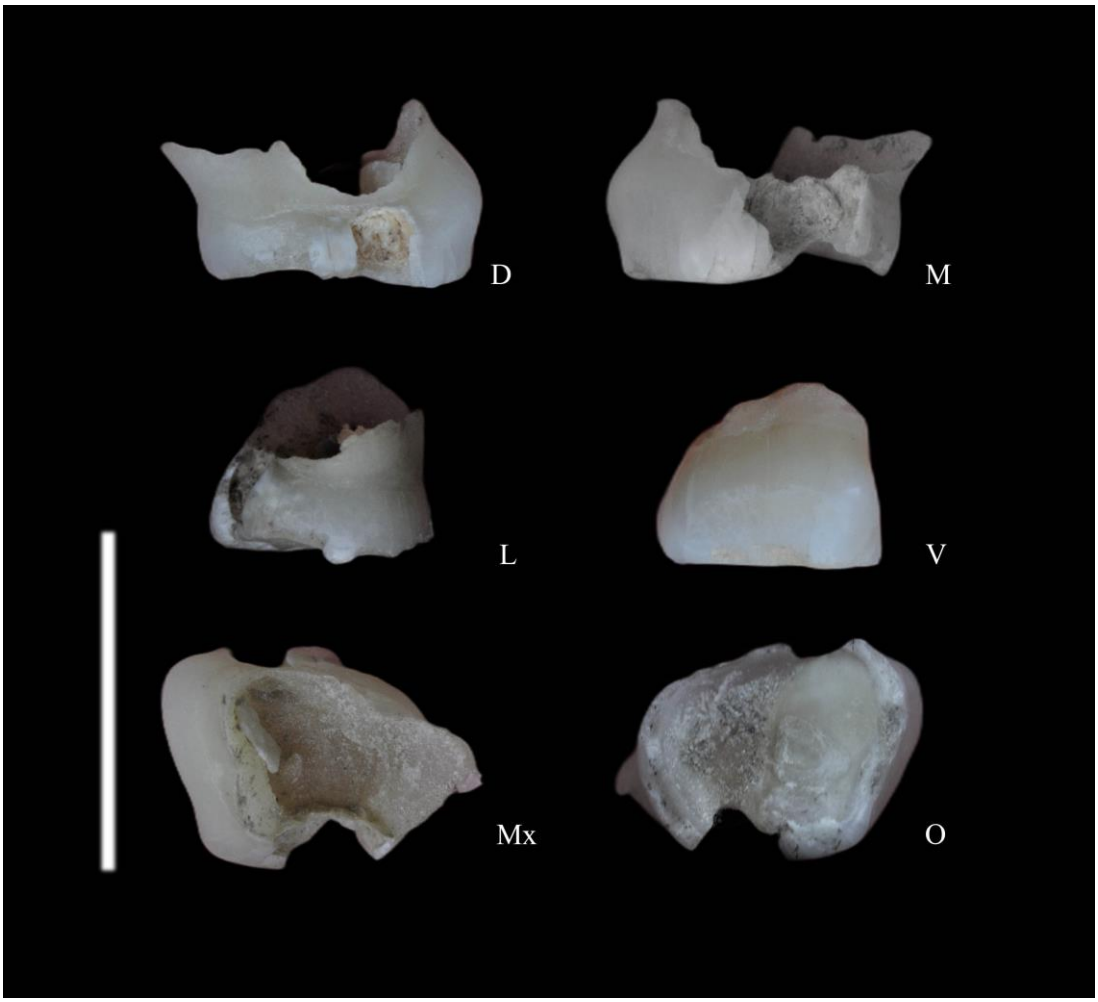

Figure 6. The human deciduous first upper left molar QK19-6169 in distal (D), mesial (M), lingual (L), vestibular (V), occlusal (O) and maxillary (Mx) views (scale, 10mm). (© FIPP 2019, G. Berillon).

A prominent *tuberculum molare* is observed at the mesiodistal corner that accentuates the asymmetrical shape of the crown in occlusal view. *Tuberculum molare* is a trait variably observed or described in archaic humans, Neanderthals and modern humans, including extant humans. By way of comparison, it is well developed in archaic humans such as Tighenif, Le Lazaret 12 and 27 and Arago 27 and moderate on Arago 12 (Tillier, 1980;

Lumley de, 2018, 2022). It is also well-developed in Neanderthals such as Shanidar 7, Chateauneuf 2 (Tillier, 1979a, Trinkaus, 1983) and Pech de l'Azé (personal observation), as well as in early *Homo sapiens* such as Qafzeh 12 and 4 (Tillier, 1979b, 1999), while it is moderate to absent on Kebara KMH25, KMH30, KMH1 and Subalyuk (Thoma, 1963; Tillier et al., 2003), as well as in Qafzeh 14, 10 and 15 (Tillier, 1999). The occurrence of a *tuberculum molare* and its prominence naturally affect the shape of the crown. In general, the outline of the crown is highly variable in archaic humans, Neanderthals and early modern humans, from elongated to quadrangular and trapezoidal, from symmetrical to asymmetrical (see above references).

The mesiodistal diameter being affected by the caries has a minimal value of 6.1mm, thus below the distributions of modern humans (European Upper Paleolithic and Near Eastern modern humans) and Neanderthals (see e.g. Becam and Chevalier, 2019 and Tillier, 1999: 6.4–9.5 mm MH and 7.1–11 mm NEA; and comparative metrics in table SI4). However, it is very likely that its actual value would fall within the lower range of both species. The buccolingual diameter is 7.2mm and falls within the lower range of the known variation for Neanderthals and below that of modern humans (see Becam and Chevalier, 2019 and Tillier, 1979a: 7.4–9.6 mm MH and 6.8–9.9 mm NEA; see table SI4). The crown diameters of the Qaleh Kurd deciduous first upper molar fall within the lower range of the known variation of Middle and Upper Pleistocene humans.

In order to observe the endostructure of the tooth, a µCTScan has been performed at the Tehran University Medical Science Preclinical Core Facility (LOTUS-inVivo µCtScan, Behin Negareh Company). A 3D reconstruction was carried out on 17.5µm-thick sections (Fig. 7). The 3D reconstructed model shows that the important crown wear and both caries deeply affect the enamel-dentin junction. The pulp cavity appears as well profoundly affected by the whole resorption process. As a consequence, reproducible measurement and morphological inference as well as quantified analyses cannot be realized as done on better preserved specimens (e.g., Fornai et al., 2014; Slimak et al., 2022).

In summary, the high degree of wear on the crown and the presence of two large caries significantly affect the morphology of the tooth, impacting the metrics and potentially taxonomically informative traits.

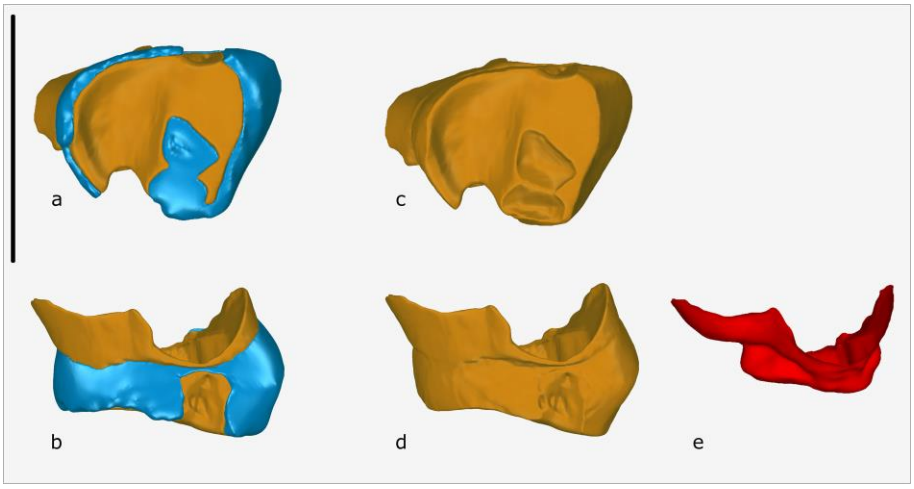

Figure 7. 3D reconstruction of the enamel (in blue), the dentine (in brown) and the pulpar cavity of the human deciduous first upper left molar QK19-6169 in occlusal (a, c) and distal (b, d, e) views (scale, 10mm). (© J. Özçelebi).

The Lithic assemblages, QK1-3

The three upper levels (QK1-3) are directly associated with the human tooth and could be observed in T1 on a large surface (contrary to the lower deposits that were excavated on less than 1m²) (Fig. 2). In total, the QK1-3 assemblages on which we focus here count for 2145 pieces of lithic artifacts collected *in-situ*.

The percentages of different raw materials is shown in Table 3. Raw materials in QK1–3 are mainly represented by sedimentary rocks comprising limestone and silicified limestone (64.3%), the chert category (24.9%, including chert and jasper, as well as flint and agate), radiolarite (1%), siltstone and sandstone (1%), and others (1.25%). Volcanic (igneous) rocks (including tuff and lithified pyroclastic debris, as well as basalt, andesite, dacite, rhyolite, and rhyodacite in very low proportions) make up about 4.68% of the assemblage. Quartzite was also used for making some few pieces (0.7%).

335 Table 3 – Lithic raw materials at Qaleh Kurd levels QK1-3.

Raw material	QK1		QK2		QK3	
	N	%	N	%	N	%
Limestone	6	31.58	16	26.23	131	40.18
Silicified limestone	5	26.32	19	31.15	84	25.77
Chert	6	31.58	4	6.56	56	17.18
Jasper	1	5.26	5	8.20	8	2.45
Quartzite	1	5.26			2	0.61
Flint			6	9.84	14	4.29
Tuff			4	6.56	5	1.53
Pyroclastic			1	1.64		0.00
Igneous			2	3.28	6	1.84
Silicified stone			2	3.28	7	2.15
Radiolarite			2	3.28	2	0.61
Dolomite					1	0.31
Andesite					1	0.31
Calcareous tufa					1	0.31
Agate					1	0.31
Bio Micrite					1	0.31
Siltstone					3	0.92
Sandstone					1	0.31
Opal					2	0.61
Total	**19**	**100**	**61**	**100**	**326**	**100**

336

337

338

Table 4. General techno-typological summary for QK1–3.

QK1	#	%	QK2	#	%	QK3	#	%	Total
Débitage	19	15.57	**Débitage**	149	59.60	**Débitage**	450	25.38	618
Tool	16	13.11	**Tool**	56	22.40	**Tool**	98	5.53	170
Core	-	-	**Core**	4	1.60	**Core**	11	0.62	15
Debris	87	71.31	**Debris**	28	11.20	**Debris**	1186	66.89	1301
Indeterminate	-	-	**Indeterminate**	13	5.20	**Indeterminate**	28	1.58	41
Total	122	100	**Total**	250	100	**Total**	1773	100	2145
Intensity of toolmaking		45.7	**Intensity of toolmaking**		27.3	**Intensity of toolmaking**		17.89	
Side scraper	3	18.75	**Side scraper**	19	33.93	**Side scraper**	26	27.08	
Mousterian Point	3	18.75	**Double side scraper**	8	14.29	**Double side scraper**	7	7.29	
simple retouched point	2	12.50	**Mousterian Point**	6	10.71	**Mousterian Point**	21	21.88	
Déjeté scraper	1	6.25	**simple retouched**	1	1.79	**simple retouched**	3	3.13	

			point			**point**		
Levallois point	1	6.25	**Levallois point**	2	3.57	**Levallois point**	5	5.21
Convergent Scraper	1	6.25	**Convergent Scraper**	6	10.71	**Convergent Scraper**	11	11.46
Endscraper	2	12.50	**Déjeté point**	1	1.79	**Déjeté point**	2	2.08
Retouched Piece	2	12.50	**Endscraper**	2	3.57	**Endscraper**	4	4.17
Other	1	6.25	**Retouched Piece**	10	17.86	**Retouched Piece**	13	13.54
Total	**16**	**100.00**	**Notched**	1	1.79	**Naturally backed knife**	1	1.04
			Total	**56**	**100.00**	**Notched**	1	1.04
						Multiple tool	2	2.08
						Total	**96**	**100.00**

The level QK1 is characterized by the production of large and elongated flakes, triangular flakes/points and, by laminar blanks. The removals were made by both non-Levallois and Levallois methods. The lithic assemblage is made up of 15.6% of débitage, 13.4% of tools and 71.3% of debris (Table 4). No core has been recovered from QK1. Flakes and blades represent 61.9% and 19% of the débitage respectively (Fig. 8). The predominance of flake production is also seen in the tool category: 68.7% of them are made on flakes, while 25% are made on blades. No bladelet tool was recorded from QK1. Elongated flakes (L/W ratio $\geqslant$ 1.5) make up about 45.4% of the flake blanks. The tool assemblage consists of simple side to transverse scrapers and retouched points. They are usually made on thick blanks, mainly with moderate to invasive retouch, and sometimes of invasive stepped types reminiscent of the Quina-type retouch (Fig. 9, g). Mousterian points are also present. Basal trimming of convergent tool types is common, perhaps for hafting purposes (Fig. 9, see b, d, f, j–l).

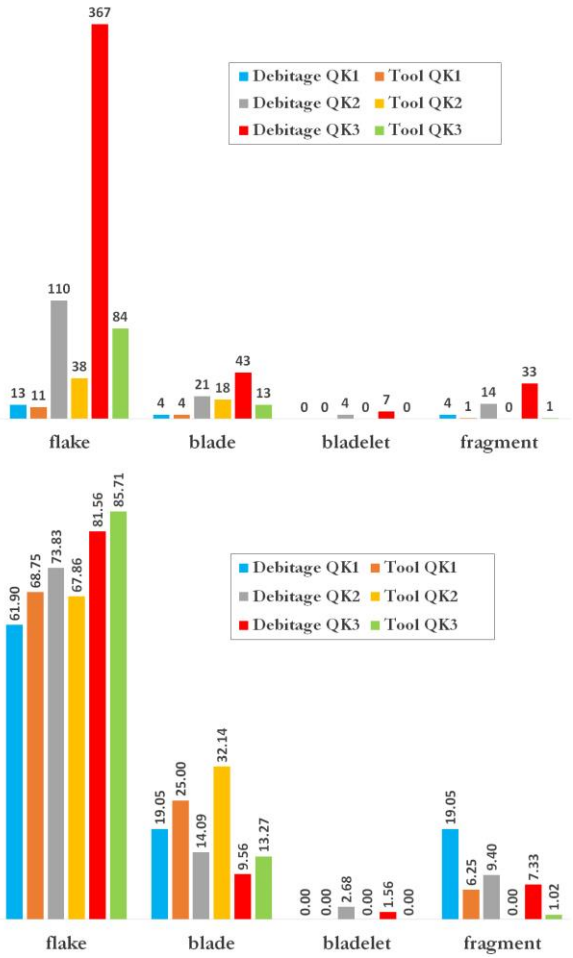

Figure 8. The composition of débitage and tools in QK1–3. Guide: the upper bar chart is based on absolute numbers, while the lower bar chart is based on percentages.

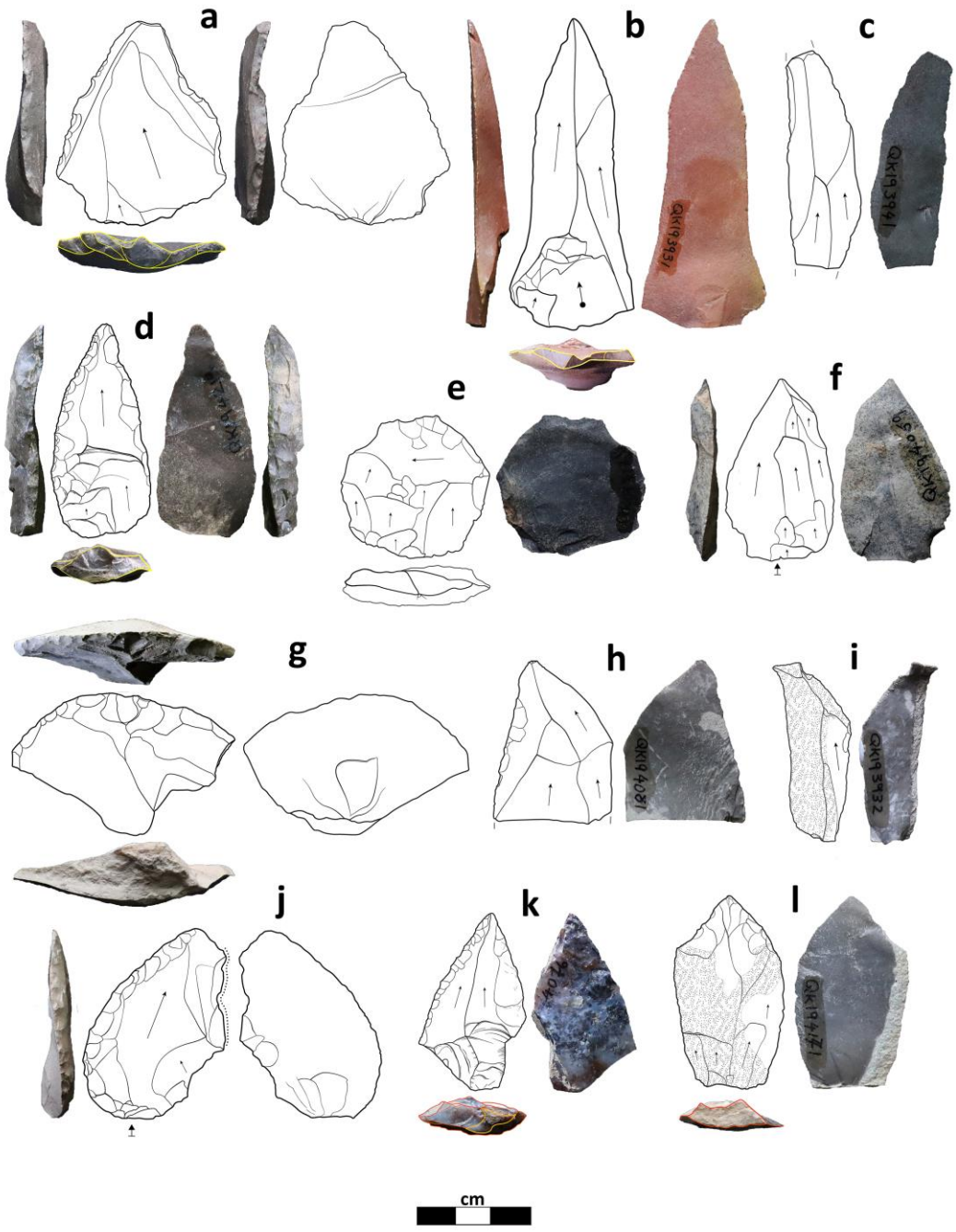

Figure 9. selected lithic artifacts from QK1. a. Retouched Levallois point; b. Pointed Levallois blade with basal thinning; c. Medial part of a blade; d. Mousterian point on an elongated thick flake with basal thinning; e. End scraper on a Levallois flake; f. point/subtriangular flake; g. Transverse scraper on a wide thick flake; h. distal part of a side-retouched piece; i. An atypical cortical plunging blade; j. Déjeté scraper; k. Mousterian point on a relatively elongated flake with basal thinning/chipping; l. Retouched point on an elongated flake. © M. Hashemi,

Full page.

The general structure of the QK2 lithic assemblage displays a mixed production of broad and elongated flakes, point or triangular flakes, and blades (Fig. 10), as in QK1. The débitage is made of both Levallois and non-Levallois, as well as laminar methods. Concerning the production of blanks, elongated varieties such as blades with convergent edges or elongated points, are more numerous here than the QK1. The assemblage is fairly retouched: more than 25% of the flakes and 46% of the blades. Cortical surfaces are observed in 27.7% of the lithics. The débitage accounts for 60% of the lithic assemblage while tools represent 22.4%. In addition to debris (11.2%), four cores were recovered in QK2. Flakes represent 73.8% of the débitage, while blades account for about 14.1% (Fig. 8). 67.9% of the tools are made on flake, and 32,1% are made on blade blanks. In addition, elongated flake blanks in QK2 are numerous (51.6%), higher than QK1.

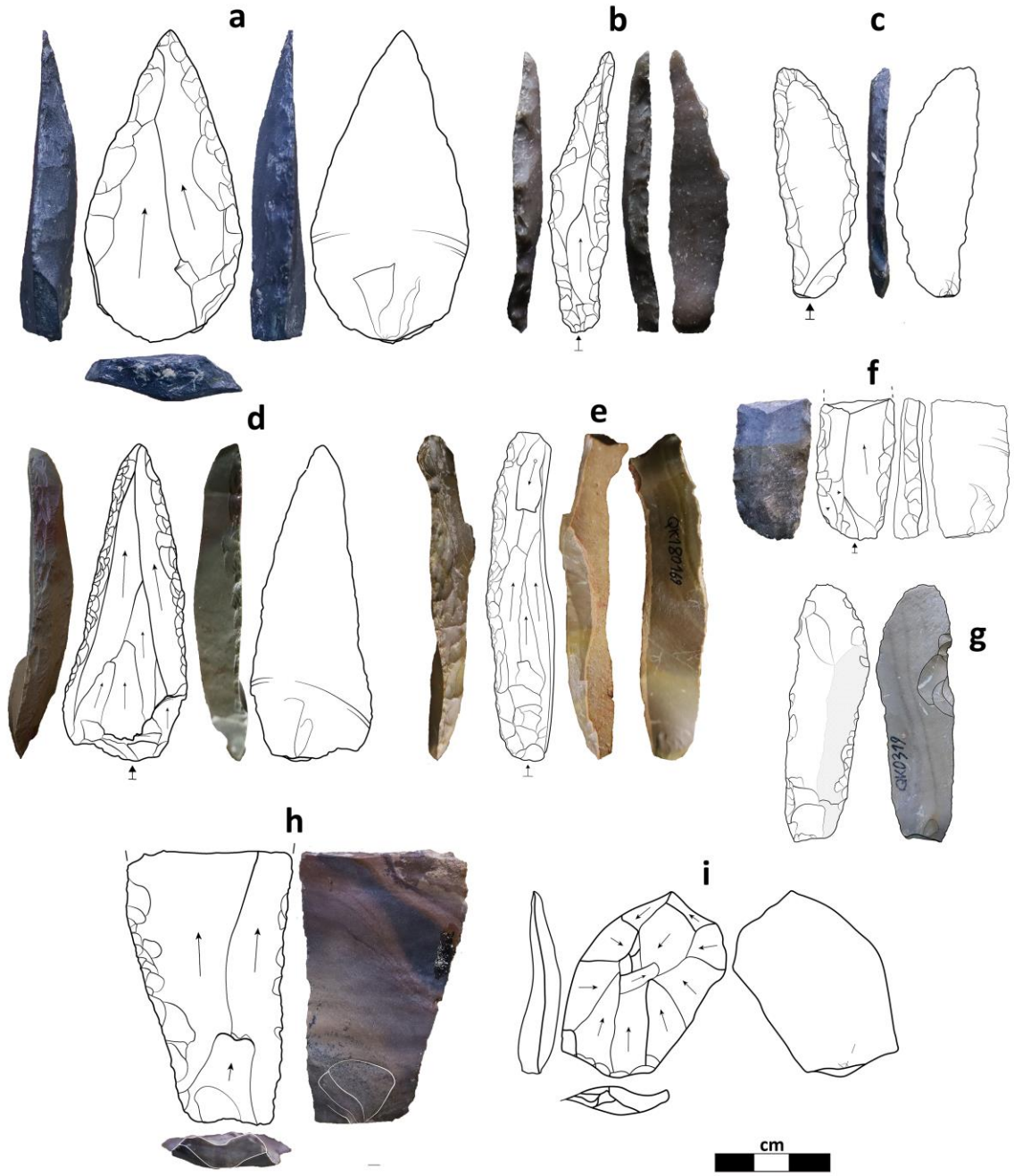

Figure 10. Selected lithic artifacts from QK2. a. Mousterian point on an elongated flake; b. Elongated point on an elongated thick blade with basal thinning; c. Double side and convergent scraper on a blade with basal chipping; d. Elongated Mousterian point with stepped retouch and basal thinning; e. Side scraper on an elongated narrow and thick cortical blade with stepped retouch; f. Double side scraper on a thick blade; g. Retouched piece made on a cortical blade with basal thinning; h. Side scraper with stepped retouch on a massive elongated flake or wide blade; i. A preferential Levallois flake with centripetal scars. © M. Hashemi.

QK3 is characterized by high occurrences of flakes and bulkier flakes and the presence of some large laminar products. Some of these laminar products were retouched to become pointed blades/elongated points (Fig. 11). The débitage is usually of non-Levallois design and laminar, which differ from the upper levels. A few signs of the discoid method are also discernible in QK3 (see the discoid core in Fig. 12a), albeit such a method is not common. The débitage accounts for 81,5% of flakes and about 9.5% of blades. 85.7% of the tools are made on flakes and 13.3% are made on blades (Fig. 8). Some bladelet débitage specimens have been recorded (as in QK2). Elongated flakes constitute 40.2% of the flake removals, and cortical pieces represent 18.9% of the lithics.

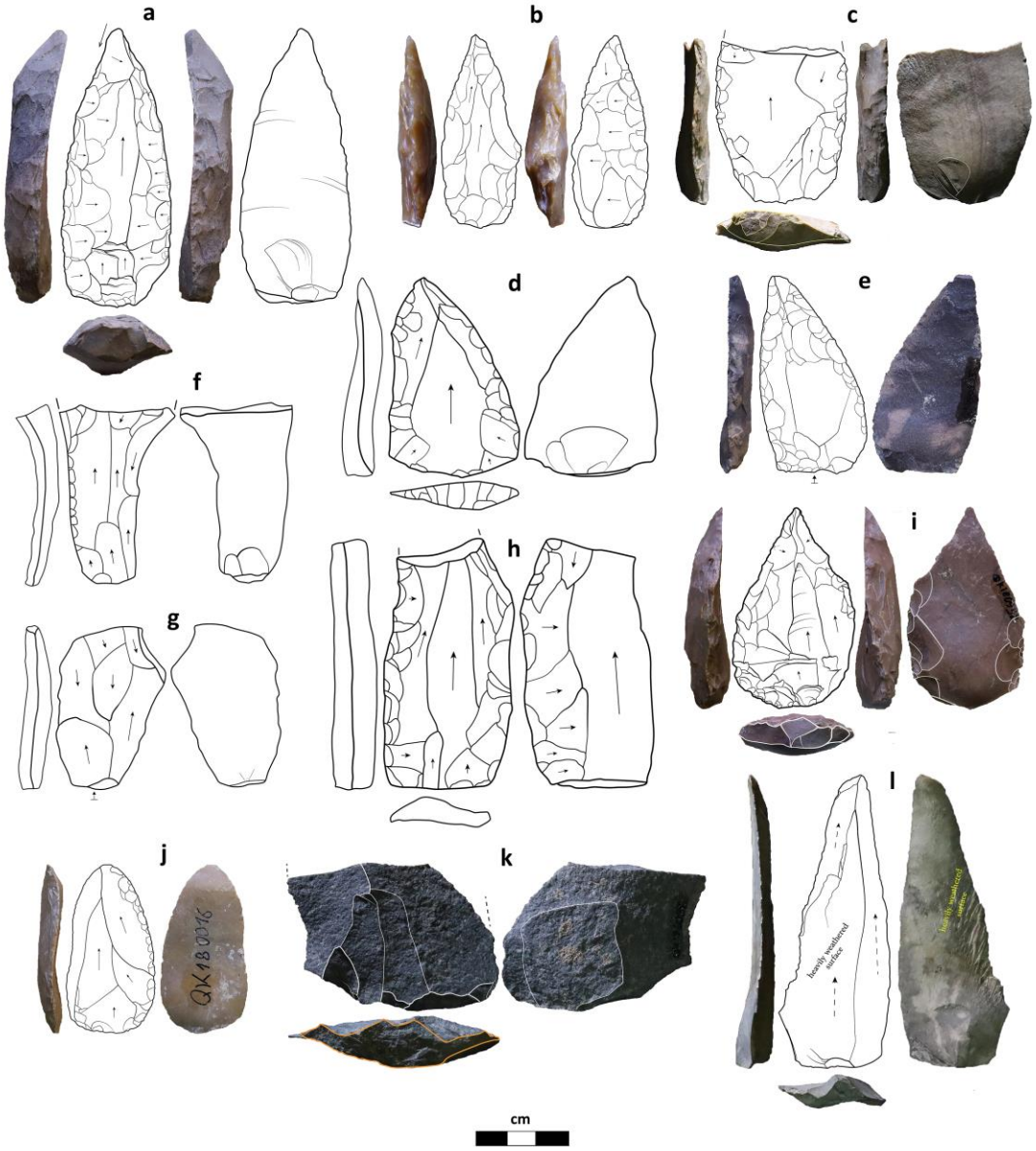

Figure 11. Selected lithic artifacts from QK3. a. Elongated Mousterian point with invasive stepped retouch on a massive elongated thick flake and with basal thinning; b. Bifacially retouched point on an elongated flake with invasive scaled-stepped retouch and ventral and basal thinning; c. Double side scraper (point?) on a massive elongated thick flake with basal thinning; d. Retouched Levallois point on a flake; e. Mousterian point with invasive scaled-stepped retouch and basal thinning (bifacially-thinned base); f. Retouched piece made on an atypical blade (laminar core trimming element of débitage surface; bidirectional opposed scheme); g. Core trimming flake (trimming of débitage surface, bidirectional scheme); h. Elongated Mousterian point made on an elongated thick flake or wide thick blade with basal and ventral thinning (invasive scaled-stepped retouch); i.

Mousterian point on a Levallois flake with invasive scaled-stepped retouch and basal-ventral thinning; j. Side scraper/retouched point on an elongated Levallois flake; k. Proximal part of an atypical massive flake; l. Elongated subtriangular flake/elongated point with (Levallois ?) with ventral nibbling in the left lateral side (not visible in the picture due to the weathering effect). © M. Hashemi.

Cores are mainly flake cores except one with mixed scars of flake-blade and one with blade scars (Figure 12). The complete cores are small (L≤4cm) to large (>7cm) in dimension in both QK2 and QK3. All cores are reduced using hard hammer technique. The number of core's negative scars range from one to two-digit flake scars (Figure 12a). The platforms are prepared both by a single blow or faceting. Most of the cores are atypical (amorphous); however, the assemblage counts also discoid cores, flat ones, Levallois cores, narrow-fronted platform cores, and core-on-flake (Figure 12). Levallois cores are recorded from both QK2 and QK3; both depict the two modes of preferential and recurrent débitage removal (Figure 12c, d). These cores usually show radial/centripetal preparations and none of them bear traces of advanced faceting for platform preparations.

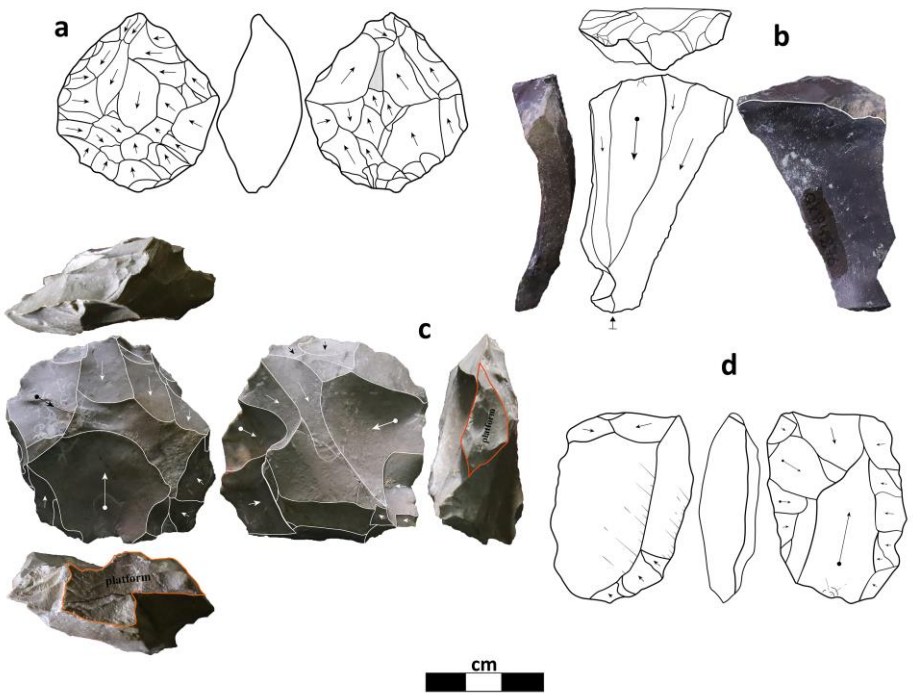

Figure 12. Lithic cores of Qaleh Kurd, Trench 1. QK2: a. discoid core; b. core-on-atypical blade with facetted platform of the core; c. recurrent Levallois core with centripetal preparation; QK3: d. preferential Levallois point core with centripetal preparation (Nubian type II core). © M. Hashemi.

The large mammal assemblages

Excavations at Qaleh Kurd delivered 4,014 faunal remains mostly in an excellent state of preservation, among which 1,886 pieces belong to large mammals. The sequence I has yielded 132 bone remains representing wild and domestic species of similar size. Cows (*Bos taurus*), sheep (*Ovis aries*), and domestic goats (*Capra hircus*) are identifiable. Small, undetermined bovids, which could be domestic or wild goats or sheep, are mainly represented by young individuals. Cutmarks made with metal knives and lithic industry attest to both recent and potentially older butchery activities.

The sequence II has yielded 1,465 *in-situ* teeth and bone remains. All long bones are fragmented pieces. As for the lithic assemblage, focus was made on the material from QK1 to QK3. Complementary observations were made on pieces from the lower levels regarding the represented taxa in the environment and the depth for time purposes. In total, nine taxa could be identified at gender or species level (Table 5), representing 408 remains (28,9 % of the total faunal material). The other remains are identified on a sub-level of gender, or undetermined. Large mammals are largely dominated by herbivores. Generally speaking, Equids represent the large majority of the fauna of each levels. At least 2 species are represented: a large horse (*Equus ferus)* (Fig. 13A) and the hydruntine (*Equus hydruntinus*), representing all age classes. The deer (*Cervus elaphus*) remains (Fig. 13D) are also common in all the deposits. Although the horse is largely dominant, some differences in faunal composition exist between levels.

QK1 yielded 123 remains, of which 26 have been identified at the species level, representing 5 taxa; each taxa is represented by a single individual (Table 5 and SI5a). The horse remains are represented by numerous pieces of limb bones and skull. The other identified species are the hydruntine, the red deer, the wild goat and the hare; they are represented by a few pieces. Marrow exploitation was particularly intense at this level, with 35.6% of the remains showing anthropogenic fractures (Fig. 14A). The stigmata visible on cortical surfaces (cutmarks,

scraping and retouch zones on bone tools) are also numerous (Fig. 13B). Their location and identification were first assessed macroscopically; when requested, we proceeded to microscopic observations using dino-lite. Carnivore trimming marks were observed on 7% of the material, which indicates a very low contribution of carnivores compared to humans in the deposit.

Table 5. Faunal list of Pleistocene levels at Qaleh Kurd

Archaeological levels	**QK1**		**QK2**		**QK3**		**QK4-6**		**TOTAL**	
	NR	%NISP	NR	%NISP	NR	%NISP	NR	%NISP	NR	%NISP
Stephanorhinus hemitoechus	-	-	-	-	-	-	1	7,7	1	0,3
Bos primigenius	-	-	1	0,7	3	1,3	-	-	4	1
Equus sp.	21	80,7	114	82,6	173	74,9	12	92,3	320	78,4
Equus hydruntinus	2	7,7	2	1,5	9	3,9	-	-	13	3,2
Cervus elaphus	1	3,9	15	10,9	27		-	-	43	10,5
Capreolus capreolus	-	-	1	0,7	3	1,3	-	-	4	1
Capra cf. *aegargus*	1	3,9	4	2,9	13	11,7	-	-	18	4,4
Ursus arctos	-	-	-	-	2	0,9	-	-	2	0,5
Lepus sp.	1	3,9	1	0,7	1	0,4	-	-	3	0,7
Total identified pieces	26		138		231		13		408	
Cetartiodactyla	2		5		9		-		16	
Indeterminate equid	6		23		21		4		54	
Indeterminate carnivore	1		1		-		1		3	
Large size herbivore	17		98		55		7		177	
Large/middle size herbivore	-		21		106		7		134	
Middle size herbivore	4		6		4		-		14	
Middle/small size herbivore	3		31		30		2		66	
Small size herbivore	16		20		26		3		65	
Indeterminate	48		195		262		20		525	
TOTAL	**123**		**538**		**744**		**1357**		**1465**	

NR=Total number of remains
%NISP=number of identified specimens

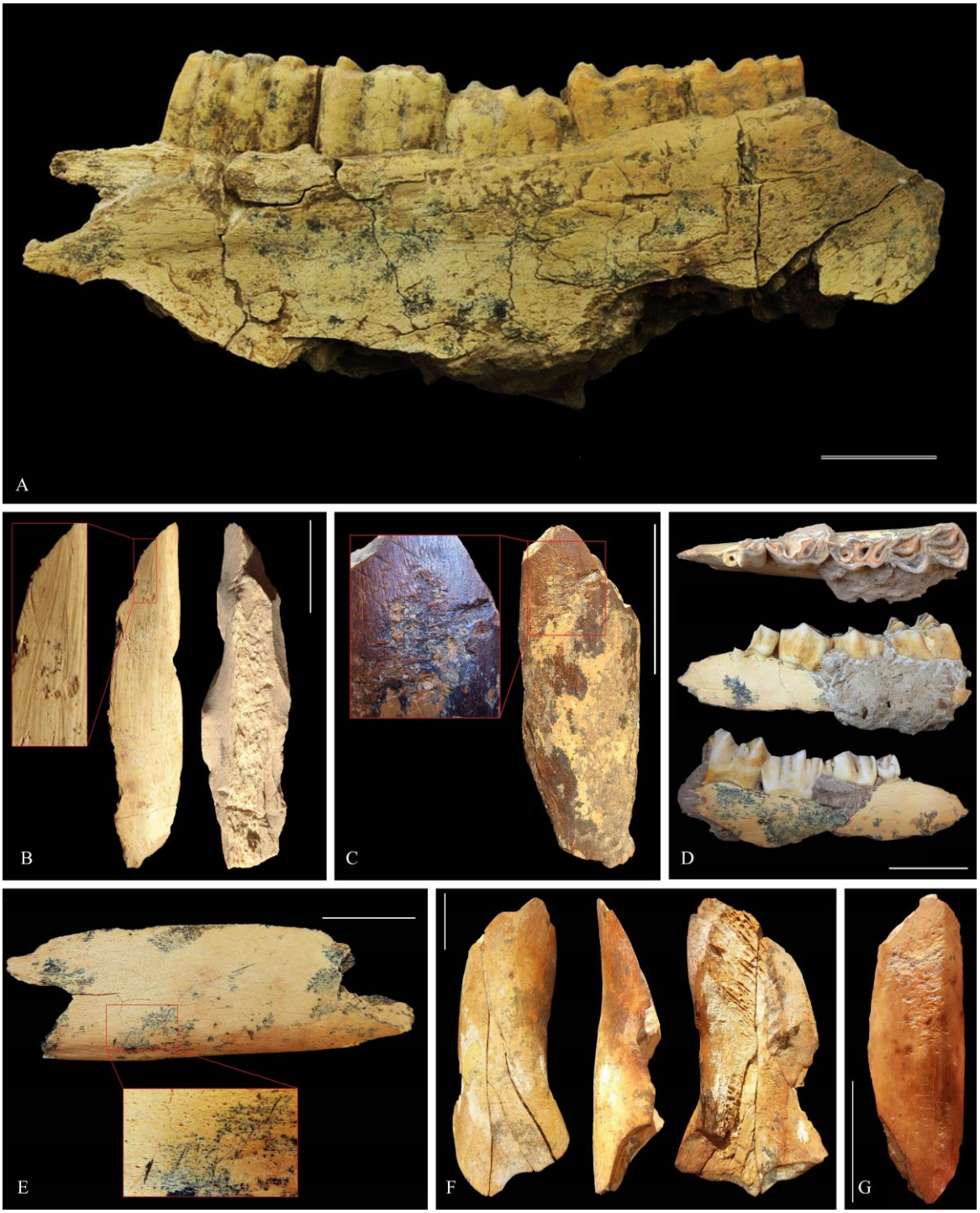

Figure 13. Mammals' remains collected at Qaleh Kurd. A. Right mandible of a horse with P2-M2. B. Long bone of a horse showing helical fracture, cutmarks and scrape marks; C. *Retouchoir* on a horse metapod associated with numerous cutmarks and scrape marks. D. Left mandible of an adult deer. E. Cutmarks on the mandible of a horse, for skin removal. F. Horse humerus with helical fracture and impact point. G. Double *retouchoir* on a deer tibia. Scale, 3cm.

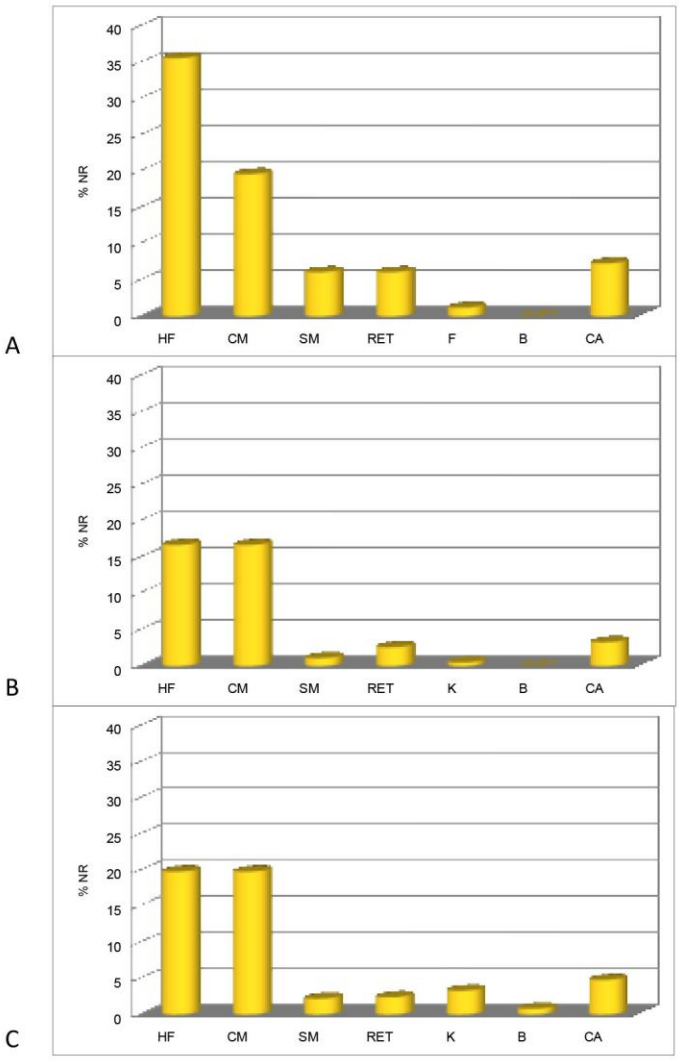

Figure 14. Percentage of remains with stigmata at Qaleh Kurd, from QK1 on top and QK3 at the bottom. HF=helical fracture; CM=cutting marks; SM=scraping marks; RET=*retouchoirs*; F=flakes; B=burnt bones; CA=carnivore marks.

QK2 yielded 538 remains representing 7 taxa (Table 5 and SI5b). The horse remains (82% of the corpus) are represented by a juvenile and an adult. All anatomical parts are represented. The deer represents 10% of the corpus and consists of a 4-5 years-old adult (Fig. 13D) and a juvenile; only the cranial parts and limbs are represented. The other species are the hydruntine (*Equus hydruntinus*), the aurochs (*Bos primigenius*), the wild goat (*Capra* cf. *aegargus)*, the roe deer (*Capreolus* sp.) and the hare (*Lepus* sp.) are represented by few remains or

single individuals. The observed stigmata, although less numerous than in QK1 (Fig. 14B), support the anthropogenic origin of this accumulation (Fig. 13F).

QK3 has been more widely excavated and yielded 744 remains, of which 231 are identified, with large majority being horses, but also the red deer, the wild goat, the hydruntine, the brown bear (*Ursus arctos*), the roe deer, the aurochs and the hare are also present (Table 5 and SI5c). The horse remains are represented by one juvenile and one adult; all anatomical parts are present in the cave, including the spine and belts, except the phalanges. The deer is represented almost exclusively by the limb bones of one adult individual. The wild goat is represented by a 6-month-old juvenile and an older adult; the cranial skeleton is particularly well represented. This suggests that both species may have been treated differently, although their masses are quite similar. The hydruntine is also represented by a juvenile and an adult. The brown bear is a juvenile, presented only with two dental remains; it is impossible to determine the cause of death. Anthropogenic stigmata are numerous, including burnt bones, helical fracturing (Fig. 13F) and cutmarks on almost 20% of the material (Fig. 14C). Percussion flakes are numerous as well, which bears witness to the in-situ location of percussion activities.

The lower deposits (QK4-6) have been little excavated. They yielded mainly horses remains that represent at least 3 individuals, one juvenile and two adults. Several helical fractures and cutmarks have been observed. Note that a steppe rhinoceros (*Stephanorhinus hemitoechus*) remain has been identified (QK4) and that some scarce remains show carnivore trimming marks (QK6).

Across the sequence, the horse appears to be the main exploited taxon. However, from a general view, for all the herbivore taxa, the skeleton is fully represented in the assemblage. Limb portions and cranial skeleton as well as the rachis are well represented. The animals therefore appear to have been transported to the site in their entirety. However, concerning the horses, given the size of these animals and the topography of the cave, they were probably dismembered prior they were brought back to the cave. The joints of the long bones and metapods have been intensely and systematically fractured, whatever the size of the animals. This is evidenced by the large quantity of bone fragments combined with the presence of numerous percussion flakes. Several mandibles are also fractured. The number of pieces with helical fractures (N=266) and cut marks (N=259) are numerous in all levels. These stigmata are indices of butchering practices. All the striations were caused by the cutting of the meat. However, the number of pieces with scraping are rarer (N=27). In summary, these first observations show

the anthropogenic nature of the faunal assemblage, for each archaeological levels, and that all herbivorous taxa and their carcasses were subject to intensive food exploitation, for meat or for the yellow marrow of the long bones or the marrow of the mandibular canal.

Moreover, some bones were also used as *retouchoirs*. Ten *retouchoirs* have been collected *in situ* (29 others were collected in the reworked sediments) (Fig. 13C and 13G). The stigmata on the cortical surfaces that allow identifying retouchoirs are numerous and can be observed macroscopically and microscopically (e.g. see Daujeard et al., 2014). They consist in characteristic cupules and notches (Fig. 13C and SI6c). These bones were used to rearrange lithic edges, and the stigmata result of the several impact points produced against the lithic material. Almost only diaphyseal fragments of long bones and metapodials of horse, deer and wild goat were used. These species are the most commonly represented in the assemblage; this indicates an opportunistic tendency and not a choice toward a given species in the collection of pieces as *retouchoirs*. Most of the *retouchoirs* have a single retouching area; this indicates that they were generally used only once.

Microvertebrate remains

Microvertabrate remains were collected through water sieving. To date, only preliminary observations were made on two test samples from T3. They revealed an interesting diversity, including several rodents (*Allactaga*, *Mesocricetus*, *Calomyscus*, *Meriones*, various voles including *Ellobius* and *Microtus* species) and, to a lesser extent, lagomorphs (Ochotonidae and Leporidae), bats, lizards (including Agamidae), snakes (including Colubridae) and small birds (See SI6). The anatomical representation of rodents is good, including small and fragile elements such as ribs and phalanges. A few traces of weak digestion have also been observed. This indicates that we are in the presence of a primary assemblage accumulated, at least in part, by predation (most probably owls). An in-depth study of the more abundant material collected during the excavation, will help to obtain more precise information on the species identifications, on the taphonomic history of the assemblages, as well as on the biochronological and palaeoenvironmental context of the human occupations.

Discussion

A Middle Pleistocene sequence

The archaeological and paleoanthropological corpus available from the Levant to the Caucasus and East Asia question the modalities and temporalities of the hominin dispersal over Eurasia during the Middle Pleistocene, as well as the diversity of hominins, their cultural traditions and possible interactions. Despite this rich regional context, no large assemblages in a clear chrono-stratigraphic framework that could be allocated to the Middle Pleistocene were available for the ICP and surroundings areas (the Zagros and the Alborz). Regarding the chronology, the Mousterian layer of Humian I, a rock shelter located in the Zagros delivered the single available date for the area; a single Th/U-series date on bone gave an age of 148±35 ka (Bewley, 1984). More recently, a late Middle Pleistocene age has been proposed for the Darband Cave assemblage based on Th/U-series analysis of two bear teeth (Biglari and Jahini, 2011; Biglari et al., 2014). However, caution is requested regarding U-series dating of faunal remains since bones and teeth are open systems for uranium; this is particularly true in case of dating a bone based on a single sample, as done on Humian I (see Grün, 2006, for a review). Concerning U-series dating of a tooth, it is also acknowledged that for a same tooth, the ages vary according to the tissues. This led to couple U-Series with ESR analyses in order to model the kinetics of U-uptake on the tissues of a same tooth and provide a single age (see Grün et al., 1988). Finally, recent works have yielded more reliable dates for the edges of the northern ICP (Heydari et al., 2020) and for the Zagros (see Becerra-Valdivia et al., 2017 for a review of available radiocarbon original dates and Bayesian models for large archaeological sequences). So far, the oldest dates for the area was reported at Gareh Boof where the Middle Paleolithic deposits of the large archaeological sequence are dated from 81 to 45ka using optically stimulated luminescence (OSL) (Heydari et al., 2021).

At Qaleh Kurd, analyses have revealed a sedimentary succession represented by more than 2.5m thick record made up of two main sequences: a karstic and clastic sequence during the Middle Pleistocene including at least six archaeological levels (Sequence II), and a Holocene sequence including isolated archaeological material (Sequence I). The 10 ESR/U-series dates obtained on equid teeth collected in the excavated archaeological

levels, provide the first chronological framework for the deposit. Although other analyses (ESR/U-series in progress and TL) are requested in order to consolidate this framework, it is consistent with the stratigraphy and supports a middle Pleistocene occupation of the cave since ca 450ka (and most probably earlier since deeper archaeological deposits could not be excavated yet) that lasted at least ca 300ka, despite the high elevation of the site (2137m asl) and the large climatic fluctuations that occurred during this period. These results would push back to more than three hundred thousand years the earliest dated evidence of human settlement in the ICP and its direct surroundings (The Zagros and the Alborz Mountains). This framework is consistent with what is known in the Levant and Central Asia for the Middle Pleistocene, where human settlements are well documented by large and well dated archaeological sequences (e.g. Mercier and Valladas, 2003; Jacobs et al., 2019; Pan et al., 2020; Finestone et al., 2022; Hershkovitz et al., 2021).

The hominins of Qaleh Kurd

Excavations at Qaleh Kurd yielded to the discovery of a deciduous human left first upper molar in the QK3 level. The crown is highly worn and the root is almost totally resorbed, suggesting that it has probably been lost naturally during the child's life and was functional for some time. The crown is also affected in depth by two large caries. Caries have long been associated with agricultural diets; yet, several Pliocene and Pleistocene cases have been described in the literature, including decidual teeth, even if they represent only a small proportion of these cases. One can quote some cases of Pliocene specimens attributed to Early *Homo* and *Paranthropus robustus* from South Africa (Towle et al., 2019, 2021) or in the Levant, on specimens of Neanderthals at Kebara (Tillier et al., 1995) and modern humans from the late Middle Pleistocene at Qafzeh (e.g., Tillier, 2021). Although diet is the primary factor in caries formation (Sheiham and James, 2015), many other contexts can lead to caries formation including fatigue of the enamel due to a high level of mastication (Sanchez-Gonzalez et al., 2020) and/or high attrition (Hillson, 2008). In the state of analysis (paleoenvironmental and surface study of the tooth) it is premature to draw any conclusions on the origins of the caries of the Qaleh Kurd’s deciduous tooth; nevertheless, given the high level of attrition, apart from diet, some functional insights could be proposed.

In terms of taxonomic affinities, the high degree of wear of the crown and the presence of two large caries significantly impact the metrics (Becam and Chevalier, 2019) and the potential taxonomically informative traits (Fornai et al., 2014). Although the bucco-lingual diameter corresponds to the range of variation known for Neanderthals and is below that of modern humans, this single measurement cannot be considered as conclusive in a taxonomic perspective. The morphology of the crown is also highly variable in archaic humans, Neanderthals and early modern humans, in occlusal view, from elongated to quadrangular and trapezoidal, from symmetrical to asymmetrical (e.g. Tillier, 1979b, 1980; Trinkaus, 1983; Tillier, 1999; Lumley de, 2018) with or without a *tuberculum molare*, as it is observed on the Qaleh Kurd specimen. This tubercule is inconstant and variably located (e.g. Thoma, 1963; Tillier, 1979b, 1980; Tillier, 1999; Tillier et al., 2003; Lumley de, 2018, 2022). In summary, the crown of deciduous upper molars is highly variable in middle Pleistocene humans, both in metrics and morphology. Given the wear of the crown, the caries and the root resorption that affected the Qaleh Kurd specimen, the taxonomic attribution of the isolated Qaleh Kurd deciduous left first upper molar appears premature.

Finally, the whole chronology of the Qaleh Kurd archaeological sequence covers more than 300 thousand years of recurrent occupations during the Middle Pleistocene, starting at least from around 450 ka. During this large period of time, the presence of archaic humans, Denisovans and Neanderthals at the east and early Modern Humans, Neanderthals and possibly other species at the west have been reported (Mercier and Valladas, 2003; Chen et al., 2019; Jacobs et al., 2019; Pan et al., 2020; Hershkovitz et al., 2021; Finestone et al., 2022; Han et al., 2022). One cannot thus exclude that several human species could have occupied the cave of Qaleh Kurd, from archaic humans (*Homo erectus*?) to Denisovans, Neanderthals and/or early modern humans.

Early Middle Paleolithic Cultural affinities

Lithic tools in the upper Qaleh Kurd assemblages (QK1-3) are usually formal (see Andrefsky, 1994), made on flake and blade blanks. There are also some opportunistic, sparsely retouched pieces made on atypical flake or blade blanks. Typologically speaking, the overall picture of tool typology depicted in table 4 is the types expected from Middle Paleolithic contexts (see, e.g., Bordes, 1961; Debénath and Dibble, 1994; Geneste, 1985).

These include side scrapers and retouched convergent tools (including retouched points and convergent scrapers) made on flakes that are the dominant tool types across QK 1–3. Within the retouched convergent tools, Mousterian points are the most recurring tool type across all the three archaeological deposits. Some of the Mousterian points in Qaleh Kurd and most of them in QK3 are elongated. Endscrapers and Déjeté points/scrapers exist, but with much lower frequencies than side scrapers and retouched points. In addition, notched pieces are unpopular across all archaeological strata in Qaleh Kurd, denticulates are absent, and this is also the case for truncated-faceted pieces.

In comparison to local assemblages, QK 1-3 appear to share typological and technological traits with the Upper Pleistocene Middle Paleolithic assemblages of the Zagros (Bisitun rock shelter: Coon, 1951; Lindly, 1997; Warwasi rock shelter and Qobeh Cave: Braidwood et al., 1961; Dibble and Holdaway, 1993; Lindly, 1997; Gar Arjeneh rock shelter: Hole and Flannery, 1967; Lindly, 1997; Mar-Tarik cave: Jaubert et al., 2009; Kaldar: Bazgir et al., 2014). These shared traits are related to the high frequency of scrapers (especially side-scraper) and points, few notches and denticulates and the comparable extent of the application of the Levallois method (Kamrani et al., 2022). In that respect, it is less similar to the ICP where these facies are unknown so far (Chahe-Jam: Vahdati Nasab and Hashemi, 2016; Mirak: Vahdati Nasab et al., 2019).

However, the QK 1-3 assemblages show also some traits that are known in the Early Middle Paleolithic of the Levant and the South Caucasus. These concern the high frequency of retouched points, either made on blades or elongated flakes (Meignen and Tushabramishvili, 2006, 2010; Mercier et al., 2010). As in the Levant and the Caucasus (Meignen and Tushabramishvili, 2010), such retouched elongated points are highly variable in their size, morphology, and retouch localization (e.g., Fig. 9a, d, j–l; Fig. 3a, b, d; Fig. 4a, b, d, e, h–j; Fig. 6). In addition, the assemblage displays symmetrical to asymmetrical points; they are sometimes reminiscent of what Neuville has called “pointes incurvées” (1951: 51, 52) or curved triangular points (Fig. 11e). In addition, in QK3, inverse retouching and hence, bifacial shaping, is observed on few points (Fig. 11h, i) as in the Caucasian early Middle Paleolithic (Meignen and Tushabramishvili, 2010). Ventral retouching/thinning, especially in the proximal and dorsal parts of the points, is less common at Qaleh Kurd than in the South Caucasus (Beliaeva and Lioubine, 1998; Golovanova and Doronichev, 2003). At QK 1-3, thinning usually occurs in proximal-basal parts

and with direct retouching/chipping; this suggests preparation for hafting (Figures 9, 10, 11). Finally, broad-based Levallois points with chapeau de gendarme striking platforms are rare in QK 1-3 contrary to the later so-called Tabun-B assemblages in the Levant (e.g., in Kebara units IX-X, Tor Faraj, Tabun I 1-17; Bar-Yosef and Meignen, 2001).

The other feature of the retouched tools at QK 1-3 is the presence of thick narrow retouched blades especially in QK2 (Figure 10b, e, f). These are similar to those recorded in the Levant in the Amudian entity in Tabun XI (Meignen and Tushabramishvili, 2010), and the early Middle Paleolithic assemblages of Abou Sif C–D (Neuville, 1951), Hummal Ia (Copeland, 1985), Hayonim lower E and F (Meignen, 1998; Meignen and Bar-Yosef, 2020), but also those of the early Middle Paleolithic "Kudaro-Djruchulian" entity in the South Caucasus (e.g., Tushabramishvili, 1963 in Meignen and Tushabramishvili, 2010). Such thick elongated blades could have been struck from narrow cores with highly oblique lateral sides in cross section (Meignen, 1998). This technic has not yet been identified at Qaleh Kurd. Regarding elongation, the lithic blanks of QK 1–3's tools mostly resemble those of Tabun-D type (Phase I Mousterian in Jelinek, 1982). They are elongated and convergent/pointed elongated and they differ from the suboval-subquadrangular blanks of the Tabun-C type (Bar-Yosef, 2008). Such blanks at Qaleh Kurd does not represent sub-parallel lateral edges, contrary to what in observed in Tabun-D type assemblages such as Abou Sif C and B (Copeland 1975, 1981). Albeit there are instances of non-elongated flake blanks in QK 1–3, they were not retouched for the most part. Preliminary analysis indicates that the flintknappers were strongly selective in choosing more elongated and thicker flakes for further retouching. This recall the Amudian as well as the Early Middle Paleolithic entities of the Levant and the Caucasus (see e.g., Meignen, 2007; Meignen and Tushabramishvili, 2010).

Few transverse and end-scrapers with Quina-like retouch and named here as demi-Quina scrapers (Figure 8g), are recorded from QK 1 to QK 3. They are made on thick and broad flakes. They belong to the Mousterian lithic type-lists of Europe (see e.g., Bordes, 1981; Bourguignon, 1997; Peresani et al., 2023). They are almost absent in the Levantine Mousterian (Agam and Zupancich, 2020), while they are known in the Acheulo-Yabrudian complex from late Lower Paleolithic or Lower-Middle Paleolithic boundary (Agam and Zupancich, 2020; Malinsky-Buller, 2016; Meignen and Bar-Yosef, 2020; Shimelmitz et al., 2014; Zaidner and Weinstein-Evron, 2006). In the South Caucasus, they are recovered from both Acheulo-Yabrudian-like lithic assemblages as in

Tsopi (Grigolia, 1963 in Golovanova and Doronichev, 2003) and early Middle Paleolithic assemblages as in sites of Kudaro-Djruchulian context (Golovanova and Doronichev, 2003). Finally, Upper Paleolithic tools types are not common in Qaleh Kurd while they are prevalent in some of the Levantine early Middle Paleolithic sites (such as Hayonim lower E and F, Hummal Ia, Abou Sif; see Meignen and Tushabramishvili, 2010; Neuville, 1951).

Blade production (laminar and elongated blanks) is significant in Qaleh Kurd but does not dominate other productions as it is the case in the Levantine early Middle Paleolithic (see e.g., Wojtczak and Malinsky-Buller, 2022). In addition, like the Levantine early Middle Paleolithic (e.g., Wojtczak, 2022; Wojtczak and Malinsky-Buller, 2022), reduction schemes in Qaleh Kurd were diverse, with the presence of Levallois, laminar, and core-on-flake strategies. However, the Levallois method is not preferably used for blade production in Qaleh Kurd Cave contrary to what is reported for the Levantine early Middle Paleolithic (see Wojtczak and Malinsky-Buller, 2022).

In summary, this first comparative analysis of the QK 1-3 lithic assemblages highlights some affinities with the Middle Pleistocene Early Middle Paleolithic of the Levant and the Caucasus that places it in an early Middle Paleolithic tradition. However, it highlights as well some affinities with the Upper Pleistocene Middle Paleolithic known in the Zagros that opens new insights in the origin of the Zagros Mousterian. Conducting new excavations and analyses at Qaleh Kurd are thus of great importance for our knowledge on the diversity of the early Middle Paleolithic cultures in the area as well as on the origin of local Mousterian facies.

Biochronological and Paleoenvironmental overview and perspectives

The Pleistocene upper units at Qaleh Kurd have yielded a faunal assemblage from which a first biochronological overview and some perspectives can be proposed. Several large mammals have been identified, including large horse (*Equus ferus* sensu lato) but also the red deer (*Cervus elaphus*), the hydruntine (*Equus hydruntinus*), the wild goat (*Capra* cf. *aegargus*), the roe deer (*Capreolus* sp.), the aurochs (*Bos primigenius*), the brown bear (*Ursus arctos*) and also the steppe rhinoceros (*Stephanorhinus hemitoechus*). Most of these taxa have a broad temporal distribution; their relevance for biochronological purposes is thus limited. They correspond to

"modern" taxa resulting from the major faunal renewal observed at the Lower-Middle Pleistocene transition. The brown bear *Ursus arctos*, identified in QK3, although known from the very beginning of the Middle Pleistocene in Asia (Zhoukoudian, Jiangzuo et al., 2018) is only described in the region in the Upper Pleistocene site of Wezmeh (Mashkour et al., 2009; Monchot et al., 2020). Aurochs is a taxon of African origin; its dispersal in Eurasia dates back to 0.7 Ma (Martinez-Navarro et al., 2007). *Bos sp.* and *Cervus elaphus* are notably identified around 0.8 Ma in the Levant (Gesher Benot Ya'aqov, Rabinovich and Biton, 2011). *Stephanorhinus hemitoechus*, identified in the lower archaeological deposit, is a species recognized mainly in Europe, although it may have spread to the Near East and North Africa (Pandolfi et al., 2021). Rhinoceros is reported from Wezmeh and Gilvaran at the west-central Zagros (Mashkour et al., 2009; Bazgir et al., 2014). It has also recently been determined in recent Middle Pleistocene deposits in Jordan (Pokines et al., 2019) and in Azerbaijan (Van der Made et al., 2016). The oldest record of *S. hemitoechus* is in Western Europe at around 0.55 Ma (Caune de l'Arago, Chen and Moigne, 2018). In Qaleh Kurd, in state of research, it is represented by a single remain which makes impossible any biochronological inference as it has been done for the Middle Pleistocene of Europe (Lacombat, 2009). Moreover, the lack of fossils makes it impossible to know whether the model is valid in Central Asia. Concerning the equids, two species have been described at Qaleh Kurd: a caballine horse and *Equus hydruntinus*, related to present-day hemiones. The later is more common in early Holocene in Iran but has also been determined in Pleistocene context (Orlando et al., 2006; Benett et al., 2017; Eisenmann and Mashkour, 1999). The two species are frequently found in sympatry. Biochronological indications could be deduced from the study of horses by combining certain evolutionary and ecomorphological characters (Boulbes and van Asperen, 2019). As a preliminary approach, a comparative analysis of the medium to large dimensions of the teeth (See SI7 for comparative metrics and clustering analysis) places the Qaleh Kurd specimens closer to the Middle Pleistocene populations (including *Equus mosbachensis* and late Middle Pleistocene caballine equids) (Forsten and Moigne, 1998; Boulbes, 2010; Uzunidis-Boutillier, 2017). However, the available material is not yet statistically representative enough to confidently address this topic. In addition, although horses in Eurasia as a whole underwent a decline in size that accelerated at the beginning of the Upper Pleistocene (Nobis, 1971; Forsten, 1991; Boulbes and van Asperen, 2019), this global reduction is not absolute (Eisenmann, 2022), and such trend remains to be verified in Central Asia and the ICP. Thanks to new excavations, Qaleh Kurd, with its

692 assemblages rich in horses, could constitute a key site for this topic as well. Finally, it is interesting to note that
693 all the species present at Qaleh Kurd are also recorded in the large revised faunal list of Middle Pleistocene
694 levels dated to 0.3-0.2 Ma from Azokh Cave in the Lesser Caucasus in Azerbaijan (Van der Made et al., 2016).
695 In summary, although preliminary, given the number of pieces collected so far, the composition of the faunal
696 sample and the metrics of the horse are consistent with a Middle Pleistocene settlement of the cave as supported
697 by the chronological data. Given the quantity of horse material collected during the first excavations at Qaleh
698 Kurd spanning all over the stratigraphic sequence, additional fieldwork could yield sufficient material in support
699 of a biochronological model for the area.
700 In a paleoecological perspective, the composition of the well represented large mammals and their relative
701 abundance do not vary in the Pleistocene deposits of Qaleh Kurd. However, the samples by levels is not
702 numerous enough yet to allow any statistical modelling. The horse, which is the dominant taxon at Qaleh Kurd,
703 is generally considered a highly specialized "grazer". However, palaeontological evidence shows that horse
704 experienced a wide range of habitats from interglacial open forests to grassy steppes during glacial episodes
705 (Pushkina et al., 2014; Rivals et al., 2015; Saarinen et al., 2016; Uzunidis, et al., 2017). Like the hemiones,
706 *Equus hydruntinus* was adapted to semi-arid and steppe conditions with a preference for temperate climates,
707 although it could tolerate a moderate cold (Boulbes and van Asperen, 2019). Among cervids, *Cervus elaphus* is a
708 eurytopic species with considerable dietary flexibility. The roe deer is tolerant of temperature variations but it is
709 more limited to a browser-type diet and prefers wooded areas (Rivals and Lister, 2016; Sommer et al., 2009).
710 Aurochs are most often linked to interglacial contexts, and their numbers generally increase in phases of
711 Pleistocene climatic improvement (Brugal et al., 2020). The steppe rhinoceros (*Stephanorhinus hemitoechus*)
712 which is identified in the lower level QK4-6, inhabited temperate open forest environments rich in low
713 vegetation. It appears to be the most ubiquitous and least moisture-dependent species of the genus; the species
714 tend to follow the Mediterranean environment during interglacial periods (Pandolfi et al., 2017; Lacombat, 2009;
715 Fortelius et al., 1993). Finally, the ibex *Capra aegargus* is one of the most widely dispersed rock mammals in
716 many habitats in Iran. The species is highly dependent on rocky substrates and steep slopes to avoid predators
717 (Sarhangzadeh et al., 2013). As a preliminary overview, the large fauna which is relatively similar from QK3 to
718 QK1 is consistent with interglacial (or interstadial) depositional conditions although the assemblage is not rich

enough to allow any robust inferences. However, the composition of the fauna of these levels implies a diversity of biotopes around the site.

The microvertebrate assemblages from Qaleh Kurd are still under study. However, preliminary observations demonstrate the presence of *Allactaga*, *Meriones*, *Ellobius* and *Mesocricetus* which indicates steppe environments. *Calomyscus* frequents rocky mountain steppe and shrubland habitats. These observations is consistent with the high elevation of the cave (over 2100m asl). Numerous samples from the whole sequence are available for sorting and study, and it makes no doubt that future investigations will provide significant biochronological and palaeoenvironmental information for the Middle Pleistocene settlement of Qaleh Kurd and the Northern ICP.

Subsistence behaviours: Intensive exploitation of the fauna by humans

Carnivores are known to be agents of bone accumulation in Pleistocene sites where they may compete with humans. This has been demonstrated from the Lower Pleistocene (e.g., in Barranco León, Spain, Courtenay et al., 2023) to the Upper Pleistocene (e.g., in Wezmeh, Zagros, Iran, Mashkour et al., 2009). However, in Qaleh Kurd, beside the two teeth of *Ursus arctos*, few pieces with carnivore traces have been collected so far, suggesting that the role of carnivores in the accumulation of the deposit was very limited.

Conversely, for the 3 levels mainly investigated, the role of humans in the accumulation of the deposits appears to be essential for food purpose as in other Pleistocene sites (e.g., Daujeard, 2008; Romandini et al., 2014; Sévêque, 2017). For all herbivore taxa, animals appear to have been transported to the site almost in their entirety. Concerning the horses, considering the size of these animals and the topography of the site, it could have been brought in pieces into the cave. The analysis of the assemblage show that anthropogenic stigmata are numerous and indicate that humans in Qaleh Kurd intensively exploited herbivor and their carcasses for meat or for the yellow marrow of the long bones or the marrow of the mandibular canal. This feature is common to both past and present hunter-gatherer populations (e.g., Binford, 1981; Abe, 2005 for present-day groups, Delpech and Villa, 1993; Farizy et al., 1994; Auguste, 1995 for Pleistocene groups). Apart from bone marrow and mandibular canal marrow, one cannot exclude that humans have recovered fat from bone tissue (joints,

phalanges, short bones) (Delpech and Villa, 1993; Brink, 1997; Speth, 2012; Costamagno and Rigaud, 2014). This process, considered universal (Outram, 2001), involves boiling, as ethno-archaeological work shows (e.g., Binford, 1981; Nelson, 2010). Nevertheless, to date, no deposits that could be interpreted as slurry discharge have been identified at Qaleh Kurd.

Bones can also be exploited as tools (e.g., Vincent, 1993; Moncel et al., 2012; Blasco et al., 2013; Daujeard et al., 2014; Moigne et al., 2016; See Hutson et al., 2018 for a review). This study show that it has been the case at Qaleh Kurd where numerous bone *retouchoirs* have been collected in the Middle Pleistocene sequence, from the earliest deposits to the most recent (Fig. 13 and SI2c). This is the first mention of *retouchoirs* in Paleolithic sites of the ICP and immediate surroundings. Finally, the *retouchoirs* at Qaleh Kurd appear consistent with those known in Pleistocene Eurasian series. As in Qaleh Kurd, almost exclusively diaphyseal fragments of long bones and metapodials were used in these Eurasian series (Vincent, 1993; Armand and Delagnes, 1998; Daujeard et al., 2014; Sévêque and Auguste, 2018).

Conclusion

Excavations at Qaleh Kurd cave, have yielded one of the largest anthropogenic assemblages of the ICP, the Zagros and the Alborz, in a precise chrono-stratigraphic framework. So far, our studies have focused on the first extensively excavated archaeological assemblages. The consistent chrono-stratigraphic framework for the whole deposit and the faunal and lithic characteristics of the upper levels, demonstrate that the cave, which is located at 2130m asl, was recurrently occupied by humans during the middle Pleistocene from ca 450ka and during at least 300ka. This makes Qaleh Kurd the oldest evidence so far of Middle Pleistocene human settlements in the ICP and immediate surroundings (the Alborz and Zagros Mountains) and pushes back the earliest evidence of human settlement in this region to more than 300ka. This fieldwork and multidisciplinary analysis at Qaleh Kurd strongly support the need of systematic surveys, including high elevated region, as well as long term excavations in the ICP and surroundings.

The reported early Middle Paleolithic cultures recalls in some traits those known in the Caucasus and the Levant but also suggest resemblance to later Zagros Mousterian facies known from the region. This opens new insights in the early stages of Middle Paleolithic cultures in the area as well as in the origin of the Zagros Mousterian. Regarding the hominin species that may have occupied the site, the taxonomic attribution of the discovered human tooth cannot be specified in state of analysis. However, the chronology of the site and the paleoanthropological knowledge from the Levant to Central Asia for this trench of time, may support the idea that several hominin species could have occupied the site, at least successively.

From a general point of view, chronological, archeological, paleontological and paleoanthropological findings make Qaleh Kurd of great interest for the knowledge of early hominin settlements, as well as biological and cultural diversity from the Levant to Central and East Asia. Fieldworks and analysis are currently conducted to enrich what we started to investigate in this contribution, and to improve our knowledge of earlier periods recorded in the Qaleh Kurd sequence.

Acknowledgements

Our work on Qaleh Kurd cave was made possible thanks to the financial support of: the Regional Service of Cultural Heritage of the Province of Qazvin, the Iranian Center for Archaeological Research (ICAR), the Ministry of Europe and Foreign Affairs of France (Commission des Fouilles archéologiques à l'étranger), Tarbiat Modares University, the French Embassy in Iran, the UMR7194 CNRS-MNHN-UPVD. We would like to express our deepest gratitude to them for their support and trust in our team. We would like to thank Dr. Sadjad Alibaigi for his generous allowance to work in this magnificent site. We would also like to express our gratitude to the Iranian Ministry of Cultural Heritage and Tourism, in particular Drs. Rouhollah Shirazi, Kourosh Roustaei, and Leyla Khosravi, directors of the Iranian Center for Archaeological Research (ICAR) at the time of our excavations, for their collaboration in the preparation of our missions and for allowing us to work in the field. We would like to thank Mrs. Solgi and her colleagues at the Tehran University Medical Science Preclinical Core Facility for providing high resolution micro-CT-Scan of the Qaleh Kurd tooth. We also thank Mr.

Hazratiha, Director of the Cultural Heritage Office of Qazvin Province at the time of first mission in 2018 and Mr. Khazaeli the current director, and Mrs. Mohammadi, Mr. Asgari, Fanaee and their Delegate for Archaeology, for their hospitality and logistical support in the field of Qaleh Kurd. We are thankful to Dr. Sébastein Nomade for his assistance in the preparation of 14C samples as well as to Dr. M. Alirezazadeh for his assistance in producing the map used in figure 1. Obviously, the field work was not possible without tremendous job of the crew, which their names were not included in the author list. In alphabetical order: L. Alinia, M. Alirezazadeh, M. Etminan, T. Izadyari, Z. Kamrani, S. Ganji, A. Khanian, D. Mahmoudi, S. Nazif, S. Shafiee, M.J. Shoaee.

Declarations

Ethical Approval

Not applicable

Funding

The Regional Service of Cultural Heritage of the Province of Qazvin for financial support of the field campaigns
The Iranian Center for Archaeological Research (ICAR) for financial support of the field campaigns
A grant from the Ministry of Europe and Foreign Affairs of France (Commission des Fouilles archéologiques à l'étranger) for financial support of the field campaigns and laboratory analyses
Tarbiat Modares University for financial support of the laboratory analyses
UMR7194 CNRS-MNHN-UPVD for financial support of the laboratory analyses. The ESR spectrometer, Q-ICP-mass spectrometer and portable gamma spectrometer of the Muséum National d'Histoire Naturelle used for part of the analyses were bought with the financial support of the Région Île-de-France' (for the two first devices) and Région Centre respectively.
The geoarchaeological analysis has been done in the frame of a doctoral scholarship (M.A. Kharazian) granted by the French Embassy in Iran.

Availability of data and materials

No data outside the submitted manuscript file

Data and materials may made available on demand to first authors; archaeological materials being under the care of the cultural heritage service of the Qazvin Province.

Bibliography

Abe, Y., 2005. Hunting and butchering patterns of the evenki in the Northern Transbaikalia Russia. Ph.D. Dissertation, Stony Brook University.

Agam, A., and Zupancich, A., 2020. Interpreting the Quina and demi-Quina scrapers from Acheulo-Yabrudian Qesem Cave, Israel: Results of raw materials and functional analyses. Journal of Human Evolution 144, 102798.

AlQahtani, S.J., Hector, M.P., Liversidge, H.M., 2014. Accuracy of dental age estimation charts: Schour and Massler, Ubelaker and the London Atlas. American Journal of Physical Anthropology. 154, 70–78

Andrefsky, W., 1994. Raw Material Availability and the Organization of Technology. American Antiquity 59, 21-35.

Armand, D., and Delagnes, A., 1998. Les retouchoirs en os d'Artenac (couche 6c) : perspectives archéozoologiques, taphonomiques et expérimentales. In: Brugal, J.-P., Meignen, L., and Patou-Mathis, M. (Eds.), Économie Préhistorique : Les Comportements de Subsistance au Paléolithique Moyen. Actes des XVIIIe Rencontres Internationales d'Archéologie et d'Histoire d'Antibes, 23-25 Octobre 1997. APDCA, Sophia Antipolis, pp. 205-214.

Auguste, P., 1995. Chasse et charognage au Paléolithique moyen: l'apport du gisement de Biache-Saint-Vaast (Pas-de-Calais). Bulletin de la Société Préhistorique Française 92, 155-167.

Bahain, J.J., Voinchet, P., Vietti, A., Shao, Q., Tombret, O., Pereira, A., Nomade, S. and Falguères, C., 2021. ESR/U-series and ESR dating of several Middle Pleistocene Italian sites: Comparison with 40Ar/39Ar chronology. Quaternary Geochronology 63, 101151.

Bar-Yosef, O., 1994. The lower Paleolithic of the Near East. Journal of World Prehistory. 8, 211–265.

Bar-Yosef, O., 2008. Asia, West: Paleolithic Cultures. In: Pearsall, D.M. (ed.), Encyclopedia of Archaeology, Academic Press, pp. 865-875.

Bar-Yosef, O., Belfer-Cohen, A., 2001. From Africa to Eurasia - early dispersals. Quaternary international. 75, 19–28.

Bar-Yosef, O., Meignen, L., 2001. The Chronology of the Levantine Middle Paleolithic Period in Retrospect. Bulletins et mémoires de la Société d'Anthropologie de Paris. BMSAP. 13, 269-289.

Bazgir, B., Ollé, A., Tumung, L., Becerra-Valdivia, L., Douka, K., Higham, T., van der Made, J., Picin, A., Saladié, P., López-García, J.M., Blain, H.-A., Allué, E., Fernández-García, M., Rey-Rodríguez, I., Arceredillo, D., Bahrololoumi, F., Azimi, M., Otte, M., Carbonell, E., 2017. Understanding the emergence of modern humans and the disappearance of Neanderthals: Insights from Kaldar Cave (Khorramabad Valley, Western Iran). Nature Scientific Reports 7, 43460.

Bazgir, B., Otte, M., Tumung, L., Ollé, A., Deo, S.G., Joglekar, P., López-García, J.M., Picin, A., Davoudi, D., van der Made, J., 2014. Test excavations and initial results at the Middle and Upper Paleolithic sites of Gilvaran, Kaldar, Ghamari caves and Gar Arjene Rockshelter, Khorramabad Valley, western Iran. Comptes Rendus Palevol. 13, 511–525.

Becam, G., Chevalier, T., 2019. Neandertal features of the deciduous and permanent teeth from Portel-Ouest Cave (Ariège, France). American Journal of Physical Anthropology. 168, 45–69.

Becerra-Valdivia, L., Douka, K., Comeskey, D., Bazgir, B., Conard, N.J., Marean, C.W., Ollé, A., Otte, M., Tumung, L., Zeidi, M., Higham, T.F.G., 2017. Chronometric investigations of the Middle to Upper Paleolithic transition in the Zagros Mountains using AMS radiocarbon dating and Bayesian age modelling. Journal of Human Evolution. 109, 57–69.

868 Beliaeva, E.V., and Lioubine, V.P., 1998. The Caucasus-Levant-Zagros: Possible relations in the Middle
869 Paleolithic. In: Prehistoire d'Anatolie: Genese des Deux Mondes (Anatolian Prehistory at the crossroads of two
870 worlds), vol. 1, M. Otte (ed.), pp. 39–55. Liege: ERAUL 85.
871 Bennett, E. A., Champlot, S., Peters, J., Arbuckle, B., Bălăşescu, A., Bar-David, S., Davis, S., Gautier, M.,
872 Germonpré, M., Gündem C., Hemami M.-R. Kaczensky P., Kuehn R., Mashkour M., Morales A., Moullé P.-E.,
873 Pucher, E., Pruvost, M., Tournepiche, J.-F., Uerpmann, H.-P., Uerpmann, M., Walzer, C., Grange, T., Geigl, E.-
874 M., 2017. Taming the Late Quaternary phylogeography of the Eurasiatic wild ass through ancient and modern
875 DNA. PNAS, 106, 21754–21759.
876 Berillon, G., Asgari Khaneghah, A. (Eds.), 2016, Garm Roud, Hunting place in Iran, Upper Paleolithic. @rchéo-
877 éditions.com/IFRI, Paris.
878 Berillon, G., Asgari Khaneghah, A., Antoine, P., Bahain, J.-J., Chevrier, B., Zeitoun, V., Aminzadeh, N.,
879 Beheshti, M., Chanzanagh, H.E., Nochadi, S., 2007. Discovery of new open-air Paleolithic localities in Central
880 Alborz, Northern Iran. Journal of Human Evolution. 52, 380–387.
881 Bewley, R.H., 1984. The Cambridge university archaeological expedition to Iran 1969. Excavations in the
882 Zagros Mountains : Houmian, Mir Malas, and Barde Spid. Iran, Journal of the British Institute of Persian Studies
883 22, 1–38.
884 Biglari, F. and Shidrang, S., 2006. The lower Paleolithic occupation of Iran. Near Eastern Archaeology, 69(3-4),
885 pp.160-168.
886 Biglari, F., Dashtizadeh, A., Zarei, S., Amini, S., Ghasimi, T., 2023. Dehtal, Evidence of the Large Flake
887 Acheulean at the North of the Persian Gulf, Iran. Parseh Journal of Archaeological Studies. 7, 7–24.
888 Biglari, F., Jahani, V., 2011. The Pleistocene Human Settlement in Gilan, Southwest Caspian Sea: Recent
889 Research. Eurasian Prehistory. 8, 3–28.
890 Biglari, F., Jahani, V., Mashkour, M., Amini, S., 2014. Test Excavations at the Lower Paleolithic Site of
891 Darband Cave, Roudbar, Gilan Province, 2012. Proceedings of the 12th Annual Symposium on the Iranian
892 Archaeology, Iranian Center for Archaeological Research, Tehran, 101–104.
893 Binford, LR., 1981. Bones: Ancient Men, Modern Myths. Academic Press, New York.

894 Blasco, R., Rosell, J., Cuartero, F., Peris, J.F., Gopher, A. and Barkai, R., 2013. Using bones to shape stones:
895 MIS 9 bone retouchers at both edges of the Mediterranean Sea. PLoS One 8, 76780.
896 Bonilauri, S., Chevrier, B., Asghar Asgari Khaneghah, U., Abolfathi, M., Ejlalipour, R., Nejab, R.S., Berillon,
897 G., 2019. Garm Roud 2, Iran: bladelet production and cultural features of a key Upper Paleolithic site south of
898 the Caspian Sea. Comptes Rendus Palevol. 20, 823-837
899 Bordes, F., 1961. Typologie du Paléolithique ancien et moyen. Delmas, Bordeaux.
900 Bordes, F., 1981. Vingt-cinq ans après : le complexe moustérien revisité. Bulletin de la Société Préhistorique
901 Française 78(3), 77–87.
902 Boulbes, N. (2010). Le cheval de Romain-la-Roche, Equus achenheimensis (Mammalia, Perissodactyla),
903 contribution à la biochronologie des équidés caballins au Pléistocène moyen. Rev. Paléobiol. 29, 747–770.
904 Boulbes, N. and Van Asperen, E.N., 2019. Biostratigraphy and palaeoecology of European Equus. Frontiers in
905 Ecology and Evolution 7, 301.
906 Bourguignon, L., 1997. Le Mousterien de type Quina: nouvelles definitions d'une entite technique. Ph.D.
907 Dissertation, Universite de Paris X, Nanterre.
908 Braidwood, R.J., Howe, B. and Reed, C.A., 1961. The Iranian Prehistoric Project: New problems arise as more is
909 learned of the first attempts at food production and settled village life. Science 133(3469), 2008-2010.
910 Brink, J.W., 1997. Fat Content in Leg Bones of Bison bison, and Applications to Archaeology. Journal of
911 Archaeological Science, 24(3), pp.259-274.
912 Brugal J.P., Argant A., Boudadi-Maligne M., Crégut-Bonnoure E., Croitor R., Fernandez P., Fourvel J.B., Fosse
913 P., Guadelli J.L., Labe B., Magniez P., Uzunidis A., 2020. Pleistocene herbivores and carnivores from France:
914 An updated overview of the litterature, sites and taphonomy. *Annales de Paléontologie*, 106 (2), 102384, 23 p.
915 Chen, F., Welker, F., Shen, C.-C., Bailey, S.E., Bergmann, I., Davis, S., Xia, H., Wang, H., Fischer, R.,
916 Freidline, S.E., Yu, T.-L., Skinner, M.M., Stelzer, S., Dong, Guangrong, Fu, Q., Dong, Guanghui, Wang, J.,
917 Zhang, D., Hublin, J.-J., 2019. A late Middle Pleistocene Denisovan mandible from the Tibetan Plateau. Nature
918 569, 409–412.

Chen, X., Moigne, A.M., 2018. Rhinoceros (*Stephanorhinus hemitoechus*) exploitation in Level F at the Caune de l'Arago (Tautavel, Pyrénées-Orientales, France) during MIS 12. *International Journal of Osteoarchaeology* 28(6), 669-680.

Chevrier, B., Berillon, G., Zeitoun, V., Khaneghah, A.A., Antoine, P., Bahain, J.-J., 2006. Moghanak, Otchounak, Garm Roud 2: nouveaux assemblages paléolithiques dans le Nord de l'Iran. Premières caractérisations typo-technologiques et attributions chrono-culturelles. Paléorient 32(2), 59–79.

Coon, C.S., 1951. Cave explorations in Iran 1949. University of Pennsylvania Press, Philadelphia.

Copeland, L., 1975. The Middle and Upper Paleolithic in Lebanon and Syria in the Light of Recent Research. In: Wendorf, F. and Close, A. (Eds.), Problems in Prehistory: North Africa and the Levant, Dallas, Southern Methodist University Press, pp. 317–350.

Copeland, L., 1981. Chronology and distribution of the Middle Paleolithic, as known in 1980. In: Cauvin, J. and Sanlaville, P. (Pds.), Lebanon and Syria, Préhistoire Du Levant Chronologie et Organisation de l'espace Depuis Les Origines Jusqu'au VIe Millénaire, Lyon, CNRS Maison de l'Orient méditerranéen, pp. 239–263.

Copeland, L., 1985. The pointed tools of Hummal Ia (El Kowm, Syria). Cahiers de l'Euphrate 4: 177–189.

Costamagno, S., and Rigaud, J.-P., 2014. L'exploitation de la graisse au Paléolithique. In: Costamagno, S. (Ed.), Histoire de l'alimentation humaine : entre choix et contraintes. CTHS, Paris, pp. 134-152.

Courtenay, L.A., Yravedra, J., Herranz-Rodrigo, D., Rodríguez-Alba, J.J., Serrano-Ramos, A., Estaca-Gómez, V., González-Aguilera, D., Solano, J.A., Jiménez-Arenas, J.M., 2023. Deciphering carnivoran competition for animal resources at the 1.46 Ma early Pleistocene site of Barranco León (Orce, Granada, Spain). Quaternary Science Reviews 300, 107912.

Daujeard, C., 2008. Exploitation du milieu animal par les Néanderthaliens dans le Sud-Est de la France. Ph.D. Dissertation, Université Lumière Lyon 2, Lyon.

Daujeard, C., Moncel, M.H., Fiore, I., Tagliacozzo, A., Bindon, P. and Raynal, J.P., 2014. Middle Paleolithic bone retouchers in Southeastern France: Variability and functionality. Quaternary International 326, 492-518.

Debénath, A., and H.L. Dibble. 1994. Handbook of Paleolithic Typology, vol. 1: Lower and Middle Paleolithic of Europe. University of Pennsylvania Press, Philadelphia.

945 Delpech F, Villa P. 1993. Activités de chasse et boucherie dans la grotte des Eglises. In: Desse, J., Audoin-
946 Rouzeau, F. (Eds), Exploitation des animaux sauvages à travers le Temps. IV. Colloque International de
947 l'Homme et l'Animal. Editions APDCA, Antibes, France, pp. 79–102.
948 Dennell, R., 2008. The Paleolithic Settlement of Asia, Cambridge World Archaeology. Cambridge University
949 Press, Cambridge.
950 Dibble, H. and Holdaway, S., 1993. The Middle Paleolithic of Warwasi Rockshelter. In: Olszewski, D.I., and
951 Dibble, H.L. (Eds), The Paleolithic Prehistory of the Zagros-Taurus. University Museum, University of
952 Pennsylvania, Philadelphia, pp.75-99.
953 Eisenmann, V., 2022. Old World Fossil Equus (Perissodactyla, Mammalia), Extant Wild Relatives and Incertae
954 Sedis Forms. Quaternary, 5(3), 38.
955 Eisenmann, V., Mashkour, M., 1999. The Small Equids (Perissodactyla, Mammalia) of the Pleistocen of
956 Binagady (Azerbaijan) and Qazvin (Iran): E. hemionus binagadensis nov. subsp. and E. Hydruntinus, Geobios,
957 32(1), 105-122.
958 Farizy, C., David, F., Jaubert, J. and Eisenmann, V., 1994. Hommes et bisons du Paléolithique moyen à Mauran
959 (Haute-Garonne). Paris: CNRS éditions.
960 Ferring, R., Oms, O., Agustí, J., Berna, F., Nioradze, M., Shelia, T., Tappen, M., Vekua, A., Zhvania, D.,
961 Lordkipanidze, D., 2011. Earliest human occupations at Dmanisi (Georgian Caucasus) dated to 1.85–1.78 Ma.
962 Proceedings of the National Academy of Sciences, 108, 10432–10436.
963 Finestone, E.M., Breeze, P.S., Breitenbach, S.F.M., Drake, N., Bergmann, L., Maksudov, F., Muhammadiyev,
964 A., Scott, P., Cai, Y., Khatsenovich, A.M., Rybin, E.P., Nehrke, G., Boivin, N., Petraglia, M., 2022. Paleolithic
965 occupation of arid Central Asia in the Middle Pleistocene. PLOS ONE. 17, e0273984.
966 Fornai, C., Benazzi, S., Svoboda, J., Pap, I., Harvati, K., Weber, G.W., 2014. Enamel thickness variation of
967 deciduous first and second upper molars in modern humans and Neanderthals. Journal of Human Evolution. 76,
968 83–91.
969 Forsten, A., 1991. Size decrease in Pleistocene-Holocene true or caballoid horses of Europe. Mammalia, 55 (3),
970 407-420.

971 Forsten, A., and Moigne, A. M. (1998). The horse from the Middle Pleistocene of Orgnac-3 (Ardèche, France).
972 Quaternaire 9, 315–323.
973 Fortelius, M., Mazza, P., Sala, B. 1993. *Stephanorhinus* (Mammalia, Rhinocerotidae) of the western European
974 Pleistocene, with a special revision of Stephanorhinus etruscus (Falconer, 1868). Palaeontographia Italica 80, 63-
975 155.
976 Geneste, J.-M., 1985. Analyse lithique d'industries moustériennes du Périgord: approche technologique du
977 comportement des groupes humaine au Paléolithique moyen. PhD thesis, Université de Bordeaux.
978 Ghasidian, E., Bretzke, K., Conard, N.J., 2017. Excavations at Ghār-e Boof in the Fars Province of Iran and its
979 bearing on models for the evolution of the Upper Paleolithic in the Zagros Mountains. Journal of
980 Anthropological Archaeology. 47, 33–49.
981 Ghasidian, E., Heydari-Guran, S., Mirazón Lahr, M., 2019. Upper Paleolithic cultural diversity in the Iranian
982 Zagros Mountains and the expansion of modern humans into Eurasia. Journal of Human Evolution. 132, 101–
983 118.
984 Ghasidian, E., Kafash, A., Kehl, M., Yousefi, M., Heydari-Guran, S., 2023. Modelling Neanderthals' dispersal
985 routes from Caucasus towards east. PLOS ONE. 18, e0281978.
986 Glantz, M., 2010. The History of Hominin Occupation of Central Asia in Review. In: Norton, C. and Braun,
987 D.R. (Eds.), Asian Paleoanthropology. From Africa to China and Beyond. Springer, Netherland, pp. 101–112.
988 Glantz, M., Viola, B., Wrinn, P., Chikisheva, T., Derevianko, A., Krivoshapkin, A., Islamov, U., Suleimanov,
989 R., Ritzman, T., 2008. New hominin remains from Uzbekistan. Journal of Human Evolution 55, 223–37.
990 Golovanova, L.V., and Doronichev, V.R., 2003. The Middle Paleolithic of the Caucasus. Journal of World
991 Prehistory 17: 71–140.
992 Gremyatskii, M. A. (1949). Skull of the Neandertal child from Teshik-Tash Cave, Southern Uzbekistan. In:
993 Gremyatskii, M. A. (Ed.), Teshik-Tash: Paleolithic Man. Moscow State University, Moscow, pp. 137–182.
994 Grigolia, G.K., 1963. Paleolit Kvemo-Kartli (Pogrebennaya peshera Tsopi I), Tbilisi, GA.
995 Grün, R., 2006. Direct Dating of Human Fossils. Yearbook of Physical Anthropology 49, 2–48.
996 Grün, R., Schwarcz, H.P., Chadam, J.M., 1988. ESR dating of tooth enamel: coupled correction for U-uptake
997 and U-series disequilibrium. Nuclear Tracks and Radiation Measurements 14, 237-241.

Han, F., Bahain, J.-J., Shao, Q., Sun, X., Voinchet, P., Xiao, P., Huang, M., Li, M., Yin, G., 2022. The Chronology of Early Human Settlement in Three Gorges Region, China—Contribution of Coupled Electron Spin Resonance and Uranium-Series Dating Method. Frontiers in Earth Science 10, 939766.

Hariryan, H., Heydari-Guran, S., Motarjem, A. and Ghasidian, E., 2021. New Evidence of a Late Pleistocene Occupation on the Southern Slopes of the Alborz Mountains. Lithic Technology 46(2), 104-110.

Henry, D.O., Belmaker, M. and Bergin, S.M., 2017. The effect of terrain on Neanderthal ecology in the Levant. Quaternary International 435, 94-105.

Hershkovitz, I., May, H., Sarig, R., Pokhojaev, A., Grimaud-Hervé, D., Bruner, E., Fornai, C., Quam, R., Arsuaga, J.L., Krenn, V.A., Martinón-Torres, M., de Castro, J.M.B., Martín-Francés, L., Slon, V., Albessard-Ball, L., Vialet, A., Schüler, T., Manzi, G., Profico, A., Di Vincenzo, F., Weber, G.W., Zaidner, Y., 2021. A Middle Pleistocene Homo from Nesher Ramla, Israel. Science. 372, 1424–1428.

Heydari, M., Guérin, G., Kreutzer, S., Jamet, G., Kharazian, M.A., Hashemi, M., Vahdati Nasab, H.V., Berillon, G., 2020. Do Bayesian methods lead to more precise chronologies? 'BayLum' and a first OSL-based chronology for the Paleolithic open-air site of Mirak (Iran). Quaternary Geochronology 59, 101082.

Heydari, M., Guérin, G., Zeidi, M., Conard, N.J., 2021. Bayesian luminescence dating at Ghār-e Boof, Iran, provides a new chronology for Middle and Upper Paleolithic in the southern Zagros. Journal of Human Evolution. 151, 102926.

Heydari-Guran, S. and Ghasidian, E., 2020. Late Pleistocene hominin settlement patterns and population dynamics in the Zagros Mountains: Kermanshah region. Archaeological Research in Asia 21, 100161.

Heydari-Guran, S., Benazzi, S., Talamo, S., Ghasidian, E., Hariri, N., Oxilia, G., Asiabani, S., Azizi, F., Naderi, R., Safaierad, R., Hublin, J.-J., Foley, R.A., Lahr, M.M., 2021. The discovery of an in situ*in situ* Neanderthal remain in the Bawa Yawan Rockshelter, West-Central Zagros Mountains, Kermanshah. PLOS ONE. 16, e0253708.

Hillson, S., 2008. The current state of dental decay. Cambridge Studies in Biological and Evolutionary Anthropology, 53, 111.

Hole, F. and Flannery, K.V., 1967. The prehistory of southwestern Iran: a preliminary report. Proceedings of the Prehistoric Society, Cambridge University Press, 33, 147-206.

Hutson, J.M., García-Moreno, A., Noack, E.S., Turner, E., Villaluenga, A., Gaudzinski-Windheuser, S., Davidson, I., Mozota, M., Rosell, J., Blasco, R., Martin-Lerma, I., Barkai, R., Gopher, A., Daujeard, C., Valensi, P., Fiore, I., Moigne, A.-M., Tagliacozzo, A., Moncel, M.-H., Santagata, C., Cauche, D., Raynal, J.-P., Sévêque, N., Auguste, P., Costamagno, S., Bourguignon, L., Soulier, M.-C., Meignen, L., Beauval, C., Rendu, W., Mussini, C., Mann, A., Maureille, B., Abrams, G., Neruda, P., Lázničková-Galetová, M., Hohenstein, U.T., Bertolini, M., Channarayapatna, S., Modolo, M., Peretto, C., Toniato, G., Münzel, S.C., Starkovich, B.M., Conard, N.J., Jéquier, C., Livraghi, A., Romandini, M., Peresani, M., Yeshurun, R., Tejero, J.-M., Barzilai, O., Hershkovitz, I., Marder, O., Vitezović, S., 2018. The origins of bone tool technologies: "Retouching the Paleolithic: Becoming Human and the Origins of Bone Tool Technology" Conference at Schloss Herrenhausen in Hannover, Germany, 21.- 23. October 2015, Propylaeum. Propylaeum.

Jacobs, Z., Li, B., Shunkov, M.V., Kozlikin, M.B., Bolikhovskaya, N.S., Agadjanian, A.K., Uliyanov, V.A., Vasiliev, S.K., O'Gorman, K., Derevianko, A.P., Roberts, R.G., 2019. Timing of archaic hominin occupation of Denisova Cave in southern Siberia. Nature 565, 594–599.

Jaubert, J., Biglari, F., Mourre, V., Bruxelles, L., Bordes, J.G., Shidrang, S., Naderi, R., Mashkour, M., Maureille, B., Mallye, J.B. and Quinif, Y., 2009. The Middle Paleolithic occupation of Mar-tarik, a new Zagros Mousterian site in Bisotun massif (kermanshah, Iran). In: Otte, M., Biglari, F., Jaubert, J. (Eds.), Iran Paleolithic, BAR International Series, Oxford, pp.7-27.

Jiangzuo, Q., Wagner, J., Chen, J., Dong, C., Wei, J., Ning, J. and Liu, J., 2018. Presence of the Middle Pleistocene cave bears in China confirmed–Evidence from Zhoukoudian area. Quaternary Science Reviews 199, 1-17.

Kamrani, Z., Vahdati Nasab, H., Bonilauri, S., Hashemi Sarvandi, S.M., Jayez, M., Kharrazian, M.A., Beheshti, S.I. and Berillon, G., 2022. Middle Paleolithic Lithic Industry from Qaleh Kurd Cave, Qazvin Province, Iran. Iranian Journal of Archaeological Studies 12(2), 1-14.

Lacombat F. 2009. Biochronologie et grands mammifères au Pléistocène moyen et supérieur en Europe occidentale : l'apport des Rhinocerotidae (genre *Stephanorhinus*). Quaternaire 20 (4), 429-435.

Leroi-Gourhan, A., 1981. La végétation et la datation de l'Abri moustérien de Houmian (Iran). Paléorient 7, 75–79.

Lindly, J.M., 1997. The Mousterian of the Zagros: A regional perspective (No. 56). Ph.D. Dissertation, Arizona State University.

Lumley de, M.-A. (Ed.), 2018. Les restes humains fossiles de la grotte du Lazaret. CNRS Editions, Paris. 658p.

Lumley de, M.-A. (Ed.), 2022. Caune de l'Arago. Tome IX. Les restes humains du Pléistocène moyen de la Caune de l'Arago. CNRS Editions, Paris. 796p.

Malinsky-Buller, A., 2016. The Muddle in the Middle Pleistocene: The Lower–Middle Paleolithic Transition from the Levantine Perspective. Journal of World Prehistory 29(1), 1-78.

Martínez-Navarro, B., Pérez-Claros, J. A., Palombo, M. R., Rook, L., Palmqvist, P. 2007. The Olduvai buffalo Pelorovis and the origin of Bos. Quaternary Research, 68 (2), 220-226.

Mashkour, M., Monchot, H., Trinkaus, E., Reyss, J.-L., Biglari, F., Bailon, S., Heydari, S., Abdi, K., 2009. Carnivores and their prey in the Wezmeh Cave (Kermanshah, Iran): a Late Pleistocene refuge in the Zagros. International Journal of Osteoarchaeology 19, 678–694.

McBurney, C.B.M., 1964. Preliminary report on Stone Age reconnaissance in north-eastern Iran. In Proceedings of the Prehistoric Society, Cambridge University Press, 30, 382-399.

Mehterian, S., Pourmand, A., Sharifi, A., Lahijani, H.A., Naderi, M. and Swart, P.K., 2017. Speleothem records of glacial/interglacial climate from Iran forewarn of future Water Availability in the interior of the Middle East. Quaternary Science Reviews 164, 187-198.

Meignen, L., 1998. Hayonim cave lithic assemblages in the context of the Near-Eastern Middle Paleolithic: a preliminary report. In: Akazawa, T., Aoki, K., and Bar-Yosef, O. (eds.), Neandertals and Modern Humans in Western Asia, Plenum Press, New York, pp. 165–180.

Meignen, L., 2007. Middle Paleolithic blady assemblages in the Near East: a reassessment. In: Caucasus and the initial dispersals in the Old World, St. Petersburg: Russian Academy of Sciences, Institute of the History of material culture, pp. 133–148.

Meignen, L., and Bar-Yosef, O., 2020. Acheulo-Yabrudian and Early Middle Paleolithic at Hayonim Cave (Western Galilee, Israel): Continuity or break? Journal of Human Evolution 139: 102733.

Meignen, L., and Tushabramishvili, N., 2006. Paléolithique moyen laminaire sur les flancs sud du Caucase: productions lithiques et fonctionnement du site de Djruchula (Géorgie). Paléorient 32(2): 81–104.

Meignen, L., and Tushabramishvili, N., 2010. Djruchula Cave, on the Southern Slopes of the Great Caucasus: An Extension of the Near Eastern Middle Paleolithic Blady Phenomenon to the North. Journal of The Israel Prehistoric Society 40, 35–61.

Mercier, N. and Valladas, H., 2003. Reassessment of TL age estimates of burnt flints from the Paleolithic site of Tabun Cave, Israel. Journal of Human Evolution, 45(5), pp.401-409.

Mercier, N., Valladas, H., Meignen, L., Joron, J.L., Tushabramishvili, N., Adler, D.S. and Bar-Yosef, O., 2010. Dating the Early Middle Paleolithic laminar industry from Djruchula Cave, Republic of Georgia. Paléorient, 163-173.

Mihailović, D., Kuhn, S.L., Bogićević, K., Dimitrijević, V., Marín-Arroyo, A.B., Marković, J., Mercier, N., Mihailović, B., Morley, M.W., Radović, P., Rink, W.J., Plavšić, S., Roksandic, M., 2022. Connections between the Levant and the Balkans in the late Middle Pleistocene: Archaeological findings from Velika and Mala Balanica Caves (Serbia). Journal of Human Evolution 163, 103138.

Moigne, A.M., Valensi, P., Auguste, P., García-Solano, J., Tuffreau, A., Lamotte, A., Barroso, C. and Moncel, M.H., 2016. Bone retouchers from Lower Paleolithic sites: Terra Amata, Orgnac 3, Cagny-l'Epinette and Cueva del Angel. Quaternary International, 409, pp.195-212.

Molnar, S., 1971. Human tooth wear, tooth function and cultural variability. American Journal of Physical Anthropology, 34. Jg., Nr. 2, S. 175-189.

Moncel, M.-H., Moigne, A.-M. and Combier, J., 2012. Towards the Middle Paleolithic in western Europe: the case of Orgnac 3 (southeastern France). Journal of Human Evolution 63, 653-666.

Monchot, H., Mashkour, M., Biglari, F., Abdi, K., 2020. The Upper Pleistocene brown bear (Carnivora, Ursidae) in the Zagros: Evidence from Wezmeh Cave, Kermanshah, Iran. Annales de Paléontologie. 106, 102381.

Narasimhan, V.M., Patterson, N., Moorjani, P., Rohland, N., Bernardos, R., Mallick, S., Lazaridis, I., Nakatsuka, N., Olalde, I., Lipson, M., Kim, A.M., Olivieri, L.M., Coppa, A., Vidale, M., Mallory, J., Moiseyev, V., Kitov, E., Monge, J., Adamski, N., Alex, N., Broomandkhoshbacht, N., Candilio, F., Callan, K., Cheronet, O., Culleton, B.J., Ferry, M., Fernandes, D., Freilich, S., Gamarra, B., Gaudio, D., Hajdinjak, M., Harney, É., Harper, T.K., Keating, D., Lawson, A.M., Mah, M., Mandl, K., Michel, M., Novak, M., Oppenheimer, J., Rai, N., Sirak, K., Slon, V., Stewardson, K., Zalzala, F., Zhang, Z., Akhatov, G., Bagashev, A.N., Bagnera, A., Baitanayev, B.,

1106 Bendezu-Sarmiento, J., Bissembaev, A.A., Bonora, G.L., Chargynov, T.T., Chikisheva, T., Dashkovskiy, P.K.,
1107 Derevianko, A., Dobeš, M., Douka, K., Dubova, N., Duisengali, M.N., Enshin, D., Epimakhov, A., Fribus, A.V.,
1108 Fuller, D., Goryachev, A., Gromov, A., Grushin, S.P., Hanks, B., Judd, M., Kazizov, E., Khokhlov, A., Krygin,
1109 A.P., Kupriyanova, E., Kuznetsov, P., Luiselli, D., Maksudov, F., Mamedov, A.M., Mamirov, T.B., Meiklejohn,
1110 C., Merrett, D.C., Micheli, R., Mochalov, O., Mustafokulov, S., Nayak, A., Pettener, D., Potts, R., Razhev, D.,
1111 Rykun, M., Sarno, S., Savenkova, T.M., Sikhymbaeva, K., Slepchenko, S.M., Soltobaev, O.A., Stepanova, N.,
1112 Svyatko, S., Tabaldiev, K., Teschler-Nicola, M., Tishkin, A.A., Tkachev, V.V., Vasilyev, S., Velemínský, P.,
1113 Voyakin, D., Yermolayeva, A., Zahir, M., Zubkov, V.S., Zubova, A., Shinde, V.S., Lalueza-Fox, C., Meyer, M.,
1114 Anthony, D., Boivin, N., Thangaraj, K., Kennett, D.J., Frachetti, M., Pinhasi, R., Reich, D., 2019. The formation
1115 of human populations in South and Central Asia. Science. 365, eaat7487.
1116 Nelson, K., 2010. Environment, cooking strategies and containers. Journal of Anthropological Archaeology,
1117 29(2), 238-247.
1118 Neuville, R., 1951. Le Paléolithique et le Mésolithique du désert de Judée. Archives de l'Institut de
1119 Paléontologie Humaine, mémoire n°24, Masson et Cie, Paris.
1120 Nikzad, M., Sedighian, H. and Ghasemi, E., 2015. New Evidence of Paleolithic Activity from South Khorasan,
1121 Eastern Iran. Antiquity 89(347), 1-7.
1122 Nobis, G. (1971). Vom Wildpferd zum Hauspferd, Studien zur Phylogenie Pleistozäner Equiden Eurasiens und
1123 das Domestikationsproblem unserer Hauspferde, Fundamenta Reihe B, Band 6. Köln: Bõhlau Verlag.
1124 Orlando, L., Mashkour, M., Burke, A., Douady, C.J., Eisenmann, V., Hanni, C., 2006. Geographic distribution
1125 of an extinct equid (Equus hydruntinus: Mammalia, Equidae) revealed by morphological and genetical analyses
1126 of fossils. Molecular Ecology 15(8), 2083-2093.
1127 Otte, M., Biglari, F., Jaubert, J. (Eds.), 2009. Iran Paleolithic, BAR International Series, Oxford.
1128 **Otte, M., Shidrang, S. and Flas, D. 2012. L'Aurignacien de la grotte Yafteh et son contexte (fouilles 2005-2008).**
1129 **ERAUL 132, Liège.**
1130 Otte, M., Shidrang, S., Zwyns, N., Flas, D., 2011. New radiocarbon dates for the Zagros Aurignacian from
1131 Yafteh cave, Iran. Journal of Human Evolution 61, 340–346.

Outram, A.K. 2001. A new approach to identifying bone marrow grease exploitation: why the indeterminate fragments should not be ignored. Journal of Archaeological Science 28, 401-410.

Pan, L., Dumoncel, J., Mazurier, A., Zanolli, C., 2020. Hominin diversity in East Asia during the Middle Pleistocene: A premolar endostructural perspective. Journal of Human Evolution 148, 102888.

Pandolfi L., Boscato P., Crezzini J., Gatta M., Moroni A., Rolfo M. and Tagliacozzo A. 2017. Late Pleistocene last occurrences of the narrow-nosed rhinoceros *Stephanorhinus hemitoechus* (Mammalia, Perissodactyla) in Italy. *Rivista Italiana Di Paleontologia E Stratigrafia*, 123 (2), 177-192.

Pandolfi, L., Bartolini-Lucenti, S., Cirilli, O., Bukhsianidze, M., Lordkipanidze, D. and Rook, L., 2021. Paleoecology, biochronology, and paleobiogeography of Eurasian Rhinocerotidae during the Early Pleistocene: The contribution of the fossil material from Dmanisi (Georgia, Southern Caucasus). Journal of Human Evolution, 156, p.103013.

Peresani, M., Bourguignon, L., Delpiano, D., and Lemorini, C., 2023. Quina on the edge. Insights from a Middle Paleolithic lithic assemblage of Grotta di Fumane, Italy. Journal of Archaeological Science: Reports 49: 103998.

Pokines J.T., Lister A.M., Ames C.J.H., Nowell A., Cordova C.E. 2019. Faunal remains from recent excavations at Shishan Marsh 1 (SI1), a Late Lower Paleolithic open-air site in the Azraq Basin, Jordan. *Quaternary Research*, 91 (2), 768-791.

Pushkina, D., Bocherens, H. and Ziegler, R., 2014. Unexpected palaeoecological features of the Middle and Late Pleistocene large herbivores in southwestern Germany revealed by stable isotopic abundances in tooth enamel. Quaternary International, 339, pp.164-178.

Rabinovich, R., Biton, R., 2011. The Early-Middle Pleistocene faunal assemblages of Gesher Benot Ya'aqov: Inter-site variability. Journal of Human Evolution 60 (4), 357-374.

Reich, D., Green, R.E., Kircher, M., Krause, J., Patterson, N., Durand, E.Y., Viola, B., Briggs, A.W., Stenzel, U., Johnson, P.L.F., Maricic, T., Good, J.M., Marques-Bonet, T., Alkan, C., Fu, Q., Mallick, S., Li, H., Meyer, M., Eichler, E.E., Stoneking, M., Richards, M., Talamo, S., Shunkov, M.V., Derevianko, A.P., Hublin, J.-J., Kelso, J., Slatkin, M., Pääbo, S., 2010. Genetic history of an archaic hominin group from Denisova Cave in Siberia. Nature. 468, 1053–1060.

1158 Rivals F., Julien M.A., Kuitems M., Van Kolfschoten T., Serangeli J., Drucker D. et al. (2015). Investigation of
1159 equid paleodiet from Schöningen 13II-4 through dental wear and isotopic analyses: archaeological implications.
1160 *Journal of Human Evolution* 89, 129-137.
1161 Rivals, F. and Lister, A.M., 2016. Dietary flexibility and niche partitioning of large herbivores through the
1162 Pleistocene of Britain. Quaternary Science Reviews 146, 116-133.
1163 Romandini M., Nannini N., Tagliacozzo A. et Peresani M. (2014) – The ungulate assemblage from layer A9 at
1164 Grotta di Fumane, Italy: Azooarchaeological contribution to the reconstruction of Neanderthal ecology.
1165 Quaternary International 337, p. 11-27.
1166 Roustaei, K., Nasab Vahdati, H., Biglari, F., Heydari, S., Clark, G.A., Lindly, M., 2004. Recent Paleolithic
1167 surveys in Luristan. Current Anthropology 45, 692–707.
1168 Saarinen, J., Eronen, J., Fortelius, M., Seppä, H. and Lister, A.M., 2016. Patterns of diet and body mass of large
1169 ungulates from the Pleistocene of Western Europe, and their relation to vegetation. Palaeontologia Electronica,
1170 19(3), pp.1-58.
1171 Sadraei, A., Mehneh, M.F., Sheikh, M., Anani, B., Minaei, Z.H., 2019. Kaftar Kouh of Ferdous, New Evidence
1172 of Paleolithic Population in Southern Khorasan, Iran. Advances in Anthropology 9, 111–123.
1173 Sadraei, A., Shipton, C., Garazhian, O., Azar, M., Zafaranlou, R., Soroush, M.R., 2023. Tracking Pleistocene
1174 occupation on the Eastern Iranian Plateau: preliminary results. Antiquity 97(391), e1.
1175 Sanchez-Gonzalez, E., Pinilla-Cienfuegos, E., Borrero-Lopez, O., Rodríguez-Rojas, F., Guiberteau, F., 2020.
1176 Contact damage of human dental enamel under cyclic axial loading with abrasive particles. Journal of the
1177 Mechanical Behavior of Biomedical Materials 102, 103512.
1178 Sarhangzadeh, J., Yavari, A.R., Hemami, M.R., Jafari, H.R. and Shams-Esfandabad, B., 2013. Habitat suitability
1179 modeling for wild goat (Capra aegagrus) in a mountainous arid area, central Iran. Caspian Journal of
1180 Environmental Sciences 11(1), 41-51.
1181 Scott, J.E., Marean, C.W., 2009. Paleolithic hominin remains from Eshkaft-e Gavi (southern Zagros Mountains,
1182 Iran): description, affinities, and evidence for butchery. Journal of Human Evolution 57, 248–259.

Sévêque, N. and Auguste, P. 2018. From West to East: Lower and Middle Paleolithic bone retouchers in Northern France. In: Hutson, J.M. et al. (Eds.), Retouching the Paleolithic, Becoming Human and the Origins of Bone Tool Technology.

Sévêque, N., 2017. Variabilité des comportements alimentaires au Paléolithique moyen en France septentrionale - Apports des études archéozoologiques. Ph.D. Université Lille 3.

Sheiham, A., James, W.P.T., 2015. Diet and Dental Caries: The Pivotal Role of Free Sugars Reemphasized. Journal of Dental Research. 94, 1341–1347.

Shidrang, S., Biglari, F., Bordes, J.G., Jaubert, J., 2016. Continuity and change in the late Pleistocene lithic industries of the central Zagros: a typo-technological analysis of lithic assemblage from Ghar-e Khar cave, Bisotun. Iran. Archaeol. Ethnol. Anthropol. Eurasia 44/1 (2016), 27–38.

Shimelmitz, R., Kuhn, S.L., Ronen, A., and Weinstein-Evron, M., 2014. Predetermined flake production at the Lower/Middle Paleolithic boundary: Yabrudian scraper blank technology. PLoS One 9(9): e106293

Shoaee, M.J., Vahdati Nasab, H., Petraglia, M.D., 2021. The Paleolithic of the Iranian Plateau: Hominin occupation history and implications for human dispersals across southern Asia. Journal of Anthropological Archaeology 62, 101292.

Slimak, L., Zanolli, C., Higham, T., Frouin, M., Schwenninger, J.-L., Arnold, L.J., Demuro, M., Douka, K., Mercier, N., Guérin, G., Valladas, H., Yvorra, P., Giraud, Y., Seguin-Orlando, A., Orlando, L., Lewis, J.E., Muth, X., Camus, H., Vandevelde, S., Buckley, M., Mallol, C., Stringer, C., Metz, L., 2022. Modern human incursion into Neanderthal territories 54,000 years ago at Mandrin, France. Science Advances 8, eabj9496.

Smith, T.M., Toussaint, M., Reid, D.J., Olejniczak, A.J., Hublin, J.-J., 2007. Rapid Dental Development in a Middle Paleolithic Belgian Neanderthal. PNAS 104(51), 20220–20225.

Solecki, R.S., 1955. Lamellar flakes versus blades, a reappraisal. American Antiquity, 20(4Part1), pp.393-394.

Solecki, R.S., 1959. Three adult neanderthal skeletons from Shanidar cave, Northern Iraq. Annual Report of the Smithsonian Institution, 603–635.

Solecki, R.S., 1963. Prehistory in Shanidar Valley, Northern Iraq: Fresh insights into Near Eastern prehistory from the Middle Paleolithic to the Proto-Neolithic are obtained. Science 139(3551), 179-193.

Soleymani, S. and Alibaigi, S., 2018. Qaleh Kurd Cave: a Middle Paleolithic site on the western borders of the Iranian Central Plateau. Al-Rāfidān, Journal of Western Asiatic Studies, 39, 43-54.

Sommer, R.S., Fahlke, J.M., Schmölcke, U., Benecke, N. and Zachos, F.E., 2009. Quaternary history of the European roe deer Capreolus capreolus. Mammal Review 39(1), pp.1-16.

Sommer, R.S., Zachos, F.E., Street, M., Jöris, O., Skog, A., Benecke, N., 2008. Late Quaternary distribution dynamics and phylogeography of the red deer (Cervus elaphus) in Europe. Quaternary Science Reviews 27 (7-8), 714-733.

Speth, J.D., 2012. Paleoanthropology and archaeology of big-game hunting. Springer, New York.

Thoma, A., 1963. The dentition of the Subalyuk Neandertal child. Zeitschrift für Morphologie und Anthropologie, 54, 127–150.

Tillier, A.M., 1979a. La dentition de l'enfant moustérien Chateauneuf 2 découvert à l'Abri de Hauteroche (Charente). L'Anthropologie (Paris) 83(3), 417-438.

Tillier, A.M., 1979b. Restes crâniens de l'enfant moustérien homo 4 de Qafzeh (Israël), la mandibule et les maxillaires. Paléorient 5, 67-85.

Tillier, A.M., 1980. Les dents d'enfant de Ternifine (Pléistocène moyen d'Algérie). L'Anthropologie 84, 413–421.

Tillier, A.M., 1995. Paléoanthropologie et pratiques funéraires au Levant méditerranéen durant le Paléolithique moyen: le cas des sujets non-adultes. Paléorient 21(2), 63-76.

Tillier, A.-M., 1999, Les enfants moustériens de Qafzeh. CNRS Editions, Paris, 239p.

Tillier, A.M., 2021. Aspects of health status in Pre-Sedentism Populations of Southwestern Asia. Evidence from Qafzeh Site, Lower Galilee. Paléorient 47(1), 31-34.

Tillier, A.-M., Arensburg, B., Rak, Y., Vandermeersch, B., 1995. Middle Paleolithic dental caries: new evidence from Kebara (Mount Carmel, Israel). Journal of Human Evolution 29, 189–192.

Tillier, A.-M., Arensburg, B., Vandermeersch, B., Chech, M., 2003. New human remains from Kebara Cave (Mount Carmel). The place of the Kebara hominids in the Levantine Mousterian fossil record. Paléorient. 29, 35–62.

Tobias, P.V., 1966. Fossil Hominid Remains from Ubeidiya, Israel. Nature 211, 130–133.

Towle, I., Irish, J.D., Groote, I.D., Fernée, C. and Loch, C., 2021. Dental caries in South African fossil hominins. South African Journal of Science, 117(3-4), pp.1-8.

Towle, I., Riga, A., Irish, J.D., Dori, I., Menter, C., Moggi-Cecchi, J., 2019. Root caries on a Paranthropus robustus third molar from Drimolen. American Journal of Physical Anthropology. 170, 319–323.

Trinkaus, E., 1983. The Shanidar Neandertals. Academic Press, New York.

Trinkaus, E., Biglari, F., 2006. Middle Paleolithic Human Remains from Bisitun Cave, Iran. Paléorient. Vol.32, 105–111.

Trinkaus, E., Biglari, F., Mashkour, M., Monchot, H., Reyss, J.L., Rougier, H., Heydari, S., Abdi, K., 2008. Late Pleistocene human remains from Wezmeh Cave, western Iran. American Journal of Physical Anthropology 135, 371–378.

Tsanova, T., 2013. The beginning of the Upper Paleolithic in the Iranian Zagros. A taphonomic approach and techno-economic comparison of Early Baradostian assemblages from Warwasi and Yafteh (Iran). Journal of Human Evolution, 65(1), pp.39-64.

Tushabramishvili, D.M., 1963. Pechtchery Dzhrutchulskogo uchtchelia. Pechtchery Gruzii. Matsnereba, Tbilisi.

Uzunidis, A., Rivals, F. and Brugal, J.P., 2017. Relation between morphology and dietary traits in horse jugal upper teeth during the middle pleistocene in Southern France. Quaternaire. Revue de l'Association française pour l'étude du Quaternaire, 28(3), pp.303-312.

Uzunidis-Boutillier, A., 2017. Grands herbivores de la fin du Pléistocène moyen au début du Pléistocène supérieur dans le sud de la France. Implications anthropologiques pour la lignée néandertalienne. Aix-Marseille université, PhD, 788 p.

Vahdati Nasab, H. and Hashemi, M., 2016. Playas and Middle Paleolithic settlement of the Iranian Central Desert: the discovery of the Chah-e Jam Middle Paleolithic site. Quaternary International 408, 140-152.

Vahdati Nasab, H., 2010. Paleolithic Archaeology of Iran. International Journal of Humanities 18(2), 63-87.

Vahdati Nasab, H., Berillon, G., Jamet, G., Hashemi, M., Jayez, M., Khaksar, S., Anvari, Z., Guérin, G., Heydari, M., Kharazian, M.A. and Puaud, S., 2019. The open-air Paleolithic site of Mirak, northern edge of the Iranian Central Desert (Semnan, Iran): Evidence of repeated human occupations during the late Pleistocene. Comptes Rendus Palevol 18(4), 465-478.

Vahdati Nasab, H., Clark, G., 2014. The upper Paleolithic of the Iranian central desert: The delazian site - A case study. Archäologische Mitteilungen aus Iran und Turan, 46, 1–20.

Vahdati Nasab, H., Clark, G.A., Torkamandi, S., 2013. Late Pleistocene dispersal corridors across the Iranian Plateau: A case study from Mirak, a Middle Paleolithic site on the northern edge of the Iranian Central desert (Dasht-e Kavir). Quaternary International, 300, 267–281.

Van der Made J., Torres T., Ortiz J.E., Moreno-Pérez L., Fernández-Jalvo Y. 2016. The new Material of Large Mammals from Azokh and Comments on the Older Collections. In Fernández-Jalvo, Y., King, T., Yepiskoposyan, L., Andrews, P. (Eds.), Azokh Cave and the Transcaucasian Corridor, Springer, Dordrecht, pp.117-159

Vandermeersch, B., 1981. Les hommes fossiles de Qafzeh (Israël). CNRS, Paris.

Vasilyev, S. and Amirkhanov, H., 2018. Paleolithic Caucasus: Paleoanthropological Panorama. Quaternary International 465, 105-116.

Vekua, A., Lordkipanidze, D., Rightmire, G.P., Agusti, J., Ferring, C.R., Maisuradze, G., Mouskhelishvili, A., Nioradzé, G., Ponce De León, M.S., Tappen, M., Tvalchrelidze, M., Zollikofer, C.P.E., 2002. A new skull of early Homo from Dmanisi, Georgia. Science. 297, 85–89.

Vincent, A. 1993. L'outillage osseux au Paléolithique moyen : une nouvelle approche. Ph.D. Dissertation, Université Paris X, Nanterre.

Wojtczak, D., and Malinsky-Buller, A., 2022. The Levantine Early Middle Paleolithic in retrospect: Reassessing the contribution of Abou-Sif to the understanding of Paleolithic record. Archaeological Research in Asia 30, 100366.

Wojtczak, D.B., 2022. More than blades. Early Middle Paleolithic of the Levant. L'Anthropologie, 126(3), p.103046.

Zaidner, Y., Druck, D., Weinstein-Evron, M., 2006. Acheulo-Yabrudian handaxes from Misliya Cave, Mount Carmel, Israel. In: Goren-Inbar, N. and Sharon, G. (Eds.), Axe Age: Acheulian Toolmaking from Quarry to Discard, Equinox Publishers, Oxford, pp. 243–266.

Zanolli, C., Biglari, F., Mashkour, M., Abdi, K., Monchot, H., Debue, K., Mazurier, A., Bayle, P., Le Luyer, M., Rougier, H., Trinkaus, E., Macchiarelli, R., 2019. A Neanderthal from the Central Western Zagros, Iran. Structural reassessment of the Wezmeh 1 maxillary premolar. Journal of Human Evolution 135, 102643.

SUPPLEMENTARY INFORMATION

SI1: Geoarcheological laboratory analysis – Applied Methods

Field naked eye observations and sketches of the deposits allowed *in situ* identification of the main units. In addition, several laboratory analyses have been started at the UMR7194's laboratories in Paris, after the samples have been exported with the authorization of the Iranian Center for Archaeological Research (ICAR).

Grain-size analysis - Grain-size Analysis gives information of transport, sorting and hence genesis for the sediment. A total of 117 sediment samples were made every 5cm accordingly to the units in both sections of T1 and the northern section of T3. The particle size distribution was then measured on crude and acid treated samples by laser granulometry using a Mastersizer 3000 from MALVERN at the sedimentology laboratory of the Musée de l'Homme (UMR 7194) in Paris. The USDA scale was used as a basis for classification of the grain sizes.

Micromorphological Analysis – In order to specify the nature and the attributes of sediments, microscopic observations of the soil micromorphology were made. Four blocks of sediments from the southern and western walls of T1 and four blocks from the southern wall of T3 were extracted, from which 10 petrographic thin sections were prepared at the sedimentology laboratory of the Institut de Paléontologie Humaine (UMR 7194) in Paris. The thin sections are described using a polarizing microscope at the sedimentology laboratory of Musée de l'Homme (UMR 7194) in Paris. Micromorphological analyses allowed recognizing some forming factors, post-depositional changes and impact of human on deposits. Thin sections are still under analysis and should allow as well contributing to some paleoenvironmental inferences.

Complementary ongoing analyses - FTIR (Fourier Transform Infrared) analysis aims at identifying organic and inorganic materials in the sediments. Seven powder samples were analyzed by FTIR-ATR, on a Bruker Vertex 70 spectrometer equipped with a globar source, a KBr beamsplitter, and a DLaTGS detector. The analyses were carried out at the *Plateau de Spectroscopie Infrarouge – Plateau Analytique du Muséum*, at Musée de l'Homme in Paris. Determination is conducted after comparison with the Plateau de Spectroscopie internal database (to be published). To complete our knowledge on mineralogy, nature and provenance of the sediments, a series of XRD analyses is implemented on 6 sediment samples from the northern section of T1 using a Bruker XRD (D2) device. Finally, the magnetic susceptibility variations along the North Section of Trench I is measured. The magnetic susceptibility is the capacity of a body to acquire an induced magnetisation in an applied magnetic field. In the sediment, the magnetic susceptibility provides information on the proportions of carbonates (diamagnetic), clays (paramagnetic) and magnetic oxides (ferro- and ferrimagnetic). Its variations

indicate changes in the mineralogy, concentration and size of magnetic grains. These magnetic minerals are sensitive to the paleoclimatic and paleoenvironmental variations. The magnetic susceptibility (χ) of sediment samples is measured with a Bartington MS-2 Susceptibility Meter coupled with a MS2B dual frequency sensor. Low frequency (χlf, 0.46 kHz) is applied and measured 3 times in an ambient temperature room; the average value is used for analysis.

SI2 : Stratigraphic divisions and character of the sediments in the trench T3

Sequence	*Unit*	*Thickness (cm)*	*Nature*	*Structure*	*Comments*
I	1	~ 15	Brown gravelly sandy silt	Reworked	Polygenetic superficial soil cover containing root traces, whitish gray slightly granular centimetric interbeds of ash and charcoal.
	2	~ 10	Whitish gray silt	Massive	Thin interbeddings of ash with lenticular geometry containing dark organic nodules.
	3	~ 7	Brown silt	Slightly granular	Polygenetic calcareous soil containing white calcareous nodules.
	4	~ 10	Light gray silt	Slightly granular	Subangular (local) gravel and centimetric charcoal.
	5	~ 7	Brown sandy silt	Slightly granular to massive	Contains soil nodules.
	6	~ 5	Light gray silt	Massive	Contains millimetric interbeddings of gray ash and charcoal. Lenticular geometry.
	7	~ 8	Brown to gray silt	Slightly granular	Contains charcoal and evidence of Fe migration. Probably a paleosol with eroded upper limit.
	8	~ 2	Whitish gray silt	Slightly granular	Contains brown soil nodules.
	9	~ 8	Black slightly sandy silt	Slightly granular	Contains reddish brown silt with granular structure that resembles a Fe segregation zone, at the bottom.
	10	~ 25	White to light gray gravelly silt	Slightly granular to massive	Contains subangular gravels and flat cobbles, interbeddings of gray sediment (ash). Affected by large bioturbation.
	11	~ 6	Black organic silt	Slightly granular	Probably an aggregated humic paleosol, with a facies of reddish brown silt with granular structure that resembles a Fe segregation zone at the bottom.
	12	~ 20	Very light gray silty sand	Slightly granular	Probably resulted from degradation of some calcareous beddings.
	13	~ 10	Cobbly gravelly sandy silt	Crudely stratified	Calcareous flat gravels (medium to coarse) and clasts.
II	14	~ 5	Gray silty sand	Granular	Consolidated by calcareous cement.
	15	~ 20	Very light brown sandy silt	Massive	Composed of very loose and well-sorted infilling sediments (loess).
	16	~ 20	Light brown gravelly sandy silt	Crudely stratified	Flat calcareous gravels.
	17	~ 2	Very dark brown organic silt (loess)	Slightly granular	Eroded top horizon of a paleosol formed in loess deposits.
	18	~ 10	Light brown silt (loess)	Slightly granular	Weakly stratified calcareous gravels.
	19	~ 6	Brown sandy silt	Slightly granular	Coarse grain and humic.
	20	~ 5	Dark brown organic silt	Slightly granular	Contains millimetric charcoal.
	21	~ 23	Greenish brown silt	Slightly granular	Evidence of gley distribution, contains Fe oxide migration zones.

22	~ 5	Gray to dark brown organic silt (ash)	Massive	Contains calcic precipitation at the bottom.
23	~ 10	Greenish brown silt	Slightly granular	Evidence of gley distribution, contains Fe oxide migration zones.
24	~ 2	Gray to dark brown organic silt	Massive	
25	~ 10	Brown silt	Granular	Calcareous flat clasts with crude stratification. This unit is probably a paleosol.
26	~ 10	Brown gravelly silt	Crudely stratified	Gravelly erosion near the top.
27	~ 30	Brown cobbly gravelly silt	Granular	Unstratified calcareous clasts.
28	~ 5	Yellowish brown silt	Granular	White calcareous gravels and sand-sized nodules.
29	~ 3	Dark brown to black organic clayey silt	Granular	Eroded.
30	~ 7	Yellowish brown gravelly silt	Granular	White calcareous gravels with lenticular geometry. Very eroded.
31	~ 5	Dark brown to black organic clayey silt	Granular	Contains yellow colored nodules of consolidated mudstone.
32	~ 7	Yellowish brown gravelly silt	Granular	White calcareous gravels. Very eroded and irregular at the upper limit.
33	~ 8	Dark brown to black organic clayey silt	Granular	
34	~ 10	Brown gravelly clayey silt	Granular	

Table SI2 *– Stratigraphic divisions and character of the sediments in the trench T3. (© M. Akhavan Kharazian and G. Jamet)*

SI3: ESR/U-series dating

Preparation - Part of an external enamel layer was mechanically extracted from each tooth, then cleaned on each side with a dental drill to avoid any contamination by sediment, cement or dentine. The cleaned enamel fragments were then grounded and sieved in order to extract the 100-200 µm grain-size fraction. This fraction was split into fourteen aliquots, thirteen of them were irradiated at the CENIEH (Burgos, Spain) using a ^{60}Co gamma source at different gamma doses ranging from 32 to 8,000 or 12,500 grays (Gy) depending on the aliquot and the sample.

ESR measurements -The fourteen aliquots, for each enamel sample, were measured using a Bruker EMX spectrometer using the following parameters: 10 mW microwave power, 0.1 mT modulation amplitude, room temperature, 10 mT scan range, 4 mins scan time and 100 kHz frequency modulation, at least four measurements for each aliquot were performed on different days. The ESR intensities were measured on each obtained spectrum from the g = 2.00018 enamel ESR peak-to-peak (T1-B2) signal according to Grün (2000).

Equivalent doses determination -The equivalent doses D_E were extrapolated from the obtained dose-intensity data sets. The growth curves were built for each sample using three different fitting functions: single saturating exponential, SSE; double saturating exponential, DSE; exponential plus linear, E+L. The obtained results are displayed in Table SI3a and the best fitting curves displayed on Figure SI3a. For the Qaleh Kurd samples, depending of the obtained curve descriptions, SSE or E+L equivalent doses were used for the age calculation.

Samples	SSE	r^2	E+L	r^2	DSE	r^2
QK18 1/1	206.65 ± 2.47	0.99974	205.36 ± 3.38	0.99973	205.05 ± 5.57	0.99970
QK18 1/2	223.25 ± 6.27	0.99857	208.97 ± 6.27	0.99926	208.97 ± 8.94	0.99917
QK19 T1/1	160.78 ± 11.24	0.99275	157.07 ± 14.01	0.9922	157.07 ± 18.05	0.99134
QK19 T1/2	152.88 ± 3.99	0.99896	151.49 ± 4.96	0.99888	148.98 ± 7.07	0.99884
QK19 T1/3	131.31 ± 6.71	0.99893	127.03 ± 4.32	0.99906	125.64 ± 6.02	0.99901
QK19T1/4	144.38 ± 3.66	0.99741	140.33 ± 8.93	0.99725	140.34 ± 12.62	0.99669
QK18 3/1	124.55 ± 3.51	0.99870	118.56 ± 3.43	0.99920	117.47 ± 4.93	0.99912
QK18 3/2	324.88 ± 5.74	0.99944	314.89 ± 6.54	0.99960	314.70 ± 9.44	0.99955
QK18 3/3	298.58± 11.65	0.99737	286.04 ± 14.85	0.99755	286.04 ± 20.84	0.99727
QK18 3/4	272.34 ± 6.14	0.99913	262.79 ± 6.90	0.99935	262.79 ± 6.90	0.99928

Table SI3a *– Equivalent doses determined for the Qaleh Kurd teeth using different mathematical extrapolation functions. The underlined values were used for the age calculation. SSE= single saturated exponential function; E+L=function composed by a linear and an exponential terms; DSE = function composed by two single saturated exponential terms. Uncertainties are given at 95% (2σ) of confidence.*

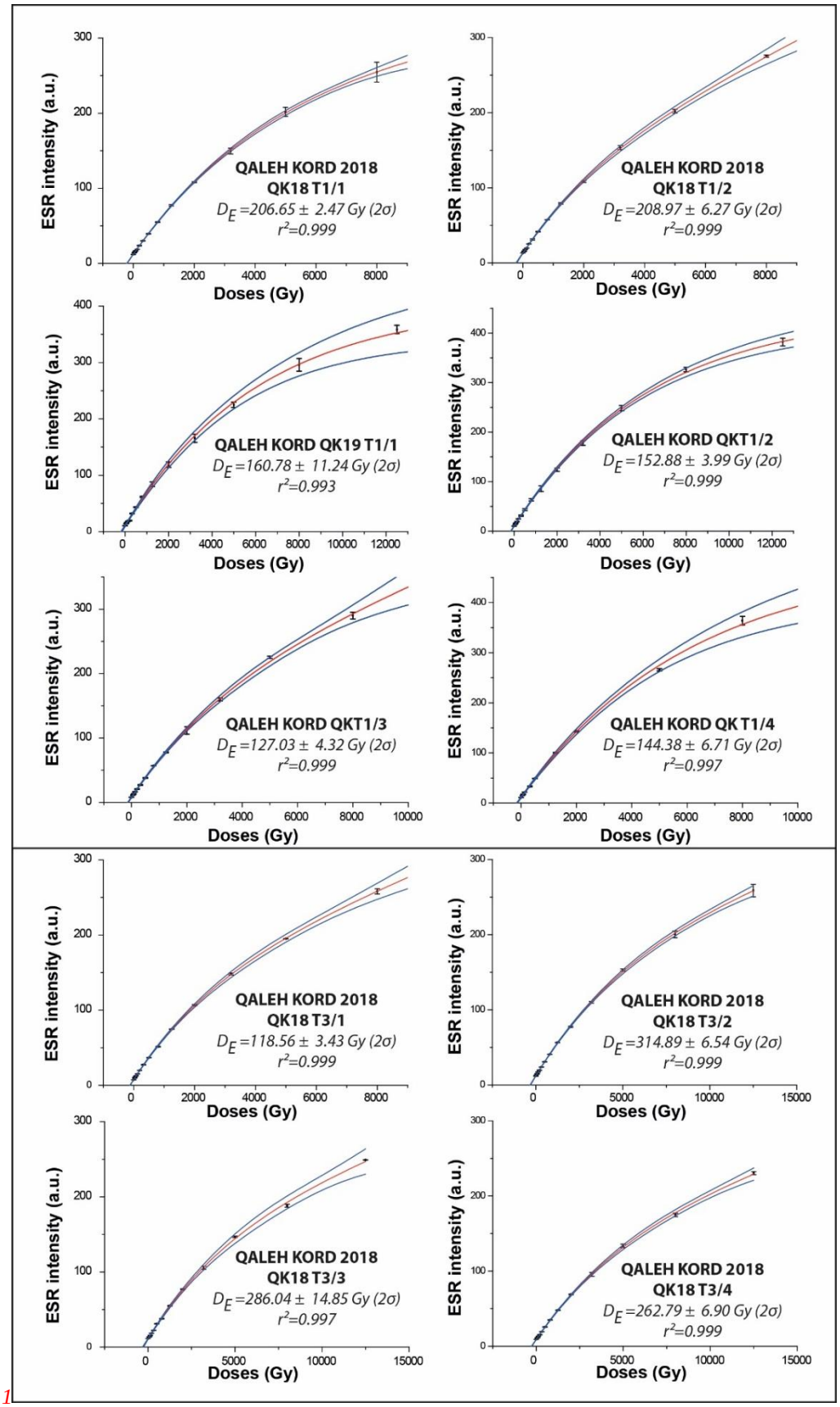

Figure SI3a – Dose growth curves obtained for the Qaleh Kurd samples.

U-series analyses - U-series analyses were performed on each dental tissue in order to determine the U-uptake parameters necessary to the dose rate contributions and age calculations (see details in Shao et al., 2015). In this work, two kinds of analyses were realized. The enamel samples were analysed on a Thermo Electron Neptune Multi-Collector Inductively Coupled Plasma Mass Spectrometer (MC-ICPMS) at Nanjing Normal University, China, and the dentine and cement samples were performed on a Thermo Electron iCAP-RQ Quadripole Inductively Coupled Plasma Mass Spectrometer (Q-ICP-MS) at MNHN, Paris. The chemical protocol of Shao et al. (2011) was used for all the analyses. The obtained results are displayed in Table SI3b.

Sample	Tissue	U (ppm)	$^{230}Th/^{232}Th$	$^{234}U/^{238}U$	$^{230}Th/^{234}U$	Apparent U-series age (ka)	$^{222}Rn/^{230}Th$	Initial thickness (µm)	Removed thickness Internal side (µm)	Removed thickness External side (µm)
QK18 T1/1	enamel	0.242 ± 0.005	288	1.473 ± 0.032	0.889 ± 0.020	192 + 13/-11	0.249	1031 ± 103	79 ± 8	172 ± 17
	dentine	8.576 ± 0.195	>9800	1.333 ± 0.029	0.668 ± 0.015	113 ± 5	0.562			
	cement	6.041 ± 0.159	>1200	1.414 ± 0.034	0.785 ± 0.021	149 +9/-8	0.058			
QK18 T1/2	enamel	0.300 ± 0.006	309	1.526 ± 0.031	1.053 ± 0.023	319 +43/-32	1.000	1580 ± 158	206 ± 21	238 ± 24
	dentine	7.824 ± 0.214	>15000	1.339 ± 0.030	0.685 ± 0.015	118 ± 5	0.352			
	cement	7.333 ± 0.157	>2400	1.403 ± 0.030	0.813 ± 0.017	160 ± 8	0.101			
QK18 T3/1	enamel	0.127 ± 0.003	75	1.394 ± 0.030	0.596 ± 0.017	94 ±4	0.749	1180 ± 118	10 ± 1	190 ± 19
	dentine	3.987 ± 0.084	>3500	1.350 ± 0.028	0.555 ± 0.012	85 ± 3	1.000			
	cement	5.018 ± 0.141	250	1.348 ± 0.036	0.716 ± 0.019	127 +7/-6	0.080			
QK18 T3/2	enamel	0.132 ± 0.003	311	1.515 ± 0.032	0.784 ± 0.018	146 ± 7	1.000	1518 ± 152	133 ± 13	306 ± 31
	dentine	5.445 ± 0.116	>3800	1.486 ± 0.031	0.835 ± 0.018	167 +9/-8	0.912			
	cement	6.000 ± 0.154	720	1.482 ± 0.038	0.823 ± 0.021	162 +10/-9	0.880			
QK18 T3/3	enamel	0.164 ± 0.004	210	1.484 ± 0.034	0.825 ± 0.020	163 ± 9	1.000	1335 ± 134	200 ± 20	34 ± 3
	dentine	7.865 ± 0.175	>4700	1.365 ± 0.029	0.823 ± 0.018	166 +9/-8	0.357			
	cement	7.120 ± 0.156	401	1.379 ± 0.029	0.874 ± 0.019	189 +12/-11	0.616			
QK18 T3/4	enamel	0.086 ± 0.002	67	1.411 ± 0.035	0.801 ± 0.021	155 +10/-9	1.000	1596 ± 160	150 ± 15	292 ± 29
	dentine	7.593 ± 0.178	>3700	1.273 ± 0.027	0.858 ± 0.018	186 +12/-11	0.303			
	cement	5.005 ± 0.106	79	1.290 ± 0.027	0.894 ± 0.021	205 +16/-14	1.000			
QK19 T1/1	enamel	0.243 ± 0.006	150	1.309 ± 0,034	0.575 ± 0.015	89 ± 4	1.000	1366 ± 137	49 ± 5	49 ± 5
	dentine	7.490 ± 0.057	>3000	1.246 ± 0.009	0.614 ± 0.005	100 ± 1	0.404			
	cement	7.107 ± 0.051	>1600	1.358 ± 0.009	0.807 ± 0.006	159 ± 3	0.377			
QK19 T1/2	enamel	0.224 ± 0.006	>500	1.432 ± 0.037	0.640 ± 0.017	104 ± 5	1.000	1310 ± 131	16 ± 2	14 ± 1
	dentine	8.727 ± 0.066	>3000	1.371 ± 0.010	0.774 ± 0.006	146 ± 3	0.277			
	cement	7.546 ± 0.052	>3000	1.421 ± 0,009	0.815 ± 0,006	160 ± 3	0.350			
QK19 T1/3	enamel	0.127 ± 0.004	70	1.280 ± 0.036	0.648 ± 0.019	108 ± 6	1.000	1681 ± 168	43 ± 4	144 ± 14
	dentine	5.675 ± 0.043	>12000	1.186 ± 0.008	0.624 ± 0.005	103 ± 1	0.369			
	cement	5.491 ± 0.040	>800	1.268 ± 0.009	0.954 ± 0.009	252 ± 9	0.392			
QK19 T1/4	enamel	0.443± 0.012	150	1.210 ± 0.031	0.566 ± 0.015	88 ± 4	1.000	556 ± 56	18 ± 2	17 ± 2
	dentine	5.446 ± 0.046	>20000	1.192 ± 0.010	6.636 ± 0.005	106 ± 2	0.440			
	cement	6.038 ± 0.041	250	1.278 ± 0.008	0.715 ± 0.006	128 ± 2	0.470			

Table SI3b *- U-series data obtained by ICP-MS, $^{222}Rn/^{230}Th$ ratios determined by check-crossing of gamma and ICP-MS data and thicknesses (measured before and after cleaning of both sides of the enamel layer) used for the ESR/U-series age calculations on the Qaleh Kurd teeth.*

Dose-rate estimations - The radioelement contents of sediment samples associated to each tooth were determined by high resolution low background gamma spectrometry using a germanium crystal (Table SI3c). The water content of the sediments was estimated after one week drying in 40°C oven and the mean value of these measurements, 10 ± 5 %, was used for the age calculations. TL Al_2O_3 dosimeters were also placed on the different dated levels during 2018 excavation campaign but it was not possible to get access to the site since this date and external gamma dose rate cannot be measured in situ. The cosmic dose rate was estimated using the formula of Prescott and Hutton (1994) using the following parameters: F=0.24; J=0.76; h=2.137 km; H=4.1. Limestone roof thicknesses of 10m above T1 and 12 m above T3 and the depth of the samples were considered in the cosmic dose rate evaluation. The following parameters were also used in the dose rate determination: k-value (α efficiency) of 0.13 ± 0.02 (Grün and Katzenberger-Apel, 1994); enamel water content of 0 wt%; dentine and cement water content of 7 wt%; radioelement contents-doses conversion factors from Guérin et al. (2011). For each dental tissue, Rn loss was estimated from both gamma and ICP measurements as preconized by Bahain et al. (1992) and the beta dose contributions were corrected from the enamel part destroyed on each side of the enamel layer during the preparation process (according to Brennan et al., 1997) (Table SI3b).

Samples	Depth	^{238}U (ppm)	^{230}Th (ppm)	^{40}K (%)
QK18 T1/1	-137cm	2.23 ± 0,09	6,52 ± 0,14	2,34 ± 0,02
QK18 T1/2	-165cm	2.30 ± 0,07	4,63 ± 0,10	1,68 ± 0,01
QK18 T3/1	-90cm	1.72 ± 0,07	2,05 ± 0,09	0,76 ± 0,01
QK18 T3/2	-163cm	1.94 ± 0,09	5,18 ± 0,14	1.95 ± 0,02
QK18 T3/3	-186cm	1.97 ± 0,07	3,61 ± 0,10	1,35 ± 0,01
QK18 T3/4	-241cm	2.01 ± 0,07	1,98 ± 0,09	0,69 ± 0,01
QK19 T1/1	-68cm	1.88 ± 0,07	4,44 ± 0,10	1,42 ± 0,01
QK19 T1/2	-90cm	1.48 ± 0,06	3,10 ± 0,09	1,01 ± 0,01
QK19 T1/3	-120cm	1.73 ± 0,06	3,15 ± 0,07	0,99 ± 0,01
QK19 T1/4	-107cm	1.92 ± 0,06	2,94 ± 0,07	0,99 ± 0,01

Table SI3c *– Radioelement contents of the sediments from Qaleh Kurd determined by high resolution low background gamma spectrometry.*

ESR/U-series age calculation - Lastly, ESR/U-series ages, U-uptake parameters and dose-rate contributions were calculated by US model (Grün et al., 1988) or AU model (Shao et al., 2012) using "USESR", "AUESR" and "combined ESR" computer programs, in which the age uncertainty (2σ) is calculated with Monte Carlo approach (Shao et al., 2014). Results are displayed in Table SI3d.

Samples	Tissue	U (ppm)	Equivalent dose (Gy)	U-uptake parameter p or *n* (a. u.)	D_α (µGy/a)	D_β (µGy/a)	$D_{(\gamma + cosm)}$ (µGy/a)	D_a (µGy/a)	ESR/U-series ages US or *AU* (ka)
QK18 T1/1	enamel dentine cement	0.242 ± 0.005 8.576 ± 0.195 6.041 ± 0.159	206,65 ± 2,47	*-0.0089 ± 0.0009* -0.6827 ±0.0632 -0.9315 ±0.0457	*55 ± 43*	*102 ± 59*	*1089 ± 43*	***1245 ± 85***	***165 ± 11***
QK18 T1/2	enamel dentine cement	0.300 ± 0.006 7.824 ± 0.214 7.333 ± 0.157	208,97 ± 6,27	*-0.0093 ± 0.0165* -0.7100 ± 0.1575 *-0.0082 ± 0.0023*	*106 ± 205*	*52 ± 57*	*1097 ± 46*	***1255 ±218***	***168 ± 29***
QK19 T1/1	enamel dentine cement	0.243 ± 0.006 7.490 ± 0.057 7.107 ± 0.051	160,78 ± 11,24	-0.2868 ± 0.0905 -0.4461 ± 0.0794 -0.9187 ± 0.0452	46 ± 34	84 ± 45	774 ± 31	**903 ± 63**	**178 ± 12**
QK19 T1/2	enamel dentine cement	0.224 ± 0.006 8.727 ± 0.066 7.546 ± 0.052	152,88 ± 3,99	-0.3656 ± 0.0888 -0.7557 ± 0.0580 -0.8379 ± 0.0514	48 ± 28	107 ± 44	592 ± 25	**746 ± 58**	**205 ± 15**
QK19 T1/3	enamel dentine cement	0.127 ± 0.004 5.675 ± 0.043 5.491 ± 0.040	127,03 ± 4,32	-0. 5131 ± 0.0764 -0.4475 ± 0.0818 *-0.0078 ± 0.0006*	*19 ± 20*	*49 ± 36*	*610 ± 25*	***687 ± 54***	***185 ± 13***
QK19 T1/4	enamel dentine cement	0.443± 0.012 5.446 ± 0.046 6.038 ± 0.041	144,38 ± 3,66	-0.2829 ± 0.1173 -0.5495 ± 0.0931 -0.7576 ± 0.0734	73 ± 47	132 ± 59	621 ± 26	**825 ± 80**	**175 ± 15**
QK18 T3/1	enamel dentine cement	0.127 ± 0.003 3.987 ± 0.084 5.018 ± 0.141	118,56 ± 3,43	0. 0076 ± 0.1131 0.0571 ± 0.1170 -0.5861 ± 0.0684	19 ± 20	44 ± 32	503 ± 24	**565 ± 44**	**210 ± 15**
QK18 T3/2	enamel dentine cement	0.132 ± 0.003 5.445 ± 0.116 6.000 ± 0.154	314,89 ± 6,54	-0.4068 ± 0.0624 -0.5746 ± 0.0508 -0.5415 ± 0.0533	40 ± 37	72 ± 47	915 ± 37	**1026 ± 70**	**307 ± 20**
QK18 T3/3	enamel dentine cement	0.164 ± 0.004 7.865 ± 0.175 7.120 ± 0.156	286,04 ± 14,85	-0.4792 ± 0.0720 -0.4952 ± 0.0716 -0.6491 ± 0.0575	54 ± 49	91 ± 63	718 ± 30	**862 ± 85**	**332 ± 28**
QK18 T3/4	enamel dentine cement	0.086 ± 0.002 7.593 ± 0.178 5.005 ± 0.106	262,79 ± 6,90	-0.0866 ± 0.0791 -0.3871 ± 0.0573 -0.4504 ± 0.0520	22 ± 18	55 ± 32	505 ± 24	**581 ± 44**	**452 ± 32**

Table SI3d *- Equivalent doses, U-uptake parameters, dose rate contributions and ESR/U-series ages obtained for the Qaleh Kurd teeth. Data obtained through AU model use are indicated in italics.*

Discussion - The equivalent doses determined for the Qaleh Kurd teeth range between 120 and 315 Gy and are quite high if we consider the relatively low U-content determined for the different dental tissues. The external dose rate estimated from the sediments varies quite highly from a level to another and impacts greatly the obtained ESR/U-series ages, ranging from ca 160 to 220 ka for T1 samples and from 195 to 485 ka for T3 ones. A Middle Pleistocene age is so confirmed for the whole set of samples and associated archaeological levels. It is however important to take in consideration that the age calculation is greatly impacted by the external dose, representing more than 75 % of the dose rate (Figure SI3.b)

and leading to the reconstruction of U-uptake kinetics quite different for the teeth issued from the two trenches. Hence, for T1 teeth, some leaching behaviors were hence determined while for T3 samples relatively recent U-uptake behaviors are reconstructed (Figure SI3c). These results need to be consolidated by in situ dosimetric measurements.

REFERENCES

BAHAIN J.J., YOKOYAMA Y., FALGUÈRES C., & SARCIA M.N., 1992 - ESR dating of tooth enamel: a comparison with K-Ar dating. *Quaternary Science reviews*, 11, 245-250.

BRENNAN B.J., RINK W.J., McGUIRL E.L., SCHWARCZ H.P. & PRESTWICH W.V., 1997. Beta doses in tooth enamel by ''One Group'' theory and the Rosy ESR dating software. *Radiation Measurements* 27, 307–314.

GRÜN, R., 2000. Methods of dose determination using ESR spectra of tooth enamel. *Radiation Measurements*, 32, 767-772

GRÜN, R., KATZENBERGER-APEL, O., 1994. An alpha irradiator for ESR dating. *Ancient TL*, 12, 35–38.

GRÜN, R., SCHWARCZ, H.P., CHADAM, J.M., 1988. ESR dating of tooth enamel: coupled correction for U-uptake and U-series disequilibrium. *Nuclear Tracks and Radiation Measurements*, 14, 237-241.

GUÉRIN, G., MERCIER, N. & ADAMIEC, G., 2011. Dose-rate conversion factors: update. *Ancient TL*, 29, 5–8.

PRESCOTT, J.R. & HUTTON, J.T., 1994. Cosmic ray contributions to dose rates for luminescence and ESR dating: large depths and long-term time variations. *Radiation Measurements*, 23, 497–500.

SHAO, Q., BAHAIN, J.-J., FALGUÈRES, C., PERETTO, C., ARZARELLO, M., MINELLI, A., HOHENSTEIN, U.T., DOLO, J.-M., GARCIA, T., FRANK, N., DOUVILLE, E., 2011. New ESR/U-series data for the early middle Pleistocene site of Isernia la Pineta, Italy. *Radiation Measurements*, 46, 847-852.

SHAO Q., BAHAIN J.-J., FALGUERES C., DOLO J.-M. & GARCIA T., 2012. A new U-uptake model for combined ESR/U-series dating of tooth enamel. *Quaternary Geochronology*, 10, 406-41.

SHAO Q., BAHAIN J.-J., DOLO J.-M. & FALGUERES C., 2014. Monte Carlo approach to calculate US-ESR ages and their uncertainties. *Quaternary Geochronology*, 22, 99-106

SHAO Q., CHADAM J., GRÜN R., FALGUÈRES C., DOLO J.-M., BAHAIN J.-J., 2015. The mathematical basis for the US-ESR dating method. *Quaternary Geochronology*, 30, 1-8

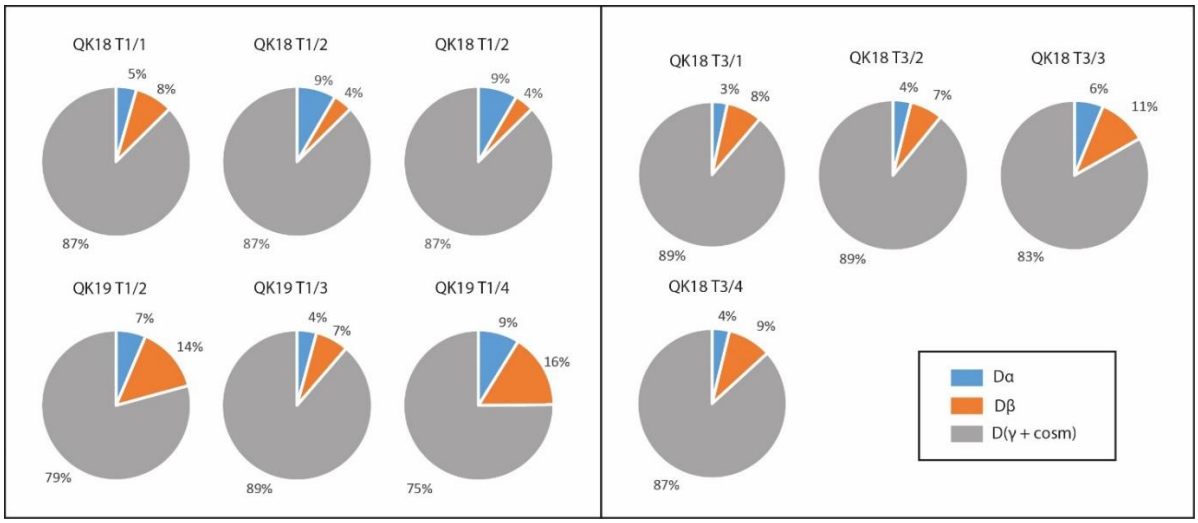

149

150 *Figure SI3b – Dose contributions reconstructed for the Qaleh Kurd teeth.*

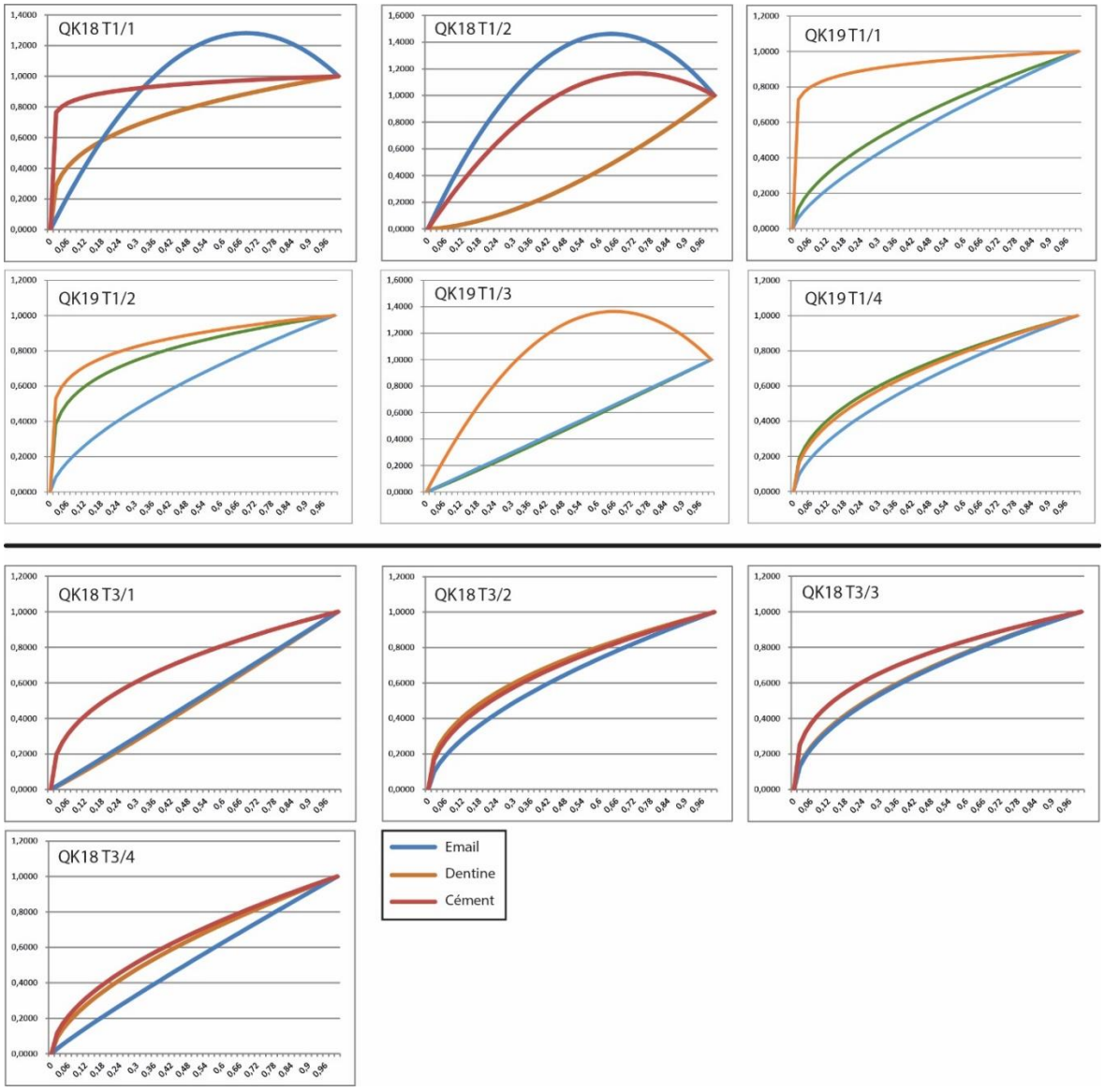

151

152 *Figure SI3c – U-uptake kinetics reconstructed for the Qaleh Kurd teeth.*

153 SI4 : The human deciduous left first upper molar. Comparative metrics.
154

			Mesiodistal diameter (mm)	Buccolingual diameter (mm)	Sources
Qaleh Kurd	**QK19-6169**	**L**	**(6.1)**	**7.2**	
Near Eastern Neanderthals	Dederiyeh cave 1 (2)	R	7.6	9.5	Tillier et al., 2003
		L	7.4	9.3	
	Dederiyeh cave 2 (1)	R	7.6	9.3	Tillier et al., 2003
	Kebara KMH 1 (2)	R	7.4	9.0	Tillier et al., 2003
		L	7.6	9.3	
	Kebara KMH 3 (1)	R	7.7	9.4	Tillier et al., 2003
	Kebara KMH 4 (1)	R	7.9	9.7	Tillier et al., 2003
	Kebara KMH 25 (1)	L	7.3	9.7	Tillier et al., 2003
	Kebara KMH 13 (1)	L	7.4	9.6	Tillier et al., 2003
	Kebara KMH 30 (1)	L	7.1	9.8	Tillier et al., 2003
	Shanidar 7 (1)	L	7.8	8.8	Trinkaus, 1983
	Amud III (1)	L	7.4	8.6	Tillier, 1979
	Range		7.1-7.9	8.6-9.8	
Near Eastern Early Modern humans	Skhul I (1)	R	8.4	7.9	Tillier et al., 2003
	Qafzeh 21 (1)	L	8.8	(7.8)	Tillier, 1999
	Qafzeh 12 (1)	R	8.8	10.0	Tillier, 1999
	Qafzeh 10 (2)	R	8.5	9.2	Tillier, 1999
		L	8.2	9.4	Tillier, 1999
	Qafzeh 4 (2)	R	8.4	8.7	Tillier, 1999
		L	8.5	9.4	Tillier, 1999
	Qafzeh 15 (2)	R	8.5	9.7	Tillier, 1999
		L	8.2	9.9	Tillier, 1999
	Range		8.2-8.8	7.9-10.0	
European Neanderthals (21)	Devil's Tower (2), Fate (1), Krapina (6), La Ferrassie 8 (1), La Quina H18 (2), Meridionale (1), Pech de l'Azé (2), Le Portel (2), Roc de Marsal (2), Subaluk (1), Teshik Tash (1)		7.1-11.0	6.8-9.9	Becam & Chevalier, 2019; Tillier, 1979, 1093; Lumley de, 2018, 2022
European Upper Paleolithic Modern Humans (30)	Abri Pataud (1), Arene Candide (4), Bruniquel (2), Dolni Vestonice (1), Hohlenstein (1), La Madeleine (1), La Roquette (1), Laugerie-Basse (2), Le Morin (1), McKay Cave (1), Muge (Arruda) (4), Muge (Moita) (3), Ofnet (8)		6.4-9.5	7.4-9.6	Becam & Chevalier, 2019
Western Middle Pleistocene humans	Lazaret 12 & 27, Arago (4), A-TD6-14 (1), Tighenif (2)		7.0-8.8	9.2-10.7	Tillier, 1980; Lumley de, 2018, 2022

155

156

REFERENCES:

Becam, G., Chevalier, T., 2019. Neandertal features of the deciduous and permanent teeth from Portel-Ouest Cave (Ariège, France). American Journal of Physical Anthropology. 168, 45–69.

Lumley de, M.-A. (Ed.), 2018. Les restes humains fossiles de la grotte du Lazaret. CNRS Editions, Paris. 658p.

Lumley de, M.-A. (Ed.), 2022. Caune de l'Arago. Tome IX. Les restes humains du Pléistocène moyen de la Caune de l'Arago. CNRS Editions, Paris. 796p.

Tillier, A.M., 1979a. La dentition de l'enfant moustérien Chateauneuf 2 découvert à l'Abri de Hauteroche (Charente). L'Anthropologie (Paris) 83(3), 417-438.

Tillier, A.M., 1980. Les dents d'enfant de Ternifine (Pléistocène moyen d'Algérie). L'Anthropologie 84, 413–421.

Tillier, A.-M., 1999, Les enfants moustériens de Qafzeh. CNRS Editions, Paris, 239p.

Tillier, A.-M., Arensburg, B., Vandermeersch, B., Chech, M., 2003. New human remains from Kebara Cave (Mount Carmel). The place of the Kebara hominids in the Levantine Mousterian fossil record. Paléorient. 29, 35–62.

Trinkaus, E., 1983. The Shanidar Neandertals. Academic Press, New York.

SI5: The faunal assemblages of QK1, QK2 and QK3

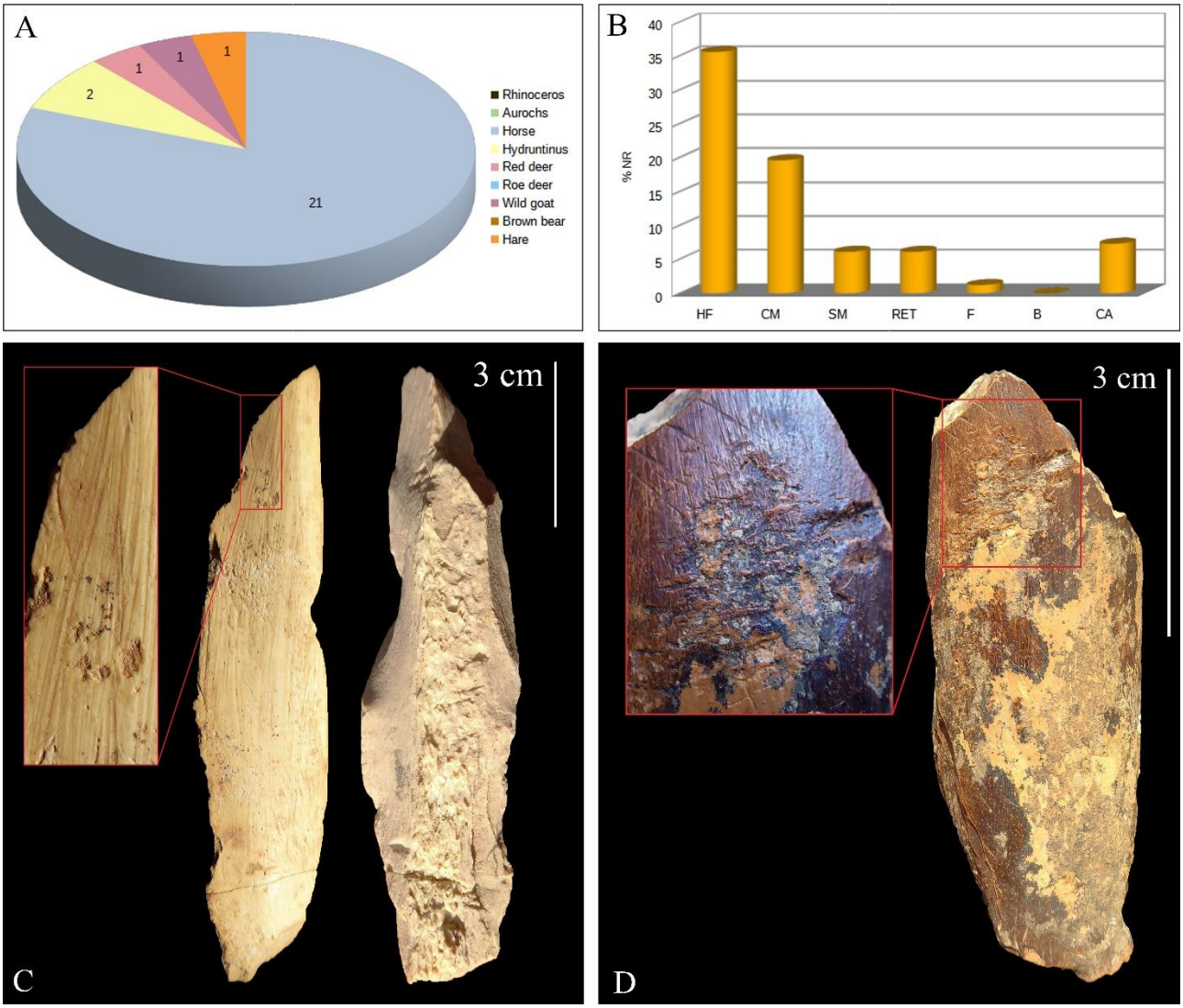

SI5a: LEVEL QK1. A. General inventory, number of rests. B. Percentage of rests with stigmata. HF=helical fracture; CM=cut marks; SM=scrapping marks; RET=*retouchoirs*; F=flakes; B=burned bones; CA=carnivore marks. C. Horse's long bone with helical fracture, cut marks and scrapping marks; D. *Retouchoir* on a horse's metapodial. Associated with a lot of cut marks and scrapping marks. (© N. Sévêque)

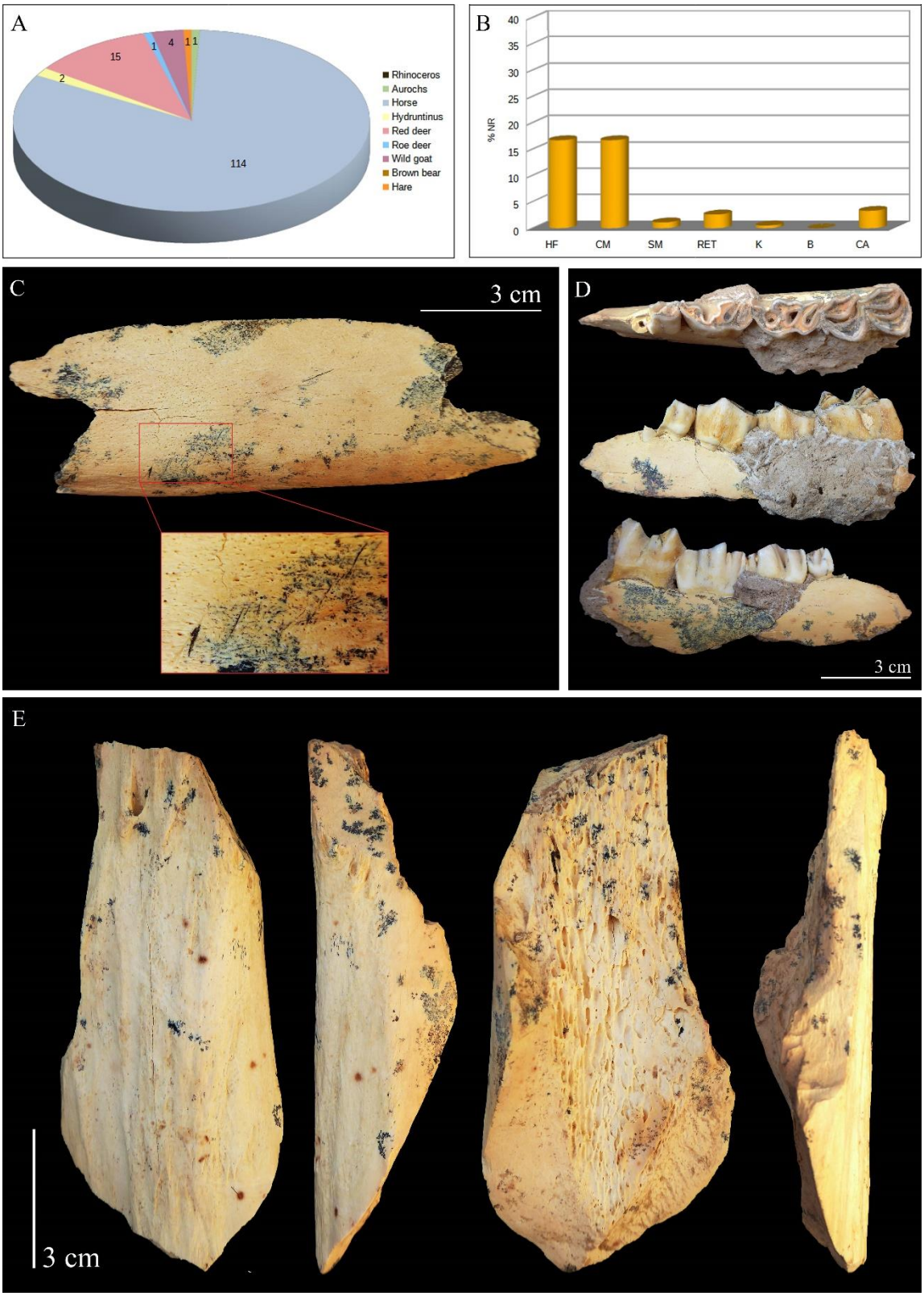

SI5b : LEVEL QK2. A. General inventory, number of rests. B. Percentage of rests with stigmata. HF=helical fracture; CM=cut marks; SM=scrapping marks; RET=*retouchoirs*; F=flakes; B=burned bones; CA=carnivore marks. C. Cut marks on a horse's mandible, for skin taking. D. Left mandible of an adult red deer. E. Helical fracture on a horse's tibia. (© N. Sévêque)

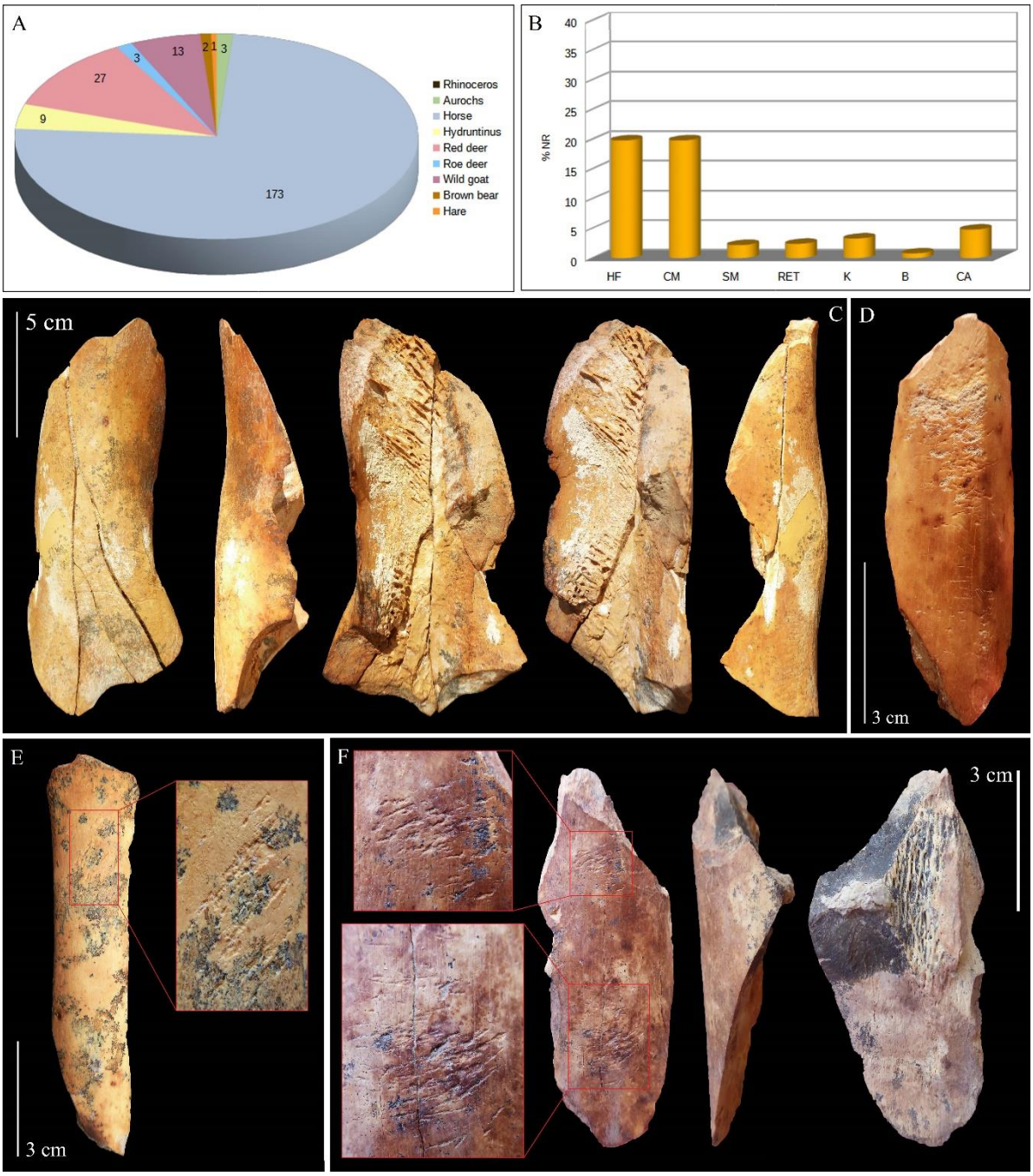

SI5c : LEVEL QK3. A. General inventory, number of rests. B. Percentage of rests with stigmata. HF=helical fracture; CM=cut marks; SM=scrapping marks; RET=*retouchoirs*; F=flakes; B=burned bones; CA=carnivore marks. C. Horse's humerus with an helical fracture and an impact point. D. Double *retouchoir* on a red deer's tibia. E. *Retouchoir* on a red deer's metapodial. F. Double *retouchoir* on a fractured horse's long bone. (© N. Sévêque)

SI6 : The Microvertebrate assemblages

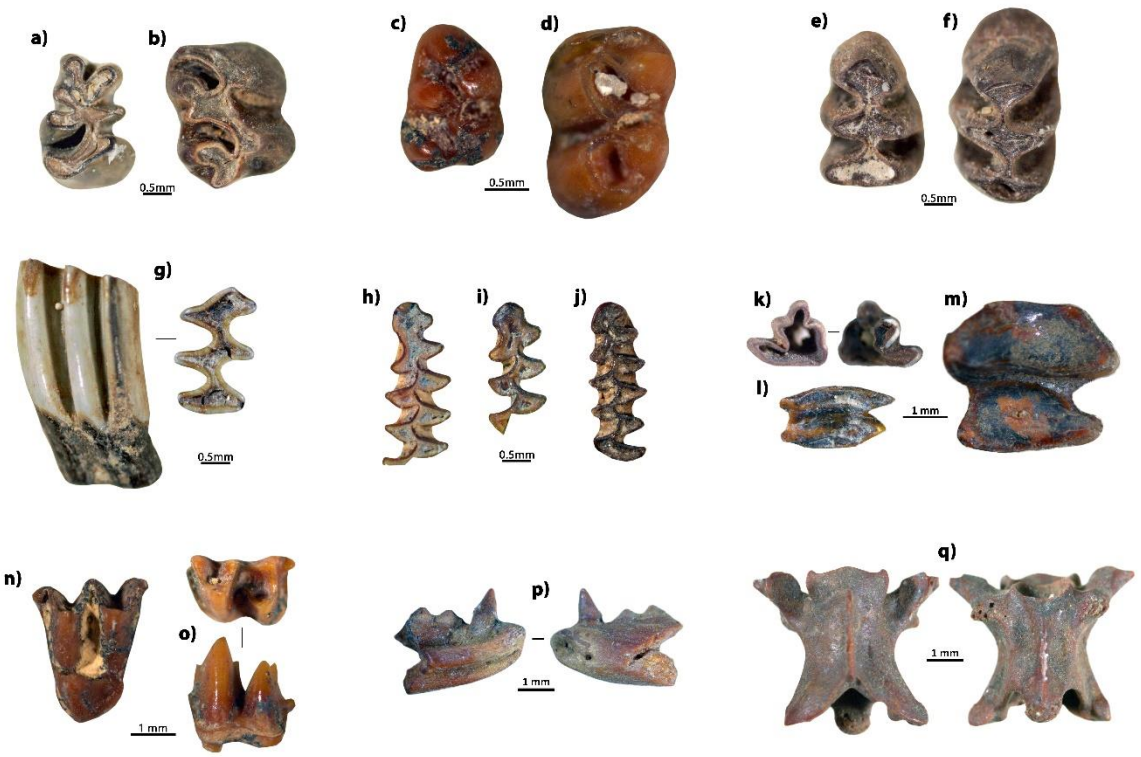

Examples of microvertebrate remains from Qaleh Kurd:
a) Allactaga sp. m1 (QK18_Trench3_Unit24-25)
b) Allactaga sp. M1 (QK18_Trench3_Unit29-31)
c) Calomyscus sp. M1 (QK18_Trench3_Unit29-31)
d) Mesocricetus sp. m3 (QK18_Trench3_Unit24-25)
e) Meriones sp. m1 (QK18_Trench3_Unit24-25)
f) Meriones sp. M1 (QK18_Trench3_Unit24-25)
g) Ellobius sp. m2 (QK18_Trench3_Unit24-25)
h) i) j) Microtus spp. m1s (QK18_Trench3_Unit24-25)
k) Ochotona sp. p3 (QK18_Trench3_Unit29-31)
l) Ochotona sp. upper molar (QK18_Trench3_Unit24-25)
m) Leporidae lower molar (QK18_Trench3_Unit29-31)
n) Chiroptera upper molar (QK18_Trench3_Unit24-25)
o) Chiroptera lower molar (QK18_Trench3_Unit24-25)
p) Agamidae dentary fragment (QK18_Trench3_Unit29-31)
q) Colubridae tronc vertebrae (QK18_Trench3_Unit29-31)

SI7 : The caballine horse at Qaleh Kurd (Sequence II). Comparative metrics of the lower teeth.

		P_{34}			M_{12}		
		DMD	DVL	(DMD+DVL)/2	DMD	DVL	(DMD+DVL)/2
	n	*6*	*6*	*6*	*9*	*9*	*9*
Qaleh Kurd	**x**	**30,5**	**17,2**	**23,9**	**28,1**	**15,8**	**21,9**
	s	1,3	1,6	1,0	2,0	1,7	1,5
Mosbach[a]	n	*46*	*45*	*45*	*44*	*43*	*43*
SIM 15/13	**x**	**32,4**	**17,9**	**25,2**	**29,8**	**15,9**	**22,8**
	s	1,5	1,0	1,0	1,7	1,1	0,9
Caune de l'Arago F[b]	n	*42*	*43*	*42*	*47*	*48*	*47*
SIM 12	**x**	**33,4**	**18,5**	**26,0**	**30,7**	**16,8**	**23,8**
	s	1,1	1,0	0,8	1,4	0,8	0,9
Steinheim[c]	n	*49*	*49*	*47*	*60*	*62*	*60*
SIM 11	**x**	**31,0**	**17,5**	**24,3**	**29,7**	**15,7**	**22,7**
	s	1,9	1,1	1,2	2,0	1,3	1,0
Orgnac 3 [2-1][b]	n	*29*	*35*	*29*	*34*	*39*	*34*
SIM 8	**x**	**30,6**	**17,1**	**23,9**	**28,4**	**15,3**	**21,8**
	s	1,1	0,8	0,7	1,1	1,0	0,7
Tabun E[a]	n	*5*	*6*	*4*	*2*	*2*	*2*
SIM 8/7 ?	**x**	**31,0**	**16,0**	**23,5**	**26,8**	**16,4**	**21,6**
	s	1,4	1,5	0,4	-	-	-
Romain-la-Roche[b]	n	*39*	*38*	*38*	*27*	*28*	*27*
SIM 6	**x**	**31,2**	**17,5**	**24,3**	**28,5**	**15,6**	**22,1**
	s	2,0	1,0	1,3	1,5	0,7	0,8
Prolom 2[a]	n	*31*	*31*	*31*	*20*	*20*	*20*
SIM 5	**x**	**29,6**	**17,6**	**23,6**	**27,5**	**16,4**	**22,0**
	s	1,3	1,0	0,8	1,2	0,8	0,6
Tournal B-D[b]	n	*31*	*32*	*31*	*29*	*30*	*28*
SIM 3	**x**	**29,0**	**17,5**	**23,3**	**27,1**	**15,6**	**21,4**
	s	1,70	0,82	1,08	1,9	0,9	1,0
Jaurens[a]	n	*26*	*25*	*26*	*26*	*26*	*26*
end SIM 3	**x**	**28,9**	**17,3**	**23,3**	**26,6**	**15,7**	**21,2**
	s	1,8	1,2	1,6	1,4	0,8	0,9

a: Eisenmann, web site

b: Boulbes, pers. datas

c: van Asperen, com. pers.

SI7a – Comparative metrics of the lower teeth of Middle and Upper Pleistocene caballine horses. DMD = Mesio-distal diameter (length); DVL = vestibulo-lingual diameter (breadth). Measurements are taken from the enamel (without cement) on the occlusal surface of the tooth.

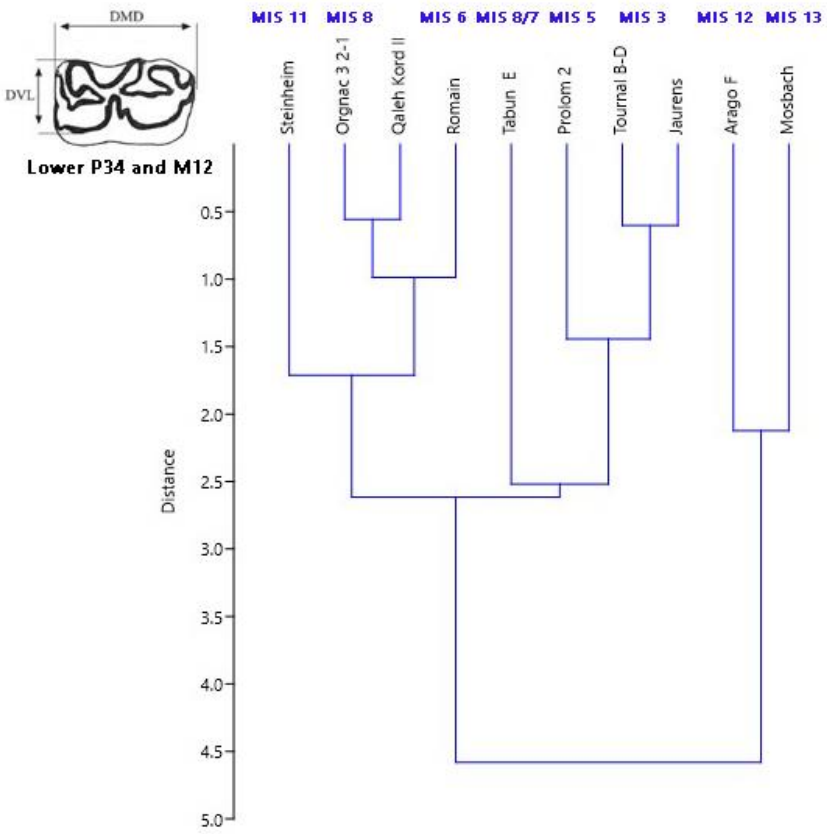

SI7b – Hierarchical clustering analysis based on the mean dimensions of the teeth (Table SI7a). Algorithm=paired group (UPGMA), Similarity index=Euclidean).